

✓

**NASA CONTRACTOR
REPORT**

NASA CR-1109



NASA CR-1

C.1

0060352



TECH LIBRARY KAFB, NM

**LOAN COPY: RETURN TO
APWL (WJL-2)
KIRTLAND AFB, N. MEX**

LUNAR ORBITER III

**Extended-Mission Spacecraft
Operations and Subsystem Performance**

Prepared by
THE BOEING COMPANY
Seattle, Wash.
for Langley Research Center



NATIONAL AERONAUTICS AND SPACE ADMINISTRATION • WASHINGTON, D. C. • JULY 1968



0060352

NASA CR-1109

LUNAR ORBITER III

Extended-Mission Spacecraft Operations and Subsystem Performance

Distribution of this report is provided in the interest of information exchange. Responsibility for the contents resides in the author or organization that prepared it.

Issued by Originator as Document No. D2-100753-4

Prepared under Contract No. NAS 1-3800 by
THE BOEING COMPANY
Seattle, Wash.

for Langley Research Center

NATIONAL AERONAUTICS AND SPACE ADMINISTRATION

For sale by the Clearinghouse for Federal Scientific and Technical Information
Springfield, Virginia 22151 - CFSTI price \$3.00

Contents

	Page
1.0 SUMMARY	1
2.0 INTRODUCTION	5
2.1 Spacecraft Description	5
2.2 Mission Objectives	5
2.3 Operational Organization	7
3.0 FLIGHT OPERATIONS	9
3.1 Spacecraft Control	10
3.1.1 Command Activity	10
3.1.2 Spacecraft Telemetry	14
3.2 Flight Path Control	14
3.2.1 Tracking Data Editing	14
3.2.2 Orbit Determination	14
3.2.3 Guidance Maneuvers	31
3.2.3.1 Orbit Phasing Maneuver for April 1967 Eclipse	31
3.2.3.2 Orbital Lifetime Adjust Maneuver	39
3.2.3.3 Maneuver into Apollo-Type Orbit	43
3.2.3.4 Terminal Transfer Maneuver	45
4.0 FLIGHT DATA	51
4.1 Environmental Data	51
4.1.1 Radiation	51
4.1.2 Micrometeoroids	51
4.2 Special Experiments	51
4.2.1 Radar Mapping Experiment	51
4.2.2 MSFN/AGNQ Support	55
4.2.3 Ionosphere Experiment	55
4.2.4 MSFN Ranging	56
5.0 SPACECRAFT SUBSYSTEM PERFORMANCE	57
5.1 Summary	57
5.2 Subsystem Performance	57
5.2.1 Attitude Control Subsystem	57
5.2.1.1 Inertial Reference Unit (IRU)	58
5.2.1.2 Star Tracker	64
5.2.1.3 Switching Assembly	71
5.2.1.4 Closed-Loop Electronics	71
5.2.1.5 Sun Sensors	71
5.2.1.6 Control Assembly	73
5.2.2 Communications Subsystem	73
5.2.2.1 Transponder	75
5.2.2.2 Traveling-Wave-Tube Amplifier	75
5.2.2.3 Command Decoder	75
5.2.2.4 Modulation Selector	75
5.2.2.5 High- and Low-Gain Antennas	75
5.2.2.6 High-Gain-Antenna Position Controller	75
5.2.2.7 Radiation Dosage Measurement System (RDMS)	77
5.2.2.8 Micrometeoroid Data	77

Continued

	page
5.2.3 Power Subsystem	77
5.2.3.1 Solar Array	77
5.2.3.2 Shunt Regulator	79
5.2.3.3 Charge Controller	79
5.2.3.4 Battery Performance	80
5.2.4 Photo Subsystem	83
5.2.4.1 Camera and Lens	83
5.2.4.2 Film Processor	84
5.2.4.3 Film Handling	84
5.2.4.4 Readout Equipment	84
5.2.4.5 Environmental Controls	85
5.2.5 Structures and Mechanisms Subsystem	85
5.2.5.1 EMD Thermal Control Coating	85
5.2.5.2 Thermal Control Coating	90
5.2.6 Velocity and Reaction Control Subsystem	90
5.2.6.1 Reaction Control Subsystem	91
5.2.6.2 Velocity Control Subsystem	95
5.3 Special Flight Tests	103
5.3.1 Canopus Tracker Glint Mapping	104
5.3.2 Tracker Degradation	109
5.3.3 Squib Firing Interaction	113
5.3.4 Maneuver Accuracy	115
5.3.5 Transponder Threshold	115
5.3.6 Focus Adjustment	115
5.3.7 V/H Tracking Roll Limit	117
5.3.8 Canopus Tracker Glint Without Earthlight	117

Figures

	Page
2-1 Lunar Orbiter Spacecraft	6
2-2 Lunar Orbiter Subsystems	7
3-1 Perilune Altitude History	40
3-2 Orbital Inclination History	40
3-3 Phasing Maneuver Two-Way Doppler — DSS-12 Day 102	42
3-4 Lighting Time History During Lunar Eclipse April 24, 1967 Based on OD-7001-8	42
3-5 S/C8(LO-III) Lifetime Adjust Maneuver	45
3-6 Predicted Perilune Altitude after Lifetime Adjust Maneuver Day 198	45
3-7 Lifetime Prediction — Apollo-Type Orbit — LRC 11/11 Lunar Model	48
3-8 Light-Dark Ratio — Apollo-Type Orbit	48
3-9 Apollo-Type Orbit Maneuver — Two-Way Doppler DSS-12	48
3-10 Terminal Maneuver — Two-Way Doppler DSS-41, Day 282, 1967.	50
4-1 Radiation Data	54
5-1 Attitude Control Subsystem	58
5-2 Prelaunch Gyro Drift Data	61
5-3 Flight Gyro Drift History	62
5-4 Flight Gyro Drift History	62
5-5 Typical Limit Cycle	64
5-6 Gyro Wheel Current and Temperature	65
5-7 Gyro Wheel Current and Temperature	66
5-8 Star Map Voltages	67
5-9 Star Map Voltages	67
5-10 <i>A Priori</i> Star Map Day 101	68
5-11 Observed Star Map Day 101	68
5-12 <i>A Priori</i> Star Map Day 196	69
5-13 Observed Star Map Day 196	69
5-14 <i>A Priori</i> Star Map Day 202	70
5-15 Observed Star Map Day 202	70
5-16 Communications Subsystem	74
5-17 Transponder Temperature Versus Power Output	76
5-18 EMD Temperature versus Transponder Power Output	76
5-19 Transponder Performance	77
5-20 TWTA Performance	78
5-21 Power Subsystem	79
5-22 Solar Array Degradation	79
5-23 Battery Performance Characteristics	80
5-24 Battery Performance Characteristics	81
5-25 Battery Performance Characteristics	81
5-26 Battery Discharge Performance	82
5-27 Photo Subsystem	83
5-28 Pitch Angle History	86
5-29 EMD Temperature History (TWTA)	86
5-30 EMD Temperature History (Transponder)	87
5-31 EMD Temperature History (IRU)	87

Continued

	page
5-32 Pitch Angle History	88
5-33 EMD Temperature History (TWTA)	88
5-34 EMD Temperature History (Transponder)	89
5-35 EMD Temperature History (IRU)	89
5-36 Velocity and Reaction Control Subsystem	90
5-37 Spacecraft Tankage Pressure Profile	91
5-38 Velocity and Reaction Control Temperature Profile	92
5-39 Nitrogen Tank Temperature Variation for Apollo-Type Orbit	93
5-40 Nitrogen Gas Usage History	94
5-41 Limit Cycle Operation (± 2 -Degree Deadband) – Apollo-Type Orbit Maneuver	96
5-42 Spacecraft Position Error – Orbital Lifetime Adjust Maneuver	97
5-43 Orbital Lifetime Adjust Maneuver (ΔV)	98
5-44 Spacecraft Position Error – Orbital Lifetime Adjust Maneuver	98
5-45 Apollo-Type Orbit Maneuver (ΔV)	98
5-46 Propellant Pressures – Apollo-Type Orbit Maneuver	99
5-47 Spacecraft Position Error – Apollo-Type Orbit Maneuver	100
5-48 TVC Actuator Position – Apollo-Type Orbit Maneuver	100
5-49 Engine Valve Temperature Characteristics – Apollo-Type Orbit Maneuver	101
5-50 Terminal Transfer Maneuver (ΔV)	101
5-51 Propellant Pressure – Terminal Transfer Maneuver	102
5-52 Spacecraft Position Error – Terminal Transfer Maneuver	102
5-53 Typical Orbit Sequence – Star Tracker Test	104
5-54 Orbital Geometry – Star Tracker Test	105
5-55 <i>A Priori</i> Star Map – Day 068, Orbit 198	107
5-56 Observed Star Map – Day 268	107
5-57 Star Map – Orbit 199	108
5-58 Star Map – Orbit 200	109
5-59 Star Map – Day 69, Orbit 200	110
5-60 Star Map Degradation Test	110
5-61 Gyro Position Versus Time	114
5-62 Star Map Versus Time	114
5-63 Transponder Threshold Test	116
5-64 <i>A Priori</i> Star Map – Orbit 316	119
5-65 Star Map and Roll Error	119
5-66 Gyro Position – Orbit 317	120
5-67 Star Map – Orbit 317	120

Tables

	Page
1-1 Orbit Parameter Summary	1
3-1 Programmer Core Map Summary	11
3-2 Spacecraft Telemetry Summary	15
3-3 Tracking Data Summary	23
3-4 Station Timing Synchronization	30
3-5 Master File — Tracking Data Tapes	30
3-6 Lunar Harmonic Coefficients	30
3-7 Orbital Elements	31
3-8 Orbit Determination Data Summary	33
3-9 Maneuver Design Data — Phasing Maneuver	41
3-10 Postmaneuver Orbit Determination Data	43
3-11 Maneuver Design Data — Lifetime Adjust Maneuver	44
3-12 Premaneuver Orbital Elements	46
3-13 Maneuver Design Data — Apollo-Type Orbit	47
3-14 Maneuver Design Data — Terminal Transfer	49
3-15 Predicted Impact Parameters	50
4-1 Radiation Data	52
4-2 Micrometeoroid Data	51
4-3 MSFN/AGNQ Tracking Summary	55
4-4 MSFN Ranging Test Data	56
5-1 Extended-Mission Activities	59
5-2 Maneuver Summary	60
5-3 Gyro Drift Data	63
5-4 Deadband Limits	63
5-5 Maneuver Rate Summary	63
5-6 Maneuver Accuracy Summary	71
5-7 Velocity Maneuver Summary	71
5-8 SIDL Data	72
5-9 Actuator Position Range	71
5-10 Deadband Data	73
5-11 Sun Sensor Null Output	73
5-12 Sun Sensor Null Offset	73
5-13 Battery Temperature Data	83
5-14 Photo Subsystem Command Sequence	84
5-15 Photo Subsystem Temperatures and Pressures	85
5-16 Major Events Using Nitrogen Gas	95
5-17 Mission III Velocity Maneuver Summary	103
5-18 Glint Mapping Sequence	106
5-19 Star Tracker Degradation Exercise Sequence	111
5-20 Squib Firing Interaction Exercise Sequence	113
5-21 Position Error	113
5-22 Maneuver Accuracy Exercise Sequence	115
5-23 Maneuver Accuracy Data	116
5-24 Canopus Tracker Glint Without Earthlight Exercise Sequence	118

Abbreviations

AGNQ	Apollo GOSS Navigation Qualification	ODGX	orbit data generation
ASU	acquire Sun	ODPL	orbit determination
BOS	bright-object sensor	OMS	optical-mechanical scanner
CAO	Canopus sensor on	PIM	pitch minus
CAO*	Canopus sensor off	PIP	pitch plus
CDZ	± 2.0 -degree deadzone	ROM	roll minus
CDZ*	± 0.2 -degree deadzone	ROP	roll plus
COGL	command generation and programmer simulation program	RTC	real-time command
DACON	data controller	SFOF	Space Flight Operations Facility
DATL	data alarm summary	SLOE	Senior Lunar Orbiter Engineer
DSIF	Deep Space Information Facility	SPA	Stored Program Address
DSN	Deep Space Network	SPAC	Spacecraft Performance Analysis and Command
DSS	Deep Space Station	SPC	stored-program command
EMD	equipment mount deck	TDPX	tracking data validation
FAT	flight acceptance test	TRJL	trajectory program
FPAC	Flight Path Analysis and Control	TSF	Track Synthesizer Frequency
GMT	Greenwich Mean Time	TTY	telemetry
GOSS	Ground Operation Support System	TVC	thrust vector control
IH	inertial hold	TWT	traveling-wave tube
IRU	inertial reference unit	TWTA	traveling-wave-tube amplifier
JPL	Jet Propulsion Laboratory	VCO	voltage controlled oscillator
LRC	Langley Research Center	V/H	velocity-height
MDE	mission-dependent equipment	YAP	yaw plus
MSFN	Manned Space Flight Network	YAM	yaw minus
NASA	National Aeronautics and Space Administration	ΔV	velocity change

1.0 Summary

The Lunar Orbiter III spacecraft was tracked from the start of its extended mission on March 9, 1967 (GMT Day 068) until it was intentionally crashed into the Moon's farside on October 9, 1967 (GMT Day 282). During this period, the primary objective of obtaining selenodetic data was successfully accomplished by ranging, tracking, and monitoring specific spacecraft telemetry channels. Secondary objectives, which included eight special exercises and four experiments in support of future missions, were also completed.

Selenodetic data acquisition was obtained to assist the Apollo mission by placing the spacecraft in an Apollo-type orbit. This was accomplished by conducting two maneuvers, one on July 17, 1967 (GMT Day 198) and one on August 30, 1967 (GMT Day 242). The first maneuver, which also precluded premature lunar impact, raised the perilune of the orbit from 57.5 km to 140.3 km, and the second lowered the apolune from 1823.7 to 316 km. See Table 1-1, a summary of all maneuvers conducted during the extended mission. Following the maneuvers, the

Table 1-1: Orbit Parameter Summary

Event	Day		Perilune Altitude (km)	Apolune Altitude (km)	Inclination (deg)	Period (min)	Comments
	GMT	Calendar					
Start Extended Mission	068	March 9	55	1845	21.05	208.5	
Phasing Maneuver $\Delta V = 5.5$ mps Sec = 3.5	102	April 12	59	$\frac{1841}{1824}$	$\frac{21.3}{22.7}$	$\frac{208.5}{207.5}$	Prepare For Lunar Eclipse On Day 114
Raise Perilune $\Delta V = 14.4$ mps Sec = 8.9	198	July 17	$\frac{60}{143}$	1824	21.05	$\frac{207.5}{212}$	Lifetime adjust
Lower Apolune $\Delta V = 198.3$ mps Sec = 128.5	242	August 30	144	$\frac{1824}{316}$	20.9	$\frac{212}{130}$	Simulate Apollo- type Orbit
Terminal Transfer Maneuver $\Delta V = 52.6$ mps Sec = 32.0	282	October 9	$\frac{102}{-15.8}$	$\frac{358}{334}$	21.2	$\frac{130}{124}$	Designed For Lunar Impact
Lunar Impact	282	October 9					Predicted time 10:27:11 GMT Lat 14.32°N Long. 92.7°W

MSFN obtained approximately 117 hours of active tracking during the remaining 40 days of Lunar Orbiter III's extended mission. Lunar environmental data of significance was a proton event first detected on May 25, 1967 (GMT Day 145) that caused an approximately 40-rad increase in loop radiation dosage. Four micrometeoroid hits were recorded during the extended mission.

Special exercises were conducted to obtain additional data on the performance characteristics of the attitude control and communication subsystems while in unique attitudes and/or environmental configurations. Hopefully, this data would verify acceptable performance of existing systems for Mission IV and assist in the development of design and operational improvements. The results of these exercises follow.

- Canopus tracker glint tests indicated that the tracker could be operated satisfactorily under Mission IV lighting conditions without adverse glint problems. A squib Canopus tracker interaction test revealed that there was no interaction between squib firing events and tracker operation.
- A roll, pitch, yaw maneuver accuracy test was conducted to obtain data that would be useful during postmission error analysis. Test results indicated that maneuver accuracies in all axes were well within the $\pm 0.3\%$ requirement.
- Transponder threshold test measurements were in agreement with transponder sensitivity measurements obtained during prelaunch ground testing and also showed that, after 6 weeks in space, drop-off in transponder sensitivity was negligible.

The following special experiments were performed to support the MSFN and to obtain additional data of a general scientific nature.

- The MSFN used Lunar Orbiter III to provide tracking data, training, and experience in tracking a spacecraft at lunar distances. This network also used the spacecraft to assist in generation of special antenna patterns, and in prelimi-

nary qualification of the basic real-time computer complex (RTCC) navigational concepts. An MSFN ranging test revealed that it was feasible for the MSFN stations to range with the spacecraft operating in Modulation Mode 4.

- A bistatic radar mapping experiment was conducted to reflect rf signals off the Moon with the intent of obtaining more information concerning the lunar image.
- An experiment was conducted to obtain additional data to assist in analysis of effects of the earth's ionosphere on doppler and ranging data.

The following events affecting spacecraft operational control occurred during the extended mission.

- MSFN tracked a lunar orbiting spacecraft in two-way lock for the first time.
- Procedures were developed for independently tracking and commanding multiple spacecraft operating within the same radio frequency band.
- A doppler resolver was used which greatly increased the confidence of the received doppler data.
- A Seattle-based team of engineers, used to supplement the regular extended-mission flight operations team, consisted of a group of engineers familiar with the spacecraft's subsystems. By using such a team, it was operationally possible at the SFOF to effectively handle the relatively long MSFN track periods.

In general, all of the spacecraft's subsystems performed satisfactorily during the extended mission. Since solar panel degradation was minimal, there was an adequate power margin at all times, which made it possible to fly the spacecraft off-Sun at large angles (50 to 60 degrees) to provide adequate thermal control.

Although there could have been considerable operational problems in selectively tracking, commanding, and monitoring telemetry from

three different Lunar Orbiter spacecraft, there were essentially no communication problems encountered. Several spurious commands were received by Lunar Orbiter III, due to antenna side-lobe problems, but these commands had no adverse effect on the spacecraft.

The lunar eclipses on April 24, 1967 (GMT Day 114) and October 18, 1967 (GMT Day 291) had considerable impact on the flight plan of Lunar Orbiter III. A phasing maneuver was performed so the spacecraft could successfully

survive the first eclipse. To preclude the risk of losing control of the spacecraft following the second eclipse, the decision was made to impact the spacecraft into the moon prior to the eclipse.

Lunar Orbiter III's extended mission officially terminated following a terminal transfer maneuver that caused the spacecraft to impact the farside of the Moon on October 9, 1967 (GMT Day 282) at a predicted time of 10:27:11 GMT and at an estimated location of 92.70° W longitude and 14.32° N latitude.

2.0 Introduction

This report covers spacecraft control and flight path analysis and control operations conducted during the Lunar Orbiter III extended mission and discusses spacecraft performance during these operations. Complete data packages have been prepared for each experiment and special exercise under separate cover and forwarded via the NASA experiment coordinator to the requestor. The highlights of each special exercise and experiment are summarized herein.

Transition from the photographic mission of Lunar Orbiter III to the extended-mission phase was completed on March 9, 1967 (Day 068). All spacecraft systems were operational — with the exception of the photo subsystem film transport mechanism, which had failed during the prime mission. The spacecraft was in an orbit inclined 21 degrees to the lunar equator with an apolune altitude of 1843 kilometers, a perilune altitude of 56.6 kilometers, and a period of 208.4 minutes. The spacecraft was operating in wide deadzone (2.0 degrees) and pitched off the sunline at minus 50 degrees for thermal relief.

2.1 SPACECRAFT DESCRIPTION

The 853-pound Lunar Orbiter spacecraft is 6.83 feet high, spans 17.1 feet from the tip of the rotatable high-gain dish antenna to the tip of the low-gain antenna, and measures 12.4 feet across the solar panels. Figure 2-1 shows the spacecraft in the flight configuration with all elements fully deployed (the mylar thermal barrier is not shown). Major components are attached to the largest of three deck structures, which are interconnected by a tubular truss network. Thermal control is maintained by controlling emission of internal energy and absorption of solar energy through the use of a special paint covering the bottom side of the deck structure. The entire spacecraft periphery above the large equipment-mounting deck is covered with a highly reflective aluminum-coated mylar shroud, providing an adiabatic thermal barrier. In addition to its structural functions, the tank deck is designed to withstand radiant energy from the velocity control engine to minimize heat losses. Three-

axis stabilization is provided by using the Sun and Canopus as primary angular references, and by a three-axis inertial system when the vehicle is required to operate off celestial references, during maneuvers, or when the Sun and/or Canopus are occulted by the Moon. The spacecraft subsystems are shown in block diagram form in Figure 2-2.

2.2 MISSION OBJECTIVES

The primary objective of the Lunar Orbiter III extended mission was to secure information that may be used to increase the scientific knowledge of the size and shape of the Moon, the properties of its gravitational field, and the lunar environment. Secondary objectives were to conduct special exercises to determine the limits of spacecraft capabilities, develop standard operating procedures, conduct experiments to provide additional scientific data, and explore the use of Lunar Orbiter subsystems for other applications. During the Lunar Orbiter III extended mission the following exercises and experiments were included.

- *Canopus tracker glint mapping test* to determine sensitivity of the star tracker;
- *Maneuver accuracy test* to provide data for postmission error analysis, and IRU and control assembly performance;
- *V/H tracking roll limit test* to establish roll angle limits for V/H sensor tracking;
- *Radar mapping experiment* to investigate methods of obtaining scientific information about the surface of celestial bodies;
- *Transponder threshold test* to determine automatic gain control degradation;
- *Canopus tracker degradation test* to determine star tracker performance;
- *Squib firing interaction test* to collect data relative to interaction with star tracker operation;
- *MSFN/AGNQ support* to qualify Apollo tracking stations;
- *Ionosphere experiment* to determine the effects of the Earth's ionosphere on doppler and ranging data;

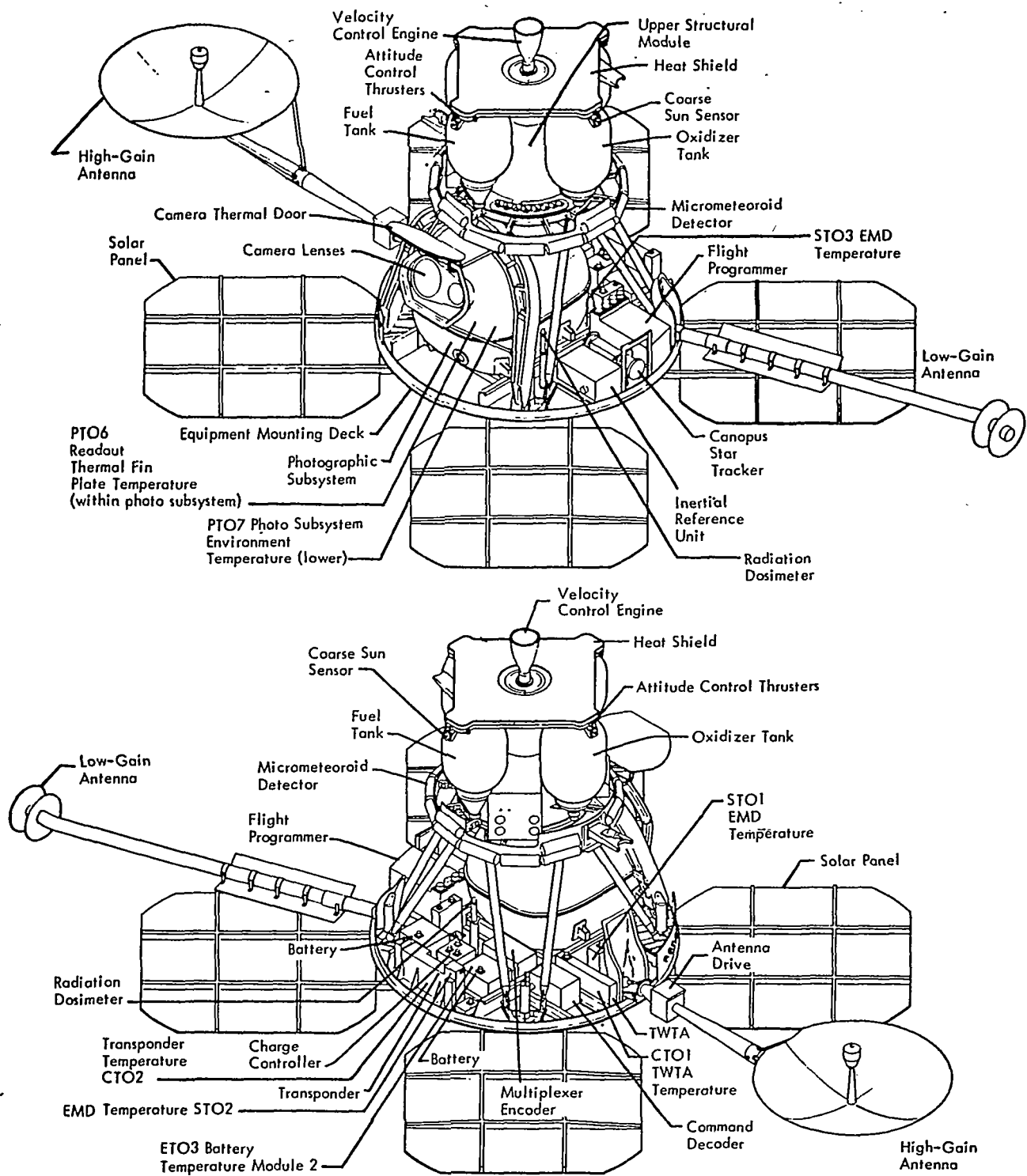


Figure 2-1: Lunar Orbiter Spacecraft

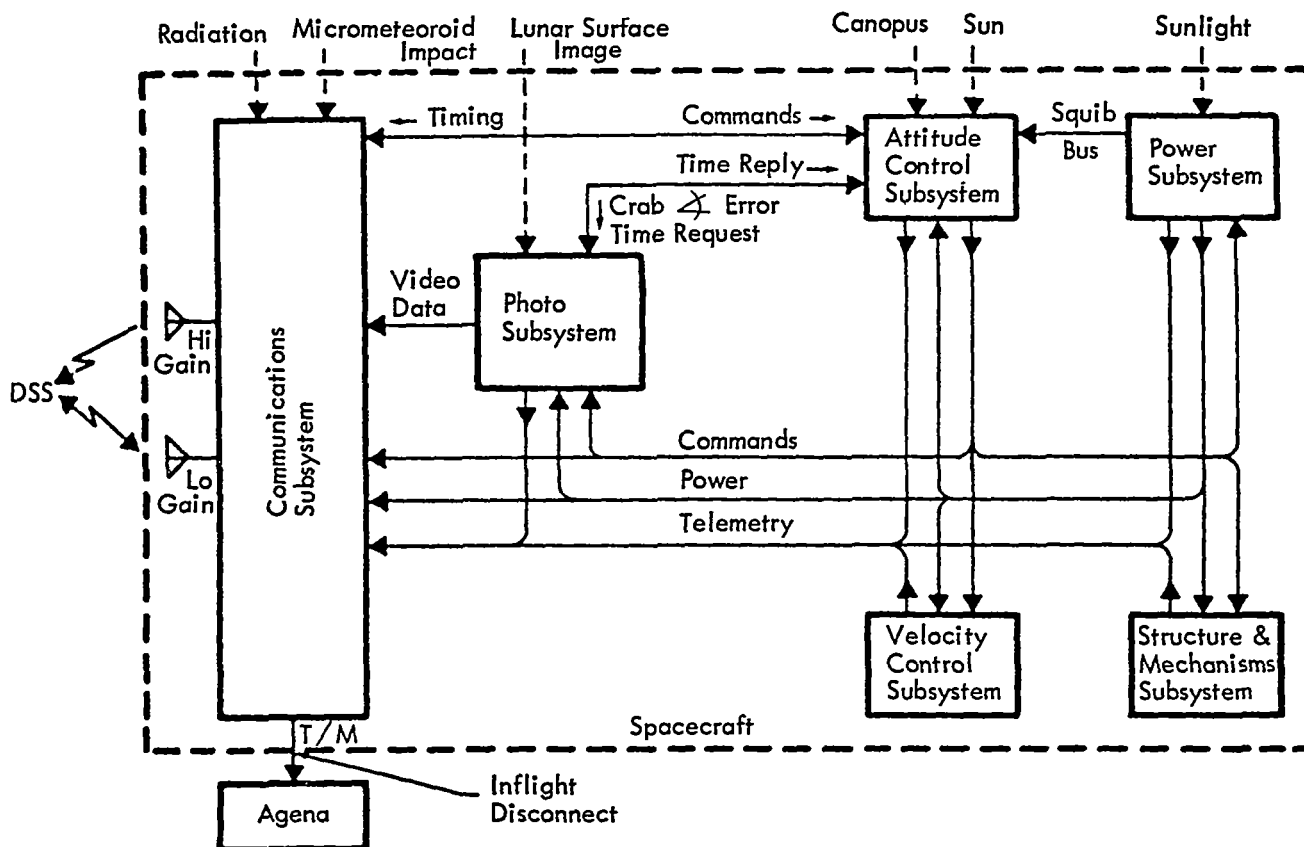


Figure 2-2: Lunar Orbiter Subsystems

- *Canopus tracker glint without earthlight test* to evaluate star tracker operation without earthlight;
- *MSFN ranging test* to determine the feasibility of MSFN ranging with the spacecraft in Mode 4;
- *Side-lobe acquisition test* to determine antenna pointing error for uplink acquisition and loss;
- *Battery discharge tests* to determine operating characteristics under lunar eclipse conditions;
- *Focus adjustment test* to determine if tiger striping could be eliminated by adjusting the line scan tube focus.

A final objective was to impact the spacecraft on the Moon (nearside if possible) prior to the loss of attitude control capability.

2.3 OPERATIONAL ORGANIZATION

The extended mission of Lunar Orbiter III was conducted using a centralized method of control

from the Space Flight Operations Facility at Pasadena, California, that was similar to that adopted for the photographic missions. Primary differences between extended and photographic mission activities are described in the following paragraphs.

Manning at the SFOF and at the DSS's was at a significantly reduced level during the extended mission than during the photographic mission. Manning at the DSS's was reduced by limiting the MDE personnel to the SLOE, assistant SLOE, and MDE systems engineer. During the photographic mission, the additional services of a video engineer, supporting film processing personnel, and telemetry operators were required. Manning at the SFOF was reduced in several areas. NASA mission advisors were no longer required; however, a small NASA scientific team located at the Langley Research Center was available for selenodetic studies and consultation. The mission director also was no longer required at the SFOF, but

available at Langley for key decisions. It was possible to reduce the size of the operational teams because of shorter tracking periods and a decrease in the level of operational activity. For those periods of increased activity such as preparation for and during a velocity maneuver, personnel from Seattle were sent to the SFOF to augment the extended-mission team. During long (but infrequent) tracking periods such as MSFN tracks, which lasted up to 32 hours, the extended-mission team was also augmented by personnel from Seattle.

A list of the manning provided by the contractor at the SFOF for extended-mission tracks is shown below. In addition to these personnel, the space flight operations director and a reduced (from the photographic mission) complement of JPL personnel such as track chief and communications personnel were required

to support the tracking periods.

A. Assistant space flight operations director

B. SPAC

1. Command programmer analyst
2. Attitude control analyst
3. Power/thermal analyst
4. Communications system analyst
5. SPAC software analyst
6. Photo subsystem analyst
7. Command coordinator

C. DACON

Data controller

D. FPAC

1. Flight chief
2. Orbit determination analyst
3. Guidance analyst

3.0 Flight Operations

The Lunar Orbiter III extended-mission period (GMT Days 068 through 282) encompassed many significant milestones of the Lunar Orbiter project. During a portion of this extended mission, three other Lunar Orbiter spacecraft were active. Therefore, the extended-mission flight operations plan underwent evolutionary changes to meet the extended-mission objectives and simultaneously control all extended-mission spacecraft.

The tracking commitment during the first 30 days consisted of a daily track of two consecutive orbits (7 to 11 hours) to be shared by the active spacecraft. In addition, an average of three of the tracking periods per month was extended to approximately 27 hours duration in support of the MSFN. After the first 30-day period, the tracking commitment was reduced to three tracks per week, each 7 to 11 hours long. The experiments and exercises to be accomplished were analyzed in relation to which spacecraft could best satisfy mission requirements. The initial portion of the Lunar Orbiter III extended mission was, therefore, devoted to selenodesy, spacecraft exercises and special experiments in support of Lunar Orbiter IV mission planning, and MSFN support and scientific data acquisition. Additional tasks were later incorporated into the flight operations plan.

A velocity maneuver was performed on April 12 (Day 102) to reduce the period that the spacecraft would be without solar power during the lunar eclipse on April 24, 1967. Also, in preparation for this eclipse, a battery discharge experiment was performed on April 22 (Day 112).

Lunar Orbiter II and III spacecraft were used between April 17 and 21 to develop procedures for tracking multiple spacecraft which operate on the same radio frequency band. Lunar Orbiter III was used as the active spacecraft during an antenna sidelobe acquisition test and as the passive spacecraft during the tests to prove offset frequencies could be employed to prevent interference with the passive space-

craft, and also to provide realistic conditions for flight operations personnel during Mission IV training.

Lunar Orbiter III was placed in the programmer-controlled extended-mission mode for thermal control and monitored at least once each day during the photo portion and the first month of the extended mission of Lunar Orbiter IV. During this period, tracking data was not retained for selenodesy.

A second velocity maneuver was performed prior to the Lunar Orbiter V photographic mission. The twofold purpose was to increase the orbital lifetime to 1 year and to enable a subsequent apolune decrease maneuver to place the spacecraft in an Apollo-type orbit. Following the maneuver, the spacecraft was placed back in the extended-mission mode for thermal control during the Lunar Orbiter V photographic mission. Daily "quick look" monitoring was used to ensure that the spacecraft status was satisfactory.

A third velocity maneuver was performed on August 30 (Day 242), 1967 to reduce the apolune altitude and approximate an Apollo orbit. The month of September was devoted primarily to selenodesy and MSFN/AGNQ support.

Studies were performed to determine whether Lunar Orbiter III could survive the October 18 (Day 291), 1967 lunar eclipse. These studies included another battery discharge test, analysis of attitude control and velocity control capabilities, analysis of power capabilities, orbit phasing and, later, controlled orbit termination. The conclusions led to the decision to design a terminal transfer velocity maneuver which would result in lunar impact on October 9 (Day 282), 1967.

Implementation of the flight plan was detailed in operations directives, which were prepared for each tracking period defining the support requirements and the sequence of events to be followed. The primary considerations used in

preparing these operations directives included:

- Amount of gaseous nitrogen available for attitude control.
- Thermal history and temperature trends.
- Electrical power loads and solar array capability at various off-Sun angles versus thermal trends at those angles.
- Note any unusual trends before they become dangerous.

3.1 SPACECRAFT CONTROL

The Lunar Orbiter III spacecraft was acquired and tracked by the DSN using the operational techniques and frequency predicts that were employed during the prime mission. After spacecraft acquisition, real-time telemetry readout was obtained at the SFOF via high-speed data line and 60-wpm teletype. The telemetry data was processed in real time by IBM 7044/7094 computer(s) and displayed on 100-wpm teletype machines, X-Y plotters, and bulk printers for analysis.

Programmer sequences were generated by the COGL and transmitted to the spacecraft to perform housekeeping functions, experiments, and special exercises. The stored-programmer routines were supplemented by pre-prepared and manually generated real-time commands as operationally required.

During the extended mission of Lunar Orbiter III, Lunar Orbiters II, IV, and V were also in the extended-mission phase. These spacecraft were operated by stored-program maps which automatically updated the Sun reference periodically. When Lunar Orbiter III was designated as the primary spacecraft for a tracking pass, the other spacecraft were also tracked for a brief period during each pass to verify programmer operation and to monitor subsystem status. Likewise, when Lunar Orbiter III was the secondary spacecraft, its status was also checked by quick-look monitoring. Spacecraft control was outlined around the following general rules.

- Minimize gas usage and extend spacecraft life.
- Maintain an acceptable thermal versus power balance.
- Minimize command activity during

periods that might allow interference with other spacecraft.

- Provide maximum safety for all spacecraft.
- Use stored-program commands in lieu of real-time commands whenever possible.
- Maintain the ability to have a controlled lunar impact at the end of the useful spacecraft life.
- Monitor each spacecraft during each scheduled tracking period.

3.1.1 Command Activity

The cruise mode programmer stored sequence consisted of acquiring the Sun reference every 60 hours and pitching minus 50 to 60 degrees for thermal relief. The pitch angles were selected by evaluating gyro drift characteristics and power/thermal requirements for each period of time. As shown in Table 3-1, the cruise program was deviated from to perform activities such as experiments and special exercises.

Real-time commands were employed to supplement stored sequences when the desired spacecraft activity was not sufficiently predictable to be pre-programmed or when a spacecraft reaction had to be evaluated prior to preceding to the next command. Virtually all activity concerned with star acquisitions was accomplished by RTC's due to the possibility of glint interfering with the Canopus star tracker operation. Real-time commands were also used to overstore discrete programmer locations (i.e., rotate the high-gain antenna, cycle the Canopus star tracker on and off, initiate velocity maneuver sequences, as a backup terminate commands for velocity maneuvers, and orient the spacecraft as required by real-time situations). A total of 1080 RTC's and 1473 SPC's were executed during the extended mission.

The communications subsystem, when operating at a received signal strength below the command threshold, can develop bit errors in the address code such that commands addressed to another spacecraft will be accepted and executed. When the DSS antenna is pointed at the prime photo mission spacecraft, the orbital geometry occasionally results in the extended-

Table 3-1: Programmer Core Map Summary

Map Number	Time Transmitted to Spacecraft (day:hr:mn)	Time Span Effectivity (day:hr:mn/day:hr:mn)	Purpose	COGL Run Number
60 Update	068:13:10	068:12:30/069:10:00	Mission IV Canopus star tracker test	068-02
63	069:18:45	069:10:00/069:11:30	Canopus star tracker ON/OFF and thermal control	069-03
64	074:03:36	069:11:30/075:04:14	V/H high-roll-angle test	074-01
65	078:03:25	075:04:14/078:03:15	Radar mapping (Stanford experiment)	078-01
66	081:18:59	078:03:15/082:01:50	Canopus star tracker degradation test	081-01
67	083:09:45	082:01:50/083:10:20	V/H high-roll-angle test	083-01
68	085:19:08	083:10:20/085:18:30	Flight plan (acquire Sun, pitch minus 50 degrees, wait 60 hours, repeat)	085-01
68 Update	095:16:15	085:18:30/099:02:00	Flight plan change (acquire Sun, pitch minus 55 degrees, wait 60 hours, repeat)	095-01
JUMP 017	099:02:00	099:02:00/100:07:07	Reflects real-time "jump" command	098-01
69	101:13:00	100:07:07/101:16:00	Lunar eclipse phasing maneuver and nitrogen isolation squib valve firing.	101-01
69 Update	102:12:40	101:16:00/102:12:58	1) Phasing burn parameter update 2) Update for actual nitrogen isolation squib valve firing 3) Extended-mission flight plan	102-01
70	112:02:45	102:12:58/113:13:54	Battery discharge test	110-02
101-105	113:13:54	113:13:54/113:17:35	Mission IV training	113-01
101 Update	113:17:35	113:17:35/114:08:30	Mission IV training	113-02

Table 3-1 (continued)

Map Number	Time Transmitted to Spacecraft (day:hr:mn)	Time Span Effectivity (day:hr:mn/day:hr:mn)	Purpose	COGL Run Number
71	114:04:54	N/A	Extended-mission flight plan	113-03
JMP 175	114:18:25	114:08:30/160:23:50	1) Readout test 2) Enter flight plan	114-02
JMP014	167:05:26	160:23:50/167:06:00	Reflects real-time "jump" command	167-01
72	168:07:08	167:06:00/180:00:00	Flight plan change (acquire Sun, pitch minus 60 degrees, wait 60 hours, repeat)	171-01
73	196:03:35	180:00:00/196:05:30	Star search for orbit adjust velocity maneuver (perilune increase)	196-01
73Update	197:22:08	196:05:30/198:02:30	Parameter update for velocity maneuver	197-01
74	198:03:10	198:02:30/198:06:00	Restore extended-mission flight plan	197-02
Seq 390 - 394	209:07:21	198:06:00/240:00:00	Telemeter memory prior to Mission V	209-01
75	241:18:00	240:00:00/241:20:00	Star search for orbit adjust velocity maneuver (apolune decrease)	241-01
76	241:23:45	241:20:00/242:01:00	Basic maneuver map for orbit adjust maneuver	241-02
76Update	242:14:52	242:01:00/242:20:00	Parameter update for velocity maneuver	242-01
77	242:21:32	242:20:00/243:00:00	Flight plan change (acquire Sun, pitch minus 58 degrees, wait 60 hours, repeat)	242-02
78	248:23:17	243:00:00/249:00:00	Flight plan change (acquire Sun, pitch minus 52 degrees, wait 60 hours, repeat)	248-01

Table 3-1 (continued)

Map Number	Time Transmitted to Spacecraft (day:hr:mn)	Time Span Effectivity (day:hr:mn/day:hr:mn)	Purpose	COGL Run Number
JMP 017	253:04:58	249:00:00/249:00:00	Reflects real-time command	253-01
79	253:08:57	249:00:00/254:14:00	TWTA on and off for MSFN pass	254-01
JMP 015	256:21:30 258:19:25	254:14:00/254:14:30	Reflects two real-time "jump" commands	256-01
80	259:00:09	254:14:30/263:00:00	TWTA on and off for MSFN pass	258-01
81	264:05:48	263:00:00/270:00:00	TWTA on and off for MSFN pass	262-01
82	274:19:03	270:00:00/277:00:00	Battery discharge test	274-01
83	278:15:02	277:00:00/280:00:00	TWTA on and off for MSFN pass	278-01
84	282:06:08	280:00:00/282:10:22	1) Terminal orbit transfer 2) Post-transfer test sequence	282-04

mission spacecraft acquiring uplink transponder lock on the signal of a side lobe and therefore operating below the command threshold. Although multiple-spacecraft tracking procedures developed after Mission III greatly reduced the number of spurious commands, three such commands were executed by the flight programmer during Mission IV and three more were executed during Mission V. The spurious commands had no detrimental effects on LO III extended-mission operation. However, due to the high probability of more than one bit error occurring, it is likely that the operation code and/or operand of the command message would also be in error and would prevent isolation of the spurious command by examining spacecraft command logs.

3.1.2 Spacecraft Telemetry

A total of 665.6 hours of telemetry data was processed during 170 tracking passes. Table 3-2 contains a summary of the telemetry data by station and includes a listing of the significant activities accomplished during each pass.

Problems encountered — such as minor communications outages and computer internal restarts — were typical of those experienced during the prime missions. Standard work-around methods such as processing TTY data and using raw hexadecimal data were employed to minimize data problems. The communications processor caused the raw TTY data to lag behind real time, which caused frequent deletion of data in order to return to real time, consequently it was not used constantly.

A data and alarm summary containing a majority of the telemetry channels for each frame was processed for all tracking passes to provide a permanent record of the telemetry data.

3.2 FLIGHT PATH CONTROL

Flight path control of the spacecraft during the extended mission is the responsibility of the FPAC portion of the flight team. The functions carried out by this team are identical to those during the primary mission (i.e., tracking data editing, orbit determination, and guidance maneuver calculations). The processes used to

perform these functions are the same as in the prime mission, except that data quantity is less due to decreased tracking time.

3.2.1 Tracking Data Editing

Tracking data editing is the process of monitoring, analyzing, and judging the quality of the doppler and range radar tracking data transmitted to the SFOF from the DSN. The data is provided from three DSN stations — Madrid, Spain (Station 62); Woomera, Australia (Station 41); and Goldstone, California (Station 12) — in three types: continuous-count doppler, ranging units, and antenna pointing angles. The pointing angles were not used due to the small arc traversed by the spacecraft in lunar orbit. Table 3-3 is a summary of the tracking data obtained during the extended mission. Computer programs TDPX and ODGX were used to edit and process the tracking data. Tables 3-3 and 3-4 provide information used for this editing and processing. Table 3-5 contains a list of master file (tracking data) tapes generated by TDPX; both tapes sent to Langley Research Center and those kept in the Jet Propulsion Laboratory tape library are listed.

During this extended mission the DSN ranging subsystems were modified to provide independent ranging data points (Mark 1A system). Prior to the modification, each set of good (not flagged bad) ranging points was one independent data point (Mark 1 system), which provided more usable data points for tracking data editing. Also, a doppler resolver was incorporated into the tracking data message, which increased doppler data accuracy by two significant figures.

3.2.2 Orbit Determination

The computer program ODPL was used to calculate the orbit determinations from the tracking data prepared by the editing programs. The program used a fourth-order spherical harmonic expansion of the lunar potential field. NASA provided the coefficients for this model on November 11, 1966 (see Table 3-6). The following procedure was used.

- Use at least two orbits of doppler data. Both two-way (CC3) and three-way (C3) doppler is to be used with data weights of 0.1 cycle per second.

Table 3-2: Spacecraft Telemetry Summary

Day	Period (GMT)	Deep Space Station	Activities
068	15:00-16:00	62	a) Selenodesy
068	15:00-20:34	12	b) Canopus tracker GLINT mapping test
068/069	21:16-07:00	41	c) Maneuver accuracy test
069	07:44-15:15	62	
069	14:43-23:05	12	
070	00:00-03:55	41	
070	06:10-07:24	41	Quick look
070	23:30-23:50	12	Quick look
072/073	19:33-03:56	12	a) MSFN
072/073	23:20-04:10	41	b) Selenodesy
075	00:04-05:07	12	a) V/H tracking roll angle test
075	01:16-06:04	41	b) Selenodesy
078	01:44-07:35	12	a) Selenodesy
078	05:15-11:06	41	b) Radar mapping experiment
079	07:51-08:00	41	Quick look
079	09:38-09:45	41	Quick look
081	10:17-16:20	41	a) Transponder threshold test
081	14:32-19:52	62	b) Canopus tracker degradation test (start) c) Selenodesy
083	04:16-10:26	12	a) Radar mapping experiment
083	08:11-13:55	41	b) V/H high-roll-angle test c) Selenodesy d) Canopus tracker degradation test

Table 3-2 (continued)

Day	Period (GMT)	Deep Space Station	Activities
085	15:37-21:41	41	a) Canopus tracker degradation test (End)
085/086	19:32-01:23	62	b) MSFN c) Selenodesy
087	10:27-10:52	12	Quick look
089	11:32-11:45	12	Quick look
092	09:53-19:00	12	a) Ionosphere experiment b) Selenodesy
094	04:12-11:25	62	a) Selenodesy b) DSS-51 performance verification
095	08:57-14:14	62	a) Selenodesy
095	12:27-18:45	12	b) MSFN ranging test
097	02:47-02:51	41	Quick look
098	17:11-23:15	12	a) MSFN
098/099	20:40-02:51	41	b) Selenodesy
101	11:34-17:39	62	a) Squib firing interaction test
101/102	15:02-00:37	12	b) Selenodesy c) Ionosphere experiment
102	12:05-21:08	62	a) Solar-eclipse phasing maneuver
102/103	15:50-01:03	12	b) Selenodesy
103	17:26-17:42	62	Quick look
104	10:31-10:49	62	Quick look
106	04:32-04:44	41	Quick look

Table 3-2 (continued)

Day	Period (GMT)	Deep Space Station	Activities
107	07:44-13:09	41	Side-lobe acquisition test
107	11:26-13:05	62	
110	15:26-17:00	62	Quick look
111	12:18-14:15	41	Quick look
112	02:14-08:21	12	a) Battery discharge test b) Selenodesy
113/114	09:30-18:42	ALL	Mission IV training
115/116	23:54-06:10	62	Selenodesy
116	06:37-13:06	12	
120	04:23-04:40	62	Quick look
126	15:09-15:43	62	Quick look
128	00:11-00:23	12	Quick look
129	00:08-00:30	12	Quick look
129	14:34-14:52	12	Quick look
130	15:17-15:28	12	Quick look
132	02:25-02:40	12	Quick look
133	01:56-02:20	41	Quick look
134	03:00-03:30	41	Quick look
135	03:35-04:00	12	Quick look
135	20:38-20:45	62	Quick look
137	23:00-23:15	12	Quick look
138	22:28-22:41	62	Quick look
139	23:25-23:30	12	Quick look

Table 3-2 (continued)

Day	Period (GMT)	Deep Space Station	Activities
141	02:05-02:20	62	Quick look
142	02:11-02:29	62	Quick look
143	02:18-02:32	12	Quick look
144	21:22-21:31	41	Quick look
145	22:25-22:32	41	Quick look
147	14:48-15:01	12	Quick look
149	01:19-01:32	41	Quick look
150	18:40-18:46	12	Quick look
151	18:15-18:35	12	Quick look
152	13:31-13:43	12	Quick look
153	18:37-19:10	41	Quick look
155	14:35-14:50	62	Quick look
156	20:11-20:25	41	Quick look
158	14:00-14:15	12	Quick look
159	22:53-23:10	41	Quick look
164	06:45-07:00	41	Quick look
164	19:51-20:22	12	Quick look
166/167	23:44-00:10	12	Quick look
167	05:17-05:44	12	Quick look
168	07:03-07:32	12	Quick look
169	00:33-00:50	62	Quick look
171	01:52-02:10	12	Quick look
174	00:50-01:06	62	Quick look

Table 3-2 (continued)

Day	Period (GMT)	Deep Space Station	Activities
176	04:32-05:00	62	Quick look
177	04:52-05:22	62	Quick look
178	12:24-12:33	12	Quick look
180	17:31-18:00	12	Quick look
186	13:00-13:55	62	Quick look
188	13:00-19:05	62	Selenodesy
188	13:40-22:34	12	
191	19:15-19:45	12	Quick look
196	02:32-07:20	12	a) Selenodesy
196	03:11-12:03	41	b) Star map
197/198	16:41-00:34	62	a) Orbital lifetime adjust maneuver
197/198	23:39-08:20	12	b) Selenodesy
198	04:52-12:46	41	
202	18:11-20:00	41	Selenodesy
202	20:40-23:35	62	
205	09:53-10:25	12	Quick look
209	06:53-11:00	12	Programmer memory verification
210	09:58-13:31	12	Quick look
215	23:31-23:45	12	Quick look
216	17:21-17:30	62	Quick look
217	22:04-22:25	41	Quick look
219	19:26-19:40	62	Quick look
220	17:31-17:50	12	Quick look

Table 3-2 (continued)

Day	Period (GMT)	Deep Space Station	Activities
221	17:45-17:50	12	Quick look
223	03:02-03:10	41	Quick look
224	20:24-20:45	62	Quick look
226	01:05-01:22	12	Quick look
226	14:16-14:35	41	Quick look
227	18:45-19:10	62	Quick look
228	14:01-14:10	41	Quick look
230	02:15-02:38	62	Quick look
230	19:30-19:40	41	Quick look
232	21:11-21:20	41	Quick look
233	21:00-21:20	62	Quick look
234	21:54-22:05	41	Quick look
235	22:19-22:32	41	Quick look
236	21:40-22:02	62	Quick look
237	22:01-22:25	41	Quick look
239	16:59-17:20	41	Quick look
240	02:46-03:00	62	Quick look
241	17:02-21:01	12	a) Selenodesy
241/242	17:16-02:20	41	b) Star search
242	00:43-05:55	62	
242	13:55-21:45	12	a) Maneuver into Apollo-type orbit
242/243	18:15-03:43	41	b) Selenodesy
243	01:35-06:56	62	

Table 3-2 (continued)

Day	Period (GMT)	Deep Space Station	Activities
244	13:00-13:30	12	Quick look
246/247	23:03-00:27	12	Quick look
248	15:00-19:07	62	Selenodesy
248/249	15:10-00:31	12	
250	12:17-19:52	62	Selenodesy
250	17:35-19:52	12	
253	01:43-04:50	12	Selenodesy
253	02:15-09:22	41	
254	10:10-15:09	41	a) MSFN
254	14:40-22:29	62	b) Selenodesy
254/255	23:15-05:01	12	
255	05:50-15:15	41	
256	14:30-17:06	41	Selenodesy
256/257	16:41-00:40	62	
258	14:31-18:07	41	Selenodesy
258/259	17:44-00:32	62	
261	05:46-13:10	12	a) MSFN
261	08:36-20:17	41	b) Selenodesy
261/262	21:34-02:49	62	
262	03:32-13:28	12	
264	03:35-08:33	62	a) MSFN
624	03:35-13:00	12	b) Selenodesy
264	12:18-20:16	41	

Table 3-2 (continued)

Day	Period (GMT)	Deep Space Station	Activities
264/265	21:18-09:00	62	
267	17:32-20:15	41	Quick look
270	19:20-19:40	12	Quick look
272	18:53-19:35	12	Quick look
273	01:54-02:00	41	Quick look
274	12:30-15:34	62	a) Selenodesy
274	16:53-23:53	12	b) Battery discharge test
274/275	21:11-00:41	41	
275	21:31-22:16	12	Quick look
276	23:23-24:00	41	Quick look
277	17:37-17:58	62	Quick look
278	08:41-18:17	62	a) MSFN
278/279	16:59-02:25	12	b) Selenodesy
278/279	22:27-11:00	41	
281/282	22:01-04:30	12	a) Terminal transfer maneuver
282	01:41-09:39	41	b) Selenodesy

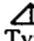
Table 3-3: Tracking Data Summary

Day of Pass	Sta	Doppler					Ranging					*Syn-freq.
		Δ Type	Start Time	Stop Time	Amount (hrs)	Trans-mitter-on time	Start Time	Stop Time	Amount (hrs)	Sta Delay	Trans-ponder Temp. (°F)	
069	62	CC3	07:47	11:14	5.35	07:47	08:32	13:58	3.84	295	62	5700
		CC3	11:14	13:58		07:47						5720
		C3	14:45	15:13	.48							5740
069	12	CC3	14:45	20:55	3.60	14:45	14:46	16:40	1.90	306	67	5690
		C3	21:43	23:00	1.24							5690
069/70	41	CC3	21:42	07:12	6.42	21:42	21:53	03:55	5.16	302	64	5730
072/3	12	CC3	19:35	23:02	6.05	19:35						5710
		CC3	23:02	01:38								5730
		C3	02:43	03:56	1.22							5660
072/3	41	C3	23:21	01:38	2.30							5680
		CC3	02:43	04:09	1.42	02:43						5700
075	12	CC3	00:30	01:17	.62	00:30						5710
		C3	01:50	03:35	1.64							5710
		C3	03:35	05:08								5720
075	41	C3	01:17	01:24	.12		02:20	04:34	.64	287	74	5670
		C3	05:04	06:02	.94							5690
		CC3	01:33	03:35	1.86	01:33						5670
078	12	CC3	03:35	04:54		01:33						5690
		CC3	01:46	05:10	4.26	01:46						5690
078	41	CC3	05:10	07:34		01:46						5700
		C3	05:15	07:35	2.34							5660
081	41	CC3	08:45	11:05	2.34	08:45	10:29	12:50	2.34	300	68	5680
		CC3	10:22	13:47	4.66	10:22						5650
081	62	CC3	13:47	16:20		10:22						5670
		C3	14:45	16:20	1.58							5630
		CC3	17:18	19:38	2.25	17:18						5640

Δ Two Way = CC3
Three Way = C3


*SYNFREQ=204XXXX.0

Table 3-3 (continued)

Day of Pass	Sta	Doppler					Ranging					*Syn-freq
		 Type	Start Time	Stop Time	Amount (hrs)	Trans-mitter-on time	Start Time	Stop Time	Amount (hrs)	Sta Delay	Trans-ponder Temp. (°F)	
083	12	CC3	04:31	07:45	5.04	04:31						5640
		CC3	07:45	10:25		04:31						5660
083	41	C3	08:10	10:23	2.22							5640
		CC3	11:18	13:53	2.58	11:18						5640
085	41	CC3	15:39	19:05	4.52	15:39						5700
		CC3	19:05	20:55		15:39						5670
		C3	21:04	21:40	.60							5670
085	62	C3	19:38	21:03	1.44							5630
085/6	62	CC3	21:04	22:35	3.46	21:04						5630
		CC3	22:35	01:20		21:04						5640
092	12	CC3	10:12	14:45	6.80	10:12	10:18	19:00	6.36	300	82	5680
		CC3	14:45	18:14		10:12						5700
		CC3	18:14	19:00		10:12						5640
095	62	CC3	09:00	11:47	2.78	09:00						5710
		C3	12:51	14:13	1.14							5680
095	12	CC3	12:29	15:55	5.42	12:29	17:30	18:45	1.02	298	86	5690
		CC3	15:55	18:45		12:29						5710
098	12	CC3	17:13	20:39	5.12	17:13						5710
		CC3	20:39	23:20		17:13						5730
098	41	C3	20:43	23:20	2.46							5690
099	41	CC3	00:12	02:51	2.65	00:12						5710
101	62	CC3	11:38	14:08	2.76	11:38	11:47	12:55	1.24	260	68	5710
101	62	C3	15:11	17:38	2.45							5720
101/2	12	CC3	15:11	18:35	7.34	15:11	15:15	00:29	5.08	310	76	5680
		CC3	18:35	22:05		15:11						5700
		CC3	22:05	00:29		15:11						5720

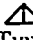
*SYNFREQ=204XXXX.0

Table 3-3 (continued)

Day of Pass	Sta	Doppler					Ranging					*Syn- freq.
		 Type	Start Time	Stop Time	Amount (hrs)	Trans- mitter- on time	Start Time	Stop Time	Amount (hrs)	Sta Delay	Trans- ponder Temp. (°F)	
102	62	CC3	12:08	15:54	2.75	12:08	12:15	14:03	1.80	265	74	5720
		C3	16:04	16:50	↑ 3.90							5720
		C3	16:50	21:07	↓							5810
102	12	C3	15:52	15:56	.06							5680
102/3	12	CC3	16:04	16:51	↑	16:04	16:20	00:45	3.46	282	62	5680
		CC3	16:51	19:05	↓ 6.84	16:04						5770
		CC3	19:05	22:34	↓	16:04						5680
		CC3	22:34	01:02		16:04						5710
107	41	CC3	07:44	09:40	1.94	07:44	08:07	09:40	1.55	299	58	5670
111	41	CC3	13:13	14:15	1.04	13:13						5620
112	12	CC3	02:20	05:42		02:20						5630
			05:42	08:13	4.28	02:20						5650
113	41	CC3	09:31	12:55	↑	09:31						5620
		CC3	12:55	16:23	↓ 7.70	09:31						5640
		CC3	16:23	18:48	↓	09:31						5670
		C3	18:50	19:52								6090
		C3	19:52	20:18	.68							5970
113	62	C3	18:20	18:48	.46							5710
		CC3	18:57	19:52		18:57						6130
113/4	62	CC3	19:52	23:20	5.42	18:57						5980
		CC3	23:20	02:04		18:57						6000
114	62	C3	02:51	05:00	1.34							5230
114	12	CC3	02:50	06:42		02:50						5190
		CC3	06:42	09:00	5.14	02:50						5210


*SYNFREQ = 204XXXX.0

Table 3-3 (continued)

Day of Pass	Sta	Doppler					Ranging					*Syn-freq.
		 Type	Start Time	Stop Time	Amount (hrs)	Trans-mitter-on Time	Start Time	Stop Time	Amount (hrs)	Sta Delay	Trans-ponder Temp (°F)	
114	41	C3	08:43	09:00	.28							5710
		CC3	09:54	13:12	↑	09:54						5190
		CC3	13:12	16:40	5.04	09:54						5210
		CC3	16:40	18:43	↓	09:54						5325
115/6	62	CC3	23:54	00:41	↑	23:54						6080
		CC3	00:41	01:07	4.54	23:54						5722
		CC3	01:07	03:26	↓	23:54						5800
		CC3	03:26	05:20	↓	23:54						5680
116	62	C3	05:21	06:09	.80							6100
116	12	C3	04:35	05:13	.64							5700
		CC3	05:23	06:49	↑	05:23						6120
		CC3	06:49	07:08	6.25	05:23						6170
		CC3	07:08	10:17	↓	05:23						6070
		CC3	10:17	13:06	↓	05:23						6090
188	62	CC3	13:11	16:35	4.55	13:11	16:52	19:04	2.20	302	72	5200
		CC3	16:35	19:04		13:11						5300
188	12	C3	13:57	16:34	4.08							5200
		C3	16:34	19:04								5300
188	12	CC3	20:10	22:24	2.24	20:10						5300
196	12	CC3	02:34	03:30	2.34	02:34						5200
		CC3	03:30	05:05		02:34						5300
196	12	C3	06:30	07:20	.84							5300
196	41	C3	03:10	03:30	1.92							5200
		C3	03:30	05:05								5300
		CC3	06:15	09:31	↑	06:15						5300
		CC3	09:31	10:50	4.78	06:15						5200
		CC3	10:50	12:03	↓	06:15						5300


*SYNFREQ = 204XXXX.0

Table 3-3 (continued)

Day of Pass	Sta	Doppler					Ranging					*Syn-freq
		 Type	Start Time	Stop Time	Amount (hrs)	Trans-mitter-on time	Start Time	Stop Time	Amount (hrs)	Sta Delay	Trans-ponder Temp. (°F)	
197	62	CC3	16:47	22:50	5.22	16:47	17:20	21:50	2.86	287	80	5300
197/8	62	C3	23:40	00:33	.88							5200
197/8	12	CC3	23:40	04:09		23:40						5600
		CC3	04:09	05:54	5.38	23:40						5300
198	12	C3	06:42	08:20	1.64							5300
198	41	C3	04:51	05:53	1.04							5300
		CC3	06:40	12:40	5.25	06:40						5300
241	12	CC3	17:04	19:13	2.14	17:04						5300
		C3	20:18	21:00	.72							5300
241	41	C3	17:20	19:13	1.92		20:20	20:30	.16	308	72	5300
241/2	41	CC3	20:10	02:20	5.12	20:10	00:50	01:48	.96	308	100	5300
242	62	C3	00:43	02:20	1.62							5300
		CC3	03:18	05:53	2.62	03:18	04:30	05:04	.56	N/A	98	5300
242	12	CC3	13:58	19:02		13:58						5300
		CC3	19:02	20:00	4.94	13:58						5608
		C3	20:53	21:45	.86							5600
242	41	C3	18:15	19:02								5300
		C3	19:02	20:00	1.50							5568
242/3	41	CC3	20:53	02:33	4.05	20:53	21:03	21:30	.45	303	88	5600
243	41	C3	03:27	03:53	.44							5600
243	62	C3	01:37	02:33	.94							5600
		CC3	03:28	06:47	2.42	03:28						5600
248	62	CC3	15:05	17:55	1.95	15:05						5570
		C3	18:50	19:07	.28							5570
248	12	C3	15:23	17:55	1.68							5570
248/9	12	CC3	18:50	00:30	4.00	18:50	21:12	22:18	1.10	280	58	5570

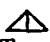
*SYNFREQ = 204XXXX.0

Table 3-3 (continued)

Day of Pass	Sta	Doppler					Ranging					*Syn- freq
		 Type	Start Time	Stop Time	Amount (hrs)	Trans- mitter - on time	Start Time	Stop Time	Amount (hrs)	Sta Delay	Trans- ponder Temp. (°F)	
250	62	CC3	12:20	19:43	4.80	12:20						5570
250	12	C3	17:36	19:43	1.30							5570
253	41	CC3	02:20	09:17	3.75	02:20	03:55	04:50	.54	245	60	5570
253	12	C3	02:20	04:50	1.50							5570
254	41	CC3	10:12	13:44	2.64	10:12						5570
		C3	14:43	15:08	.42							5690
254	62	CC3	14:48	21:30	3.75	14:48	15:12	19:53	2.15	282	72	5570
		C3	21:31	22:30	.98							5570
254	12	CC3	23:30	24:00	.50	23:30						5570
255	12	C3	00:05	05:00	3.86							5570
255	41	C3	05:50	13:46	4.58							5570
		CC3	14:35	15:15	.66	14:35						5570
256	41	CC3	15:13	15:58	.75	15:13						5690
		C3	16:43	17:05	.30							5690
256/7	62	CC3	16:46	00:25	4.16	16:46	21:35	00:25	1.35	291	78	5690
258	41	CC3	14:35	18:06	2.70	14:35	15:05	18:05	2.08	306	76	5690
258	62	C3	17:53	18:07	.24							5690
258/9	62	CC3	18:55	23:25	4.20	18:55	19:30	22:28	1.66	288	76	5690
		CC3	23:25	00:44		18:55						5400
261	12	CC3	05:47	09:23	2.84	05:47						5690
		C3	10:12	13:38	2.44							5690
261	41	C3	08:37	09:22	.75							5690
		CC3	10:12	15:55	4.14	10:12	15:15	15:55	.66	309	74	5690
		C3	16:55	17:40	.75							5690
		C3	19:48	20:16	.46							5690

*SYNFREQ=204XXXX.0

Table 3-3 (continued)

Day of Pass		Sta	Doppler				Ranging					*Syn-freq
			 Type	Start Time	Stop Time	Amount (hrs)	Trans-mitter-on time	Start Time	Stop Time	Amount (hrs)	Sta Delay	
261/2	62	CC3	21:06	21:19	.22	21:06						5400
		CC3	23:18	23:34	.26	23:18						5400
		C3	21:23	22:28	1.08							5400
		C3	23:38	02:50	2.16							5400
262	12	C3	03:40	09:22	3.02							5690
		CC3	10:09	13:28	2.58	10:09						5690
264	12	CC3	03:27	11:32	5.12	03:07	08:40	09:20	.66	310		5690
		C3	12:20	13:00	.66							5690
264	62	C3	03:27	07:10	2.46							5690
264	41	CC3	11:27	13:00	.75	11:27						5690
		C3	13:06	13:45	.65							5690
274	12	CC3	16:55	18:59	3.50	16:55						5800
		CC3	18:59	22:29		16:55						5640
		C3	23:26	23:52	.34							5640
274	41	C3	19:42	22:29	1.84							5640
274/5	41	CC3	23:26	00:40	1.24	23:26						5640
278	62	C3	08:44	13:55	3.25							5690
		CC3	14:43	16:05	1.36	14:43						5640
		C3	17:02	18:16	1.24							5640
278	12	CC3	17:02	22:39	3.08	17:02						5640
278/9	12	C3	23:35	00:25	.68							5640
278	41	C3	22:28	22:39	.18							5640
278/9	41	CC3	23:33	00:20	.78	23:33	23:40	00:20	.66	311		5640
279	41	C3	00:27	11:00	5.75							5640
281/2	12	CC3	22:03	03:05	3.34	22:03						5640
282	12	C3	03:56	04:29	.55							5640
282	41	C3	01:40	03:05	1.42							5640
		CC3	03:56	09:40	4.08	03:56						5640

*SYNFREQ = 204XXXX.0

Table 3-4: Station Timing Synchronization

		<u>Day Time (GMT)</u>		<u>Station Number</u>		<u>Timing Bias*</u>	
039	00:00	62	-780.	129	17:26	62	+379.6
039	00:00	41	+350.	130	23:40	41	+762.3
125	20:46	41	+768.9	131	00:32	41	+780.9
126	14:22	62	+307.5	156	00:00	41	+834.
126	21:20	41	+756.1	156	00:01	62	+812.0
127	06:14	41	+365.3	161	00:01	62	+859.0
127	14:20	62	+321.4	164	20:48	62	+865.0
129	06:20	41	+384.2	242	00:00	41	+255.3
				264	00:00	62	+612.4

*Deviation from DSS-12's clock in microseconds.

Table 3-5: Master File—Tracking Data Tapes

<u>Time Interval</u>		<u>Langley</u>	<u>JPL</u>
		<u>Tape</u>	<u>Tape</u>
<u>Start Time</u>	<u>Stop Time</u>	<u>Number</u>	<u>Number</u>
GMT/Day	GMT/Day		
07:47/069	06:02/075	LT327	8447,8850
07:47/069	01:21/086	LT328	8447,8850
07:47/069	18:06/102	LT329	8447,8850
16:30/102	15:58/114	LT330	8889,11291
16:30/102	13:06/116	LT331	8889,11291
16:30/102	12:45/198	LT332	8889,11291
16:30/102	17:42/261	LT333	8889,11291
16:30/102	04:26/279	LT335	8889,11291
16:30/102	10:36/282	LT336	8889,11291

- Each data arc is to consist of doppler data from at least two different stations.
- Range units are to be calculated for visual assistance of the determination.
- First determine a solution estimating only state vector and doppler bias, and then eight or ten high-order harmonic co-

Table 3-6: Lunar Harmonic Coefficients

(LRC 11/11)	
GM = 4902.58	C33 = +0.0091 E-4
J40 = -0.209 E-4	S21 = -0.411 E-4
C41 = -0.051 E-4	S22 = -0.058 E-4
C42 = +0.028 E-4	S33 = -0.033 E-4
C44 = +0.00094 E-4	J30 = -0.446 E-4
S41 = -0.102 E-4	C31 = +0.435 E-4
S42 = -0.083 E-4	C32 = -0.052 E-4
S44 = +0.0017 E-4	C43 = -0.0047 E-4
J20 = +2.07 E-4	S31 = +0.107 E-4
C21 = +0.088 E-4	S32 = +0.0187 E-4
C22 = +0.276 E-4	S43 = -0.026 E-4

efficients are to be added to the list of estimated items.

- True anomaly of spacecraft at epoch as close to 180 degrees (apolune) as possible.

The Keplerian state vectors resulting from the extended-mission orbit determinations are contained in Table 3-7. Table 3-8 describes the

tracking data and statistics used for the orbit determinations. Perilune altitude and orbit inclination change history are displayed in Figures 3-1 and 3-2, respectively.

3.2.3 Guidance Maneuvers

3.2.3.1 Orbit Phasing Maneuver for April 1967 Eclipse

Preliminary analysis of the LO III premaneuver orbit indicated that the spacecraft would be in total darkness over 4 hours during the lunar eclipse on April 24, 1967. Graphical techniques verified by FPAC computer programs were used

to determine the sequence of events during eclipse passage which would minimize time spent in total darkness.

To compute the phasing maneuver, it was necessary to choose a reference time as a targeting parameter in the maneuver design program. The reference epoch (Day 114, 11:29 GMT) was chosen as the time of apoapsis passage during the eclipse which, if satisfied, would establish the proper phasing for optimum lighting. The maneuver design (Table 3-9) was accomplished using orbit determination solution OD 6019-8. Using this state vector, the epoch of apoapsis passage (corresponding to the reference epoch)

Table 3-7: Orbital Elements (Selenographic, True of Date)

OD	Epoch (GMT) (Day:Hr:Mn:Sc)	a(km)	e	w (deg)	Ω (deg)	i (deg)	Tp(sec)
6000-8	055:04:10:00	2688.08	0.331948	185.553	103.9920	20.8158	5799.32
6001-8	058:05:10:00	2688.27	0.333210	187.620	62.4747	20.8394	-6224.32
6002-8	060:02:20:00	2687.78	0.336335	188.854	36.9206	20.8777	5999.27
6003-8	062:03:00:00	2688.52	0.338662	191.456	9.2300	20.9557	6085.97
6004-8	065:03:50:00	2688.41	0.336810	194.639	328.0800	21.1262	5609.34
6005-8	066:11:00:00	2688.24	0.335080	196.456	309.9120	21.0170	5237.20
6006-8	067:04:35:00	2688.25	0.334052	197.048	300.0120	21.0570	6000.28
6007-8	067:15:00:00	2688.21	0.333438	197.735	293.8130	21.0300	5978.49
6008-8	068:11:45:00	2688.13	0.332356	198.648	281.9110	21.0529	5635.39
6009-8	072:19:35:00	2688.59	0.330453	201.713	222.6000	21.2102	4249.74
6010-8	075:01:45:00	2689.00	0.332500	*	*	*	*
6011-8	078:01:45:00	2688.36	0.333972	204.410	152.2940	21.0272	-4330.20
6012-8	081:10:20:00	2688.50	0.331367	206.960	106.7370	21.0021	-1925.83
6013-8	083:05:10:00	2688.52	0.329774	208.676	82.0277	21.0402	2183.11
6014-8	085:16:30:00	2688.70	0.329996	209.714	48.7475	20.9354	3174.52
6015-8	092:10:10:00	2688.11	0.336877	218.524	315.2070	20.6894	-2735.53

Table 3-7 (continued)

OD	Epoch (GMT) (Day:Hr:Mn:Sc)	a(km)	e	w (deg)	Ω (deg)	i (deg)	Tp (sec)
6016-8	095:09:00:00	2687.68	0.333845	221.417	275.256	21.0926	2084.54
6017-8	098:17:10:00	2688.87	0.330260	224.202	229.242	21.2537	3016.03
6018-8	101:11:40:00	2688.61	0.330323	224.833	192.192	21.1628	4784.83
6019-8	101:11:40:00	2688.47	0.330358	224.942	192.083	21.2902	4784.60
7000-8	102:19:05:00	2680.00	0.329300	*	*	*	*
7001-8	113:10:45:00	2679.61	0.327492	233.029	30.659	21.0230	4460.60
7002-8	116:01:00:00	2680.20	0.331630	235.216	355.334	21.2972	4480.84
7003-8	188:13:05:00	2680.35	0.329598	299.194	83.149	21.0286	-6217.97
7004-8	196:04:00:00	2679.97	0.328770	304.732	340.081	21.1047	4786.69
8000-8	198:01:22:00	2721.65	0.308818	305.739	314.289	21.0138	-6333.61
8001-8	241:17:10:00	2721.82	0.306775	341.515	79.730	20.8920	-6228.18
9001-8	242:20:55:00	1968.12	0.043475	354.311	63.932	20.8839	-3599.66
9002-8	248:15:05:00	1968.46	0.049304	348.760	344.051	21.1622	614.498
9003-8	250:12:21:00	1967.75	0.050217	350.045	317.692	21.1532	- 879.887
9004-8	253:02:18:00	*	*	*	*	*	*
9005-8	254:10:30:00	1968.12	0.052269	355.078	261.316	21.2365	1314.13
9006-8	256:16:50:00	1967.57	0.055826	3.169	228.929	21.3340	1015.34
9007-8	258:14:35:00	1967.83	0.057866	10.373	202.209	21.4803	1140.27
9008-8	261:06:00:00	1967.57	0.059062	21.235	165.382	21.3139	2156.11
9009-8	264:03:37:32	1968.13	0.062018	29.530	123.947	20.8215	2092.87
9010-8	274:16:55:00	1967.52	0.055996	31.072	335.664	21.0999	-2197.34
9011-8	278:14:45:00	1968.37	0.053903	35.206	280.007	21.0725	-1140.91
9012-8	281:22:00:00	1967.92	0.059631	40.591	233.378	21.1076	2188.43

*Results known to be erroneous because of data problems.

Table 3-8: Orbit Determination Data Summary

OD	Station	Data* Type	Start Time (GMT) Day: Hr: Mn	End Time (GMT) Day: Hr: Mn	Number of Points	Standard Deviation
6000-8	62	C3	055:04:10	055:04:54	42	0.223
	62	C3	055:18:03	055:18:48	45	0.197
	12	CC3	055:04:11	055:11:54	333	0.148
	41	C3	055:09:58	055:11:54	116	0.146
	41	CC3	055:12:48	055:18:48	307	0.157
6001-8	62	CC3	058:05:15	058:06:19	55	0.176
	12	CC3	058:07:04	058:13:17	318	0.322
	12	C3	058:14:04	058:16:04	112	0.252
	41	CC3	058:14:00	058:19:09	249	0.497
6002-8	62	CC3	060:02:20	060:07:08	203	0.476
	62	C3	060:07:50	060:08:57	37	0.314
	12	CC3	060:07:49	060:14:06	298	0.346
	41	CC3	060:14:46	060:16:19	68	0.261
6003-8	62	CC3	062:03:00	062:09:09	262	0.185
	62	C3	062:09:17	062:10:22	41	0.0642
	12	CC3	062:09:18	062:16:59	382	0.157
6004-8	41	CC3	065:03:50	065:04:53	61	0.0358
	41	C3	065:05:03	065:05:20	18	0.0660
	62	C3	065:04:45	065:04:53	9	0.0391
	62	CC3	065:05:03	065:12:29	341	0.0987
	12	CC3	065:13:10	065:17:47	231	0.0831
6005-8	62	CC3	066:11:00	066:12:51	89	0.186
	62	C3	066:13:34	066:14:14	33	0.0859

*CC3 = two-way doppler, C3 = three-way doppler.

Table 3-8 (continued)

OD	Station	Data* Type	Start Time (GMT) Day:Hr:Mn	End Time (GMT) Day:Hr.:Mn	Number of Points	Standard Deviation
6005-8 (cont)	12	CC3	066:13:33	066:19:50	326	0.141
	12	C3	066:20:36	066:22:09	88	0.0618
	41	CC3	066:20:30	067:01:58	256	0.159
6006-8	41	CC3	067:04:35	067:06:11	85	0.157
	62	CC3	067:06:59	067:13:13	305	0.133
	62	C3	067:13:59	067:15:18	51	0.142
	12	CC3	067:13:58	067:18:29	228	0.147
6007-8	62	C3	067:15:00	067:15:18	14	0.019
	12	CC3	067:15:00	067:20:11	266	0.196
	12	C3	067:20:58	067:23:29	86	0.092
	41	CC3	067:20:53	068:05:58	408	0.139
	41	RU	067:21:00	068:05:05	119	18.900
6008-8	62	CC3	068:11:45	068:13:35	92	0.220
	62	C3	068:14:21	068:15:58	85	0.181
	12	CC3	068:14:20	068:20:32	317	0.219
	41	CC3	068:21:19	069:01:49	196	0.226
6009-8	12	CC3	072:19:35	073:01:38	308	0.112
	12	C3	073:02:43	073:03:54	64	0.0564
	41	C3	072:23:24	073:01:38	122	0.121
	41	CC3	073:02:43	073:04:08	83	0.0346
6010-8	41	CC3	075:01:48	075:04:53	84	0.259
	12	C3	075:01:49	075:04:53	92	0.245

Table 3-8 (continued)

OD	Station	Data Type	Start Time (GMT) Day:Hr:Mn	End Time (GMT) Day:Hr:Mn	Number of Points	Standard Deviation
6011-8	12	CC3	078:01:46	078:07:33	227	0.219
	41	C3	078:05:16	078:07:33	135	0.240
	41	CC3	078:08:45	078:11:04	139	0.209
6012-8	41	CC3	081:10:21	081:16:19	237	0.123
	62	C3	081:14:51	081:16:19	84	0.140
	62	CC3	081:17:24	081:19:37	112	0.129
6013-8	12	CC3	083:05:10	083:10:24	253	0.0830
	41	C3	083:08:13	083:10:23	124	0.150
	41	CC3	083:11:18	083:13:53	150	0.0955
6014-8	41	CC3	085:16:30	085:20:53	197	0.0714
	62	C3	085:19:38	085:20:53	67	0.0594
	62	CC3	085:21:05	086:01:15	183	0.0856
6015-8	12	CC3	092:10:13	092:18:59	405	0.453
6016-8	62	CC3	095:09:00	095:11:43	137	0.1160
	62	C3	095:12:55	095:14:11	33	0.0918
	12	CC3	095:12:31	095:18:44	285	0.2190
6017-8	12	CC3	098:17:13	098:23:20	272	0.0948
	41	C3	098:20:50	098:23:20	123	0.0990
	41	CC3	098:23:43	099:01:39	79	0.0496
6018-8	62	CC3	101:11:40	101:14:08	144	0.254
	62	C3	101:15:11	101:17:37	128	0.251
	12	CC3	101:15:11	101:21:07	275	0.477

Table 3-8 (continued)

OD	Station	Data Type	Start Time (GMT) Day: Hr: Mn	End Time (GMT) Day: Hr: Mn	Number of Points	Standard Deviation
6019-8	62	CC3	101:11:40	101:14:08	144	0.288
	62	C3	101:15:11	101:17:37	128	0.230
	12	CC3	101:15:11	102:00:28	414	0.251
7000-8	62	C3	102:19:07	102:21:06	103	0.610
	12	CC3	102:19:07	103:01:01	272	1.100
7001-8	41	CC3	113:10:45	113:18:41	354	0.125
	62	C3	113:18:21	113:18:37	17	0.0333
	62	CC3	113:18:57	113:22:29	134	0.124
7002-8	62	CC3	116:01:00	116:05:09	161	0.0712
	62	C3	116:05:25	116:06:08	37	0.0594
	12	C3	116:04:35	116:05:09	35	0.0404
	12	CC3	116:05:25	116:13:09	354	0.0756
7003-8	62	CC3	188:13:13	188:19:03	204	0.0283
	12	C3	188:13:57	188:19:03	156	0.0371
	12	CC3	188:20:10	188:22:32	98	0.0242
7004-8	12	CC3	196:04:04	196:05:04	59	0.0117
	12	C3	196:06:31	196:07:19	49	0.0218
	41	C3	196:04:00	196:05:04	64	0.0201
	41	CC3	196:06:31	196:12:02	231	0.0399
8000-8	12	CC3	198:01:26	198:05:45	174	0.0432
	12	C3	198:07:01	198:08:19	79	0.0304
	41	C3	198:04:53	198:05:44	52	0.0281
	41	CC3	198:07:03	198:12:39	222	0.0439

Table 3-8 (continued)

OD	Station	Data Type	Start Time (GMT) Day: Hr: Mn	End Time (GMT) Day: Hr: Mn	Number of Points	Standard Deviation
8001-8	12	CC3	241:17:10	241:19:12	123	0.209
	12	C3	241:20:18	241:21:00	41	0.0425
	41	C3	241:17:19	241:19:12	114	0.218
	41	CC3	241:20:12	242:02:18	289	0.188
	62	C3	242:00:44	242:02:19	92	0.240
9001-8	41	CC3	242:20:56	243:02:32	225	0.246
	41	RU	242:21:02	242:21:28	24	7.80
	41	C3	243:03:28	243:03:42	11	0.178
	62	C3	243:01:37	243:02:32	44	0.218
	62	CC3	243:03:28	243:06:32	119	0.322
	12	C3	242:20:55	242:21:44	44	0.234
9002-8	62	CC3	248:15:06	248:17:56	112	0.220
	62	C3	248:18:50	248:19:06	17	0.136
	12	C3	248:15:23	248:17:56	82	0.192
	12	CC3	248:18:50	249:00:29	214	0.193
	12	RU	248:21:12	248:22:19	65	9.57
9003-8	62	CC3	250:12:21	250:19:42	249	0.251
	12	C3	250:17:36	250:19:46	74	0.255
9004-8	12	C3	253:02:18	253:04:48	70	1.20
	41	CC3	253:02:20	253:09:21	193	2.33
9005-8	41	CC3	254:10:30	254:13:43	126	0.205
	41	C3	254:14:49	254:15:07	17	0.261
	62	CC3	254:14:49	254:21:23	214	0.191

Table 3-8 (continued)

OD	Station	Data Type	Start Time (GMT) Day: Hr: Mn	End Time (GMT) Day: Hr: Mn	Number of Points	Standard Deviation
9006-8	41	C3	256:16:50	256:17:03	14	0.0877
	62	CC3	256:16:50	257:00:24	235	0.0936
9007-8	41	CC3	258:14:35	258:18:06	162	0.185
	62	C3	258:17:52	258:18:06	13	0.156
	62	CC3	258:18:55	259:00:31	235	0.218
9008-8	12	CC3	261:06:00	261:09:21	138	0.147
	12	C3	261:10:12	261:13:08	117	0.117
	41	C3	261:08:37	261:09:21	43	0.122
	41	CC3	261:10:12	261:15:54	234	0.129
9009-8	62	C3	264:03:38	264:07:09	125	0.142
	12	CC3	264:03:38	264:11:31	287	0.152
	12	C3	264:12:20	264:11:58	39	0.116
	41	CC3	264:12:20	264:12:59	36	0.112
9010-8	12	CC3	274:16:55	274:22:28	194	0.220
	12	C3	274:23:26	274:23:51	19	0.119
	41	C3	274:19:41	274:22:28	98	0.236
	41	CC3	274:23:26	275:00:39	63	0.214
9011-8	62	CC3	278:14:45	278:16:04	78	0.477
	62	C3	278:17:07	278:18:15	63	0.407
	12	CC3	278:17:01	278:22:36	216	0.411
	12	C3	278:23:35	279:00:24	35	0.489
	41	C3	278:22:28	278:22:38	9	0.0937
	41	CC3	278:23:34	279:00:19	45	0.458

Table 3-8 (continued)

OD	Station	Data Type	Start Time (GMT) Day:Hr:Mn	End Time (GMT) Day:Hr:Mn	Number of Points	Standard Deviation
9012-8	12	CC3	281:22:03	282:03:04	191	0.137
	12	C3	282:03:57	282:04:26	28	0.162
	41	C3	282:01:46	282:03:04	77	0.163
	41	CC3	282:03:56	282:09:14	201	0.168

was computed using TRJL. The total timing change (77 minutes, 49.5 seconds) required for the spacecraft to arrive at apoapsis at the desired time was determined. The number of orbits between the phasing maneuver and the reference epoch (81.48) was chosen and the necessary orbital period change (58.476 seconds) computed. Constraints on the velocity control system (minimum ΔV greater than 5 meters per second) made it necessary to dissipate ΔV on changing other orbital parameters; therefore, a change in inclination of 0.075 degree was used.

Canopus was out of view of the star tracker; therefore, it was necessary to use the star α -Lyra (Vega) as the roll reference for the maneuver. The results of the maneuver design are shown in Table 3-9.

Maneuver monitoring was accomplished by DSS-12. Predicted and actual two-way doppler is plotted on Figure 3-3. The fact that the two curves were parallel indicated the maneuver execution was as planned. The slight bias (14.5 Hz) is caused by the epoch forwarding of the OD state vector (OD 6019-8) to the burn time (a period of 30 hours).

A series of postmaneuver orbit determinations was used to evaluate the event sequence and lighting conditions during the lunar eclipse. A series of parameters concerning the eclipse was tabulated for each OD. Table 3-10 contains the results of all postmaneuver OD's and these data show that the maneuver was executed as designed.

Telemetry measurements of solar array current were monitored during the eclipse to indicate percent sunlight visible to the spacecraft. Figure 3-4 is a plot of predicted lighting time histories. Points based on telemetry data are provided as a comparison.

3.2.3.2 Orbital Lifetime Adjust Maneuver

The purpose of the maneuver was to increase perilune altitude such that a lunar impact would not occur within a year, and to adjust perilune so that following Mission V a maneuver could be performed to place the spacecraft in an Apollo-type orbit within existing ΔV constraints.

Analysis of the perilune altitude history (Figure 3-1) indicated that the spacecraft would impact the Moon approximately Day 260, 1967 on the farside of the Moon. To guarantee that the spacecraft would not impact the Moon, it was necessary to increase perilune altitude by 83 kilometers. This would allow a predicted miss of 20 kilometers at the lowest perilune altitude occurring on Day 6 of 1968. The 20-kilometer miss was chosen to accommodate execution errors and uncertainties in the lunar gravitational field and surface elevation.

The second constraint on this maneuver required that perilune altitude be between the limits of 111.2 and 185.3 kilometers when a second maneuver could be performed. The second maneuver would be required to lower the orbit apolune to simulate an Apollo orbit as closely as possible within ΔV constraints. The maneuver design was accomplished using the orbit determination results of OD 7004-8, which is presented in Table 3-11. The "solved

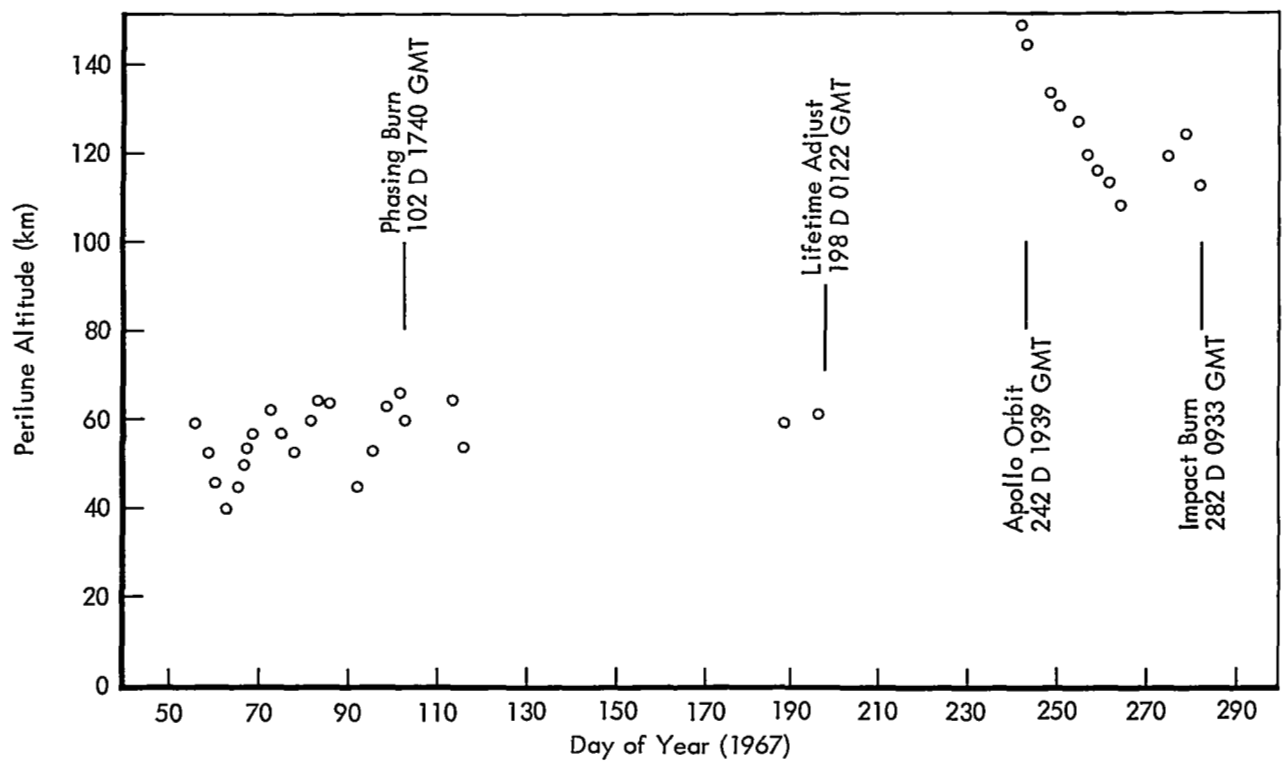


Figure 3-1: Perilune Altitude History

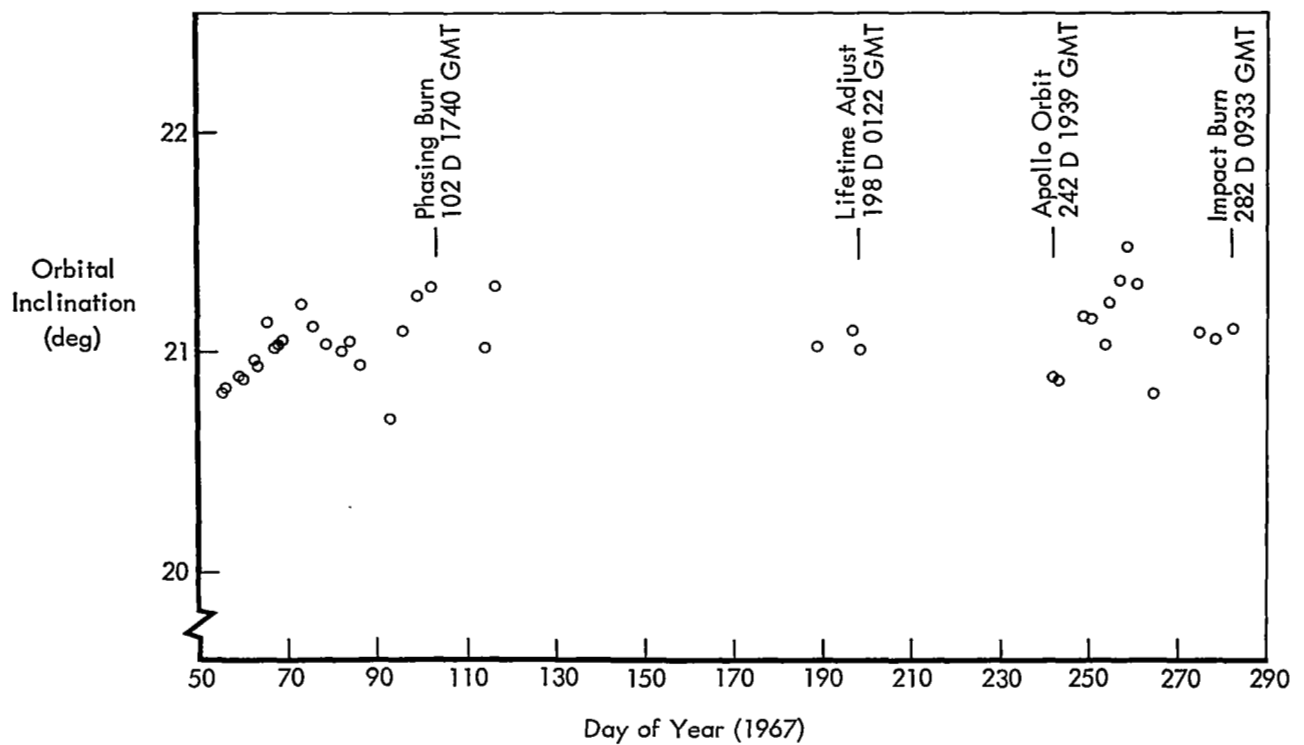


Figure 3-2: Orbital Inclination History

Table 3-9: Maneuver Design Data – Phasing Maneuver

Orbit Determination No.	6019-8	
Roll reference star	α LYRA (VEGA)	
Right ascension (deg)	278.77	
Declination (deg)	38.75	
Required ΔV (m/sec)	5.50	
Ignition time (GMT)	102:17:40:28.23	
Burn duration (sec)	3.6	
Attitude (deg)		
Roll	101.63	
Pitch	-113.84	
Yaw	0	
Orbit Elements	Prior To Maneuver	After Maneuver
Semi-major Axis (km)	2688.4011	2680.0159
Eccentricity	0.33143346	0.32920162
Argument of perilune (deg)	225.28262	225.09570
Longitude of ascending node (deg)	175.49502	175.85379
Inclination (deg)	21.330864	21.405958
Orbit period (sec)	12508.6	12450.1
Apolune altitude (km)	1841.337	1824.192
Perilune altitude (km)	59.285	59.660

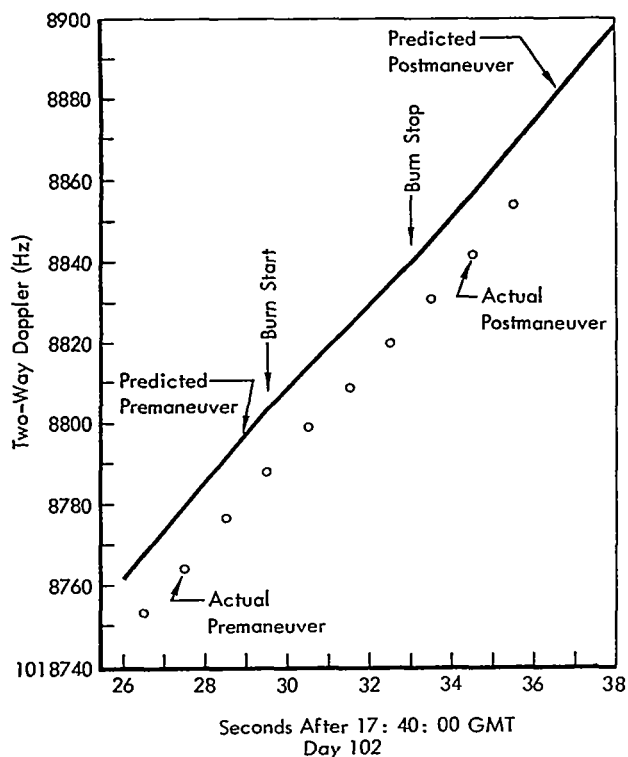


Figure 3-3: Phasing Maneuver Two-Way Doppler - DSS 12, Day 102

for" state vector was mapped forward to the maneuver time using the LRC 11/11 lunar harmonics.

The attitude maneuvers required to position the spacecraft for the burn were computed from a Sun - α CRU (ACURX) orientation since Canopus was out of view of the star tracker.

During the maneuver the spacecraft was tracked by DSS-12. Predicted and actual two-way doppler is plotted on Figure 3-5 with a doppler shift of 212 Hz being observed during the burn. A comparison of the predicted and actual doppler curves indicates that ignition and cutoff occurred on schedule. The 36-Hz bias between the two curves is caused by the epoch forwarding of the OD state vector (OD 7004-8) to the burn time (a period of 45 hours). All indications were that the maneuver was performed as designed. The pre- and post-burn perilune altitude history is shown in Figure 3-6.

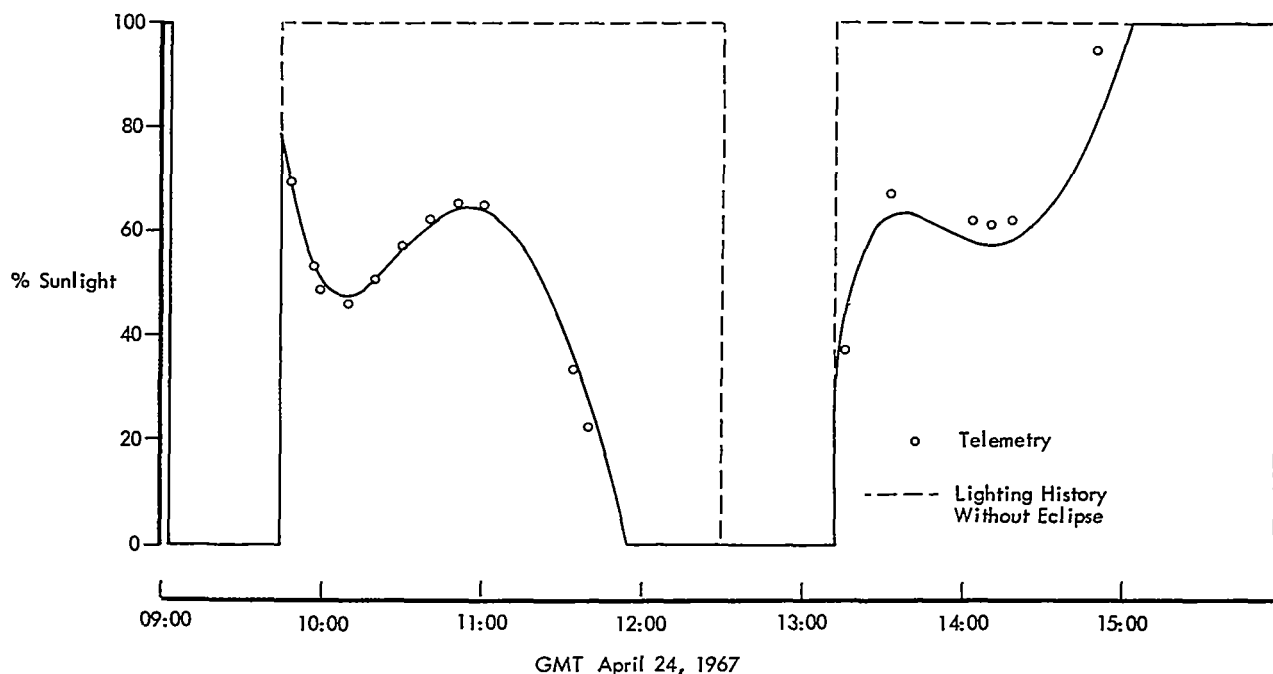


Figure 3-4: Lighting Time History During Lunar Eclipse April 24, 1967, Based on OD 7001-8

Table 3-10: Postmaneuver Orbit Determination Data

OD Number	OD Data Arc Length hr:min	OD Epoch Time Before Eclipse* day:hr:min	Orbital Period (sec)	Time of Apoapsis Passage (GMT) Day 114	Time in Total Darkness (min)	Time Below 30% Sunlight (min)	Enter Umbra (GMT) Day 114	Exit Umbra (GMT) Day 114
Maneuver Design			12,450.1	11:29:00	80	96	1154	1314
7000-8	5:51	11:17:2	12,450.2	11:26:31	79	94	1153	1312
7001-8	11:45	1:1:22	12,447.3	11:26:36	78	94	1154	1312

*Referred to center of eclipse GMT 114:12:07:00

A postmaneuver orbit determination (OD 8000-8) was used to evaluate the maneuver execution. The results are shown in Table 3-11. The pre-maneuver prediction was based on OD 7004-8, which had an epoch 45 hours prior to the burn, which is the major reason for the discrepancies in the orbital parameters.

Orbit determination (OD 7005-8) was made using the tracking data prior to the maneuver to verify that the burn was successfully accomplished. Table 3-12 includes the orbital elements at the end of the OD data arc. Comparison of this data with the elements prior to the maneuver Table 3-11 indicates that the preburn perilune altitude was 2.02 kilometers high and apolune altitude was 2.92 kilometers low. Using this information, the preburn prediction of perilune and apolune altitude would be 142.27 and 1823.82 kilometers, respectively, which compares favorably with values determined in the postburn orbit determination.

3.2.3.3 Maneuver Into Apollo-Type Orbit

The following objectives were to be satisfied by this velocity maneuver.

- Orbital geometry similar to an Apollo-type orbit (which is 80 to 100 kilometers circular) within ΔV constraints.
 perilune altitude 100 km
 apolune altitude 330 km
 inclination 21 deg.
- Orbital lifetime greater than supply of attitude control gas.
- Minimum light-to-dark ratio of 1.8.
- Maintain velocity control adequate for crash capability.

- Attempt to phase the spacecraft such that no long periods of darkness would be encountered during the eclipse on October 18, 1967 (Day 291).

The maneuver design was accomplished using the orbit determination results of OD 8001-8, which are presented in Table 3-13. The resulting state vector was mapped forward 26.5 hours to the maneuver time using the LRC 7/28B lunar harmonics modified in the OD solution. Attitude maneuvers required to orient the spacecraft for the burn were computed from a Sun α Lyra orientation, since Canopus was out of view of the star tracker.

The prediction of perilune altitude in the low-altitude orbit is shown in Figure 3-7, which also shows the results of OD solutions following the burn. The resulting light-to-dark ratio of the spacecraft in the Apollo-type orbit is shown in Figure 3-8.

The spacecraft was tracked during the maneuver by DSS-12 and -41. Predicted and actual two-way doppler from Station 12 is plotted in Figure 3-9. A doppler shift of 2050 Hz was observed during the burn. The close agreement between the actual and predicted curves both before and after the burn indicate that the maneuver was performed as commanded. The deviation in the curves during the burn indicates that the preburn prediction of thrust level was slightly in error which had no effect on the total velocity change imparted to the spacecraft since both curves terminate at essentially the same point. A postmaneuver orbit determination (OD 9001-

Table 3-11: Maneuver Design Data – Lifetime Adjust Maneuver

Orbit Determination Number	7004.8		
Roll reference star	α CRU (ACURX)		
Right ascension (deg)	185.97		
Declination (deg)	62.83		
Required ΔV (m/sec)	14.37		
Ignition time (GMT)	198:01:21:46.30		
Burn duration (sec)	8.93		
Attitude (deg)			
Roll	-48.59		
Pitch	108.00		
Yaw	0		
Orbit Elements	Prior To Maneuver	After Maneuver	Actual After Maneuver*
Semi-major axis (km)	2680.23	2721.59	2721.65
Eccentricity	0.330048	0.309835	0.308818
Argument of perilune (deg)	306.256	306.239	305.739
Longitude of ascending node (deg)	313.889	313.888	314.289
Inclination (deg)	21.137	21.137	21.014
Orbit period (min)	207.53	212.35	212.356
Apolune altitude (km)	1826.74	1826.74	1824.05
Perilune altitude (km)	57.53	140.25	143.06

*O.D. No. 8000-8

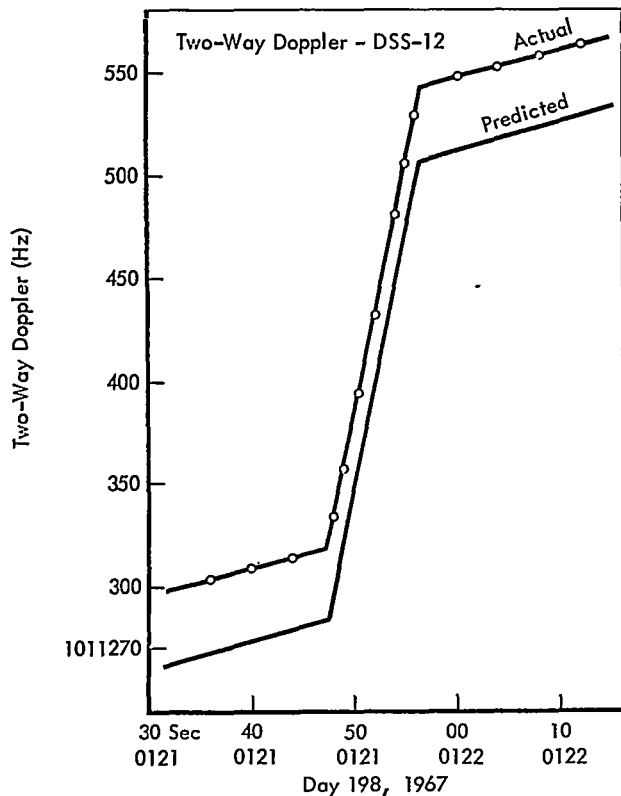


Figure 3-5: SC/8 (LOIII) Lifetime Adjust Maneuver

8) was used to evaluate the maneuver execution. The comparison with premaneuver orbital elements can be seen in Table 3-13.

Figure 3-7 indicates the lack of ability to predict perilune altitude in this low-altitude orbit. After a period of 20 days, the actual OD solutions indicated a perilune altitude 30 kilometers higher than premaneuver predictions. There are two primary causes for this difference: first, the best lunar model available for predictions (LRC 11/11) was developed for an orbit with a higher apolune altitude and a lower inclination than the Apollo-type orbit, and second, a mechanical model exactly representing the actual Moon's gravitational field is very complex and has not been determined.

3.2.3.4 Terminal Transfer Maneuver

The object of this maneuver was to impact Lunar Orbiter III on the lunar surface. An impact on the nearside of the Moon was desired if within the ΔV capability of the spacecraft.

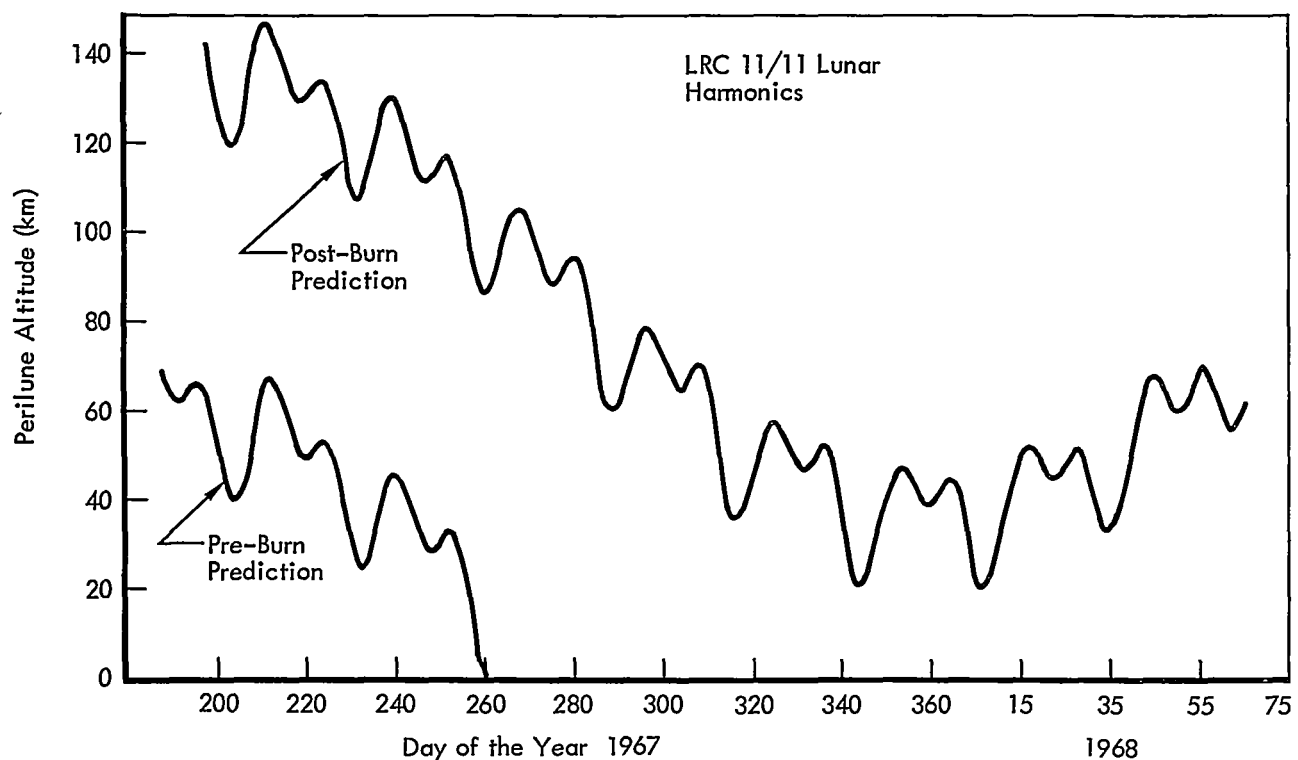


Figure 3-6: Predicted Perilune Altitude after Lifetime Adjust Maneuver - Day 198

Table 3-12:
Premaneuver Orbital Elements of 7005-8
(Selenographic of date coordinates)

Epoch day 198 01 hr 18 min 48.75 sec	
Semimajor axis (km)	2679.78
Eccentricity	0.329181
Perilune altitude (km)	59.55
Apolune altitude (km)	1823.82
Inclination (deg)	21.106
Argument of perilune (deg)	305.382
Longitude of node (deg)	314.720
Period (min)	207.474

This capability appeared to exist with only a small chance of success due to the following:

- Low flight path angle;
- Lunar surface terrain uncertainty;
- Maneuver design based on an OD state vector 80 hours in the past.

Even considering the small chance of success, it was decided to attempt a controlled impact on the lunar front face.

The maneuver design was accomplished using the orbit determination results of OD 9011-8, which was mapped forward to the maneuver

time using the LRC 11/11 lunar harmonics and is presented in Table 3-14. Canopus was within the field of view of the star tracker and was used as the roll reference for the maneuver. Use of Canopus as a roll reference has been impossible from Day 95 to Day 278 of 1967 due to the orientation of the star tracker on the spacecraft.

Predicted and actual two-way doppler from DSS-41 is plotted in Figure 3-10, with a doppler shift of 210 Hz being observed during the burn. A comparison of predicted and actual doppler curves indicates that engine ignition and cutoff occurred on time. The bias (368 Hz) between the two curves at ignition results from the epoch forwarding of OD 9011-8 to the burn time (a period of 80 hours).

Orbit determination (OD 9012-8) was computed subsequent to the maneuver OD 9011-8. Table 3-15 shows the predicted impact points from both solutions. The most probable point of impact is at the location from OD 9012-8.

The major reason for the large discrepancies between preburn and postmaneuver predictions was epoch forwarding, which had to be accomplished prior to maneuver design. Prediction of the Lunar Orbiter III trajectory in the low-altitude orbit was inadequate due to the lack of an effective lunar gravitational model, which can be seen by a comparison of the orbital elements prior to the maneuver and OD 9012-8 Table 3-14. A significant difference is evident in perilune altitude. The fact that actual perilune altitude was 10 kilometers lower than predicted guaranteed that impact occurred on the farside of the moon.

Table 3-13: Maneuver Design Data – Apollo-Type Orbit

Orbit Determination Number	8001-8		
Roll Reference Star	α Lyr (VEGA)		
Right ascension (deg)	278.77		
Declination (deg)	38.75		
Required ΔV (m/sec)	198.30		
Ignition time (GMT)	242:19:39:19:60		
Burn duration (sec)	128.5		
Attitude (deg)			
Roll	-176.10		
Pitch	-78.31		
Yaw	0		
Orbit Elements	Prior To Maneuver	After Maneuver	Actual After Maneuver*
Semi-major axis (km)	2722.0	1967.86	1968.12
Eccentricity	0.30823	0.43791	0.43475
Argument of perilune (deg)	342.42	354.42	354.31
Longitude of ascending node (deg)	64.34	64.34	63.93
Inclination (deg)	20.94	20.93	20.88
Orbit period (min)	212.47	130.56	130.58
Apolune altitude (km)	1823.70	315.95	315.59
Perilune altitude (km)	145.32	143.60	144.46
*O.D. NO 9001-8			

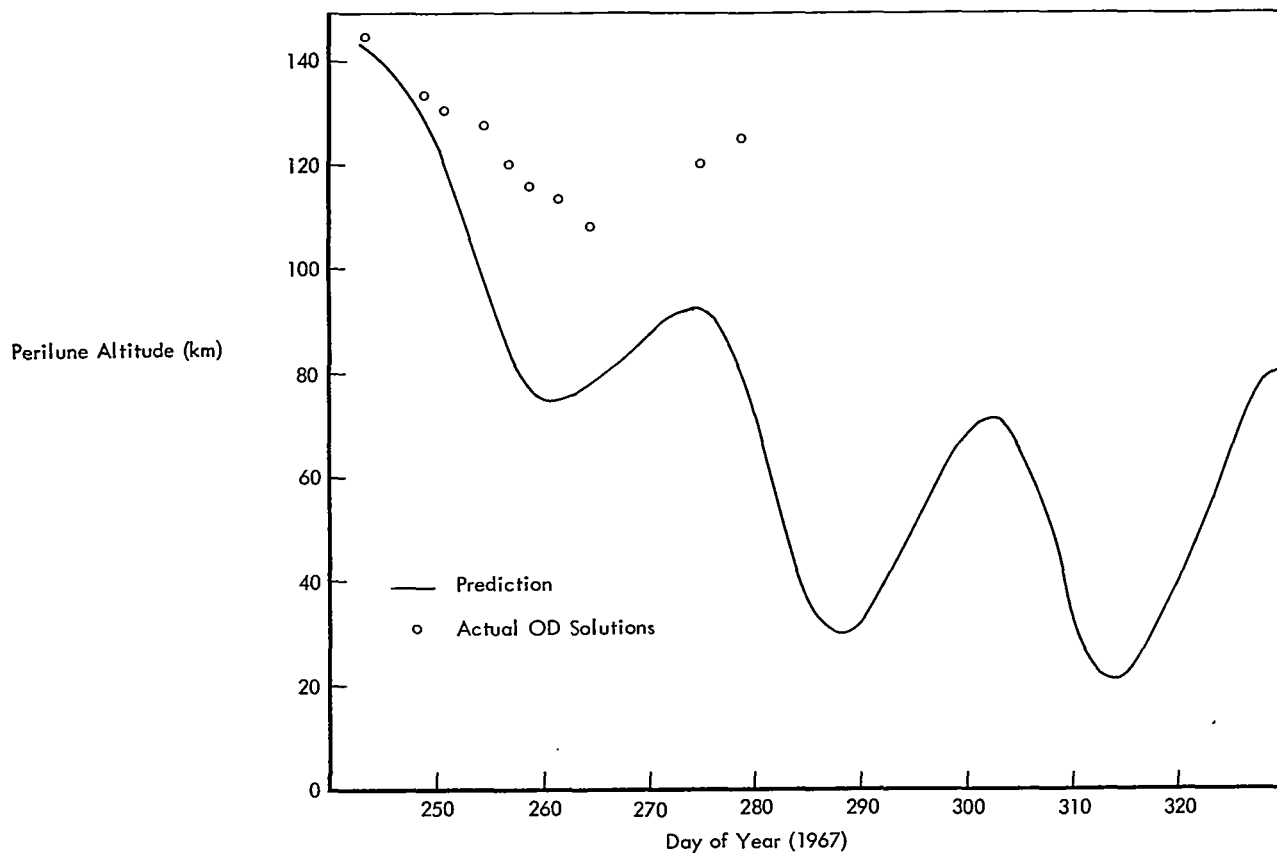


Figure 3-7: Lifetime Prediction - Apollo-Type Orbit - LRC 11/11 Lunar Model

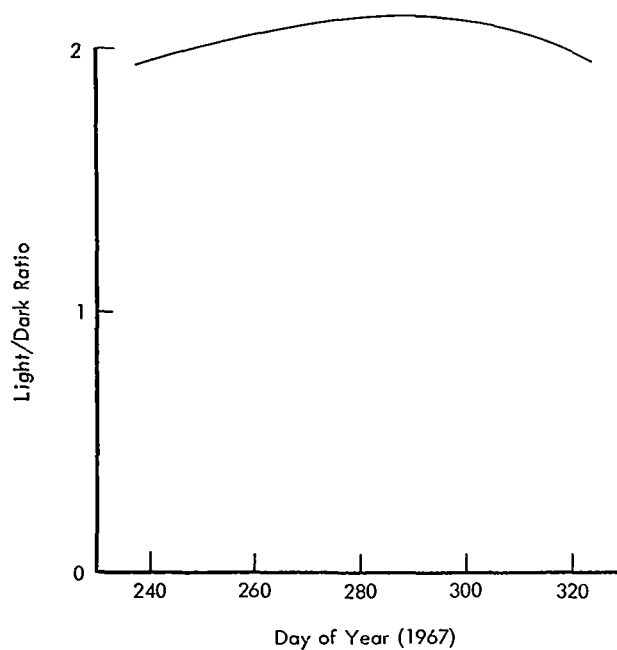


Figure 3-8:
Light/Dark Ratio - Apollo-Type Orbit

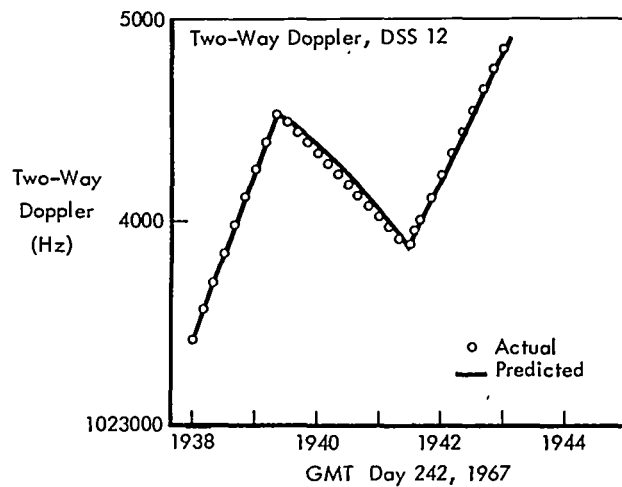


Figure 3-9:
Apollo-Type Orbit Maneuver -
Two-Way Doppler DSS-12

Table 3-14: Maneuver Design Data – Terminal Transfer

Orbit Determination No.	9011.8		
Roll reference star	Canopus		
Right ascension (deg)	95.71		
Declination (deg)	-52.67		
Required ΔV (m/sec)	52.6		
Ignition time (GMT)	282:09:33:05.90		
Burn duration (sec)	32.00		
Attitude (deg)			
Roll	35.74		
Pitch	31.83		
Yaw	0		
Orbit elements	Prior To Maneuver	After Maneuver	Predicted After Maneuver*
Semimajor axis (km)	1968.28	1907.23	1897.90
Eccentricity	0.065146	0.092684	0.0919807
Argument of perilune (deg)	40.874	66.379	69.19
Longitude of ascending node (deg)	227.469	227.296	226.05
Inclination (deg)	21.747	21.717	21.16
Orbit period (min)	130.60	124.57	123.66
Apolune altitude (km)	358.42	345.19	334.38
Perilune altitude (km)	101.97	-7.63	-15.76

*O.D. 9012-8

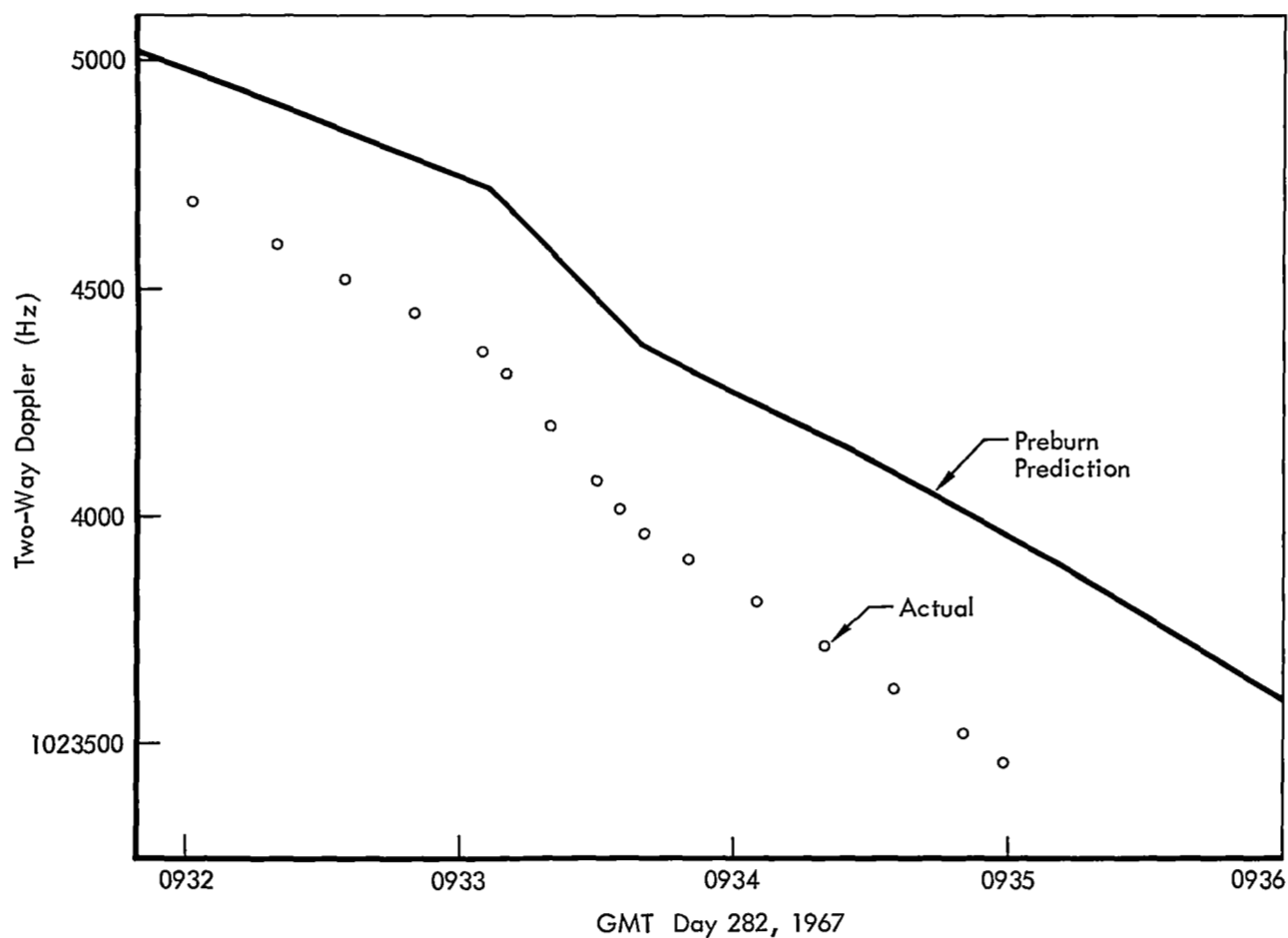


Figure 3-10: Terminal Maneuver — Two-Way Doppler DSS-41, Day 282, 1967

Table 3-15:
Predicted Impact Parameters*

Orbit Determination	9011-8	9012-8
Longitude (Deg W)	88.40	92.70
Latitude (Deg N)	15.70	14.32
Time (GMT)	282:10:30:37	282:10:27:11

*Most probable location of impact.

4.0 FLIGHT DATA

4.1 ENVIRONMENTAL DATA

A prime objective of the extended mission was collection of lunar environmental data during long lunar flight periods. Spacecraft telemetry was monitored during each tracking period to determine if there had been any increase in radiation flux or micrometeoroid activity. Because the activity was frequently monitored in real time, however, the exact location or time was unknown.

4.1.1 Radiation

Table 4-1 shows radiation data collected during the extended mission. The scintillation counter located near the film cassette recorded 5.50 rads; the one near the film looper recorded 6.00 at the beginning of the extended mission. Figure 4-1 shows the increasing radiation trend.

The data suggests that looper scintillation counter experienced a change in background level after Day 150 due possibly to a leak in the structure of the counter. The scope of the background level shown after Day 150 was not reflected by any other extended mission spacecraft.

4.1.2 Micrometeoroids

The micrometeoroid detection system received one hit during the prime mission and four during the extended mission. Table 4-2 lists the detectors that record impact and the time period during which each impact occurred.

Table 4-2: Micrometeoroid Data

Detector Number	Activity Recorded Between		
	Day/GMT	—	Day/GMT*
19	087/10:52	—	089/11:32
10	111/12:18	—	112/12:18
16	227/19:10	—	230/02:15
08	265/09:00	—	267/17:32

*See Tables 3-9, 3-11, and 3-13 for orbital parameters during these time periods.

4.2 SPECIAL EXPERIMENTS

During the extended mission, the spacecraft was used to obtain scientific data and as a tool

to conduct special experiments. The purpose of the experiment and the types of data collected are furnished in this report. Data analysis is the responsibility of the requesting agency.

4.2.1 Radar Mapping Experiment

The purpose of this experiment was to reflect, from the high-gain antenna off the lunar surface, an rf signal that could be received by an Earth-based tracking station. The reflected signal, along with a direct signal from the spacecraft low-gain antenna, was used to obtain information about the surface image.

Two experiments were conducted on Day 78, one on Orbit 263 and one on Orbit 264. The object was to reflect the rf signal in the region of the crater Langrenus (61° E longitude, 10° S latitude). It was necessary to orient the spacecraft approximately 35 degrees off the sunline during the period the TWTA was on because of power and thermal constraints. This was done by rotating the high-gain antenna to an angle of 51 degrees so that, after a two-axis attitude maneuver to point the high-gain-antenna beam at the target area, the spacecraft was at the desired off-Sun angle. To obtain the proper reflected signal, it was required that the incidence angle (angle between the incoming signal and the surface normal at the point of reflection) be in the range of 40 to 50 degrees. Each orbit the TWTA was turned on approximately 20 minutes after sunrise, for temperature stabilization, and allowed to remain on for 19 minutes.

The third experiment took place on Day 83 during Orbit 299. The object was to have the point of reflection at the Moon's prime meridian with the spacecraft high-gain antenna pointed northward. The constraints on incidence angle (between 40 and 50 degrees) and off-Sun angle (approximately 35 degrees) also applied for this experiment.

The high-gain antenna was rotated to 337 degrees to satisfy the off-Sun constraint. The TWTA was turned on for a period of 19 minutes.

The reflected signal was received by the track-

Table 4-1: Radiation Data

Tracking Period (GMT day)	Cassette Radiation (rads)	Looper Radiation (rads)	Tracking Period (GMT day)	Cassette Radiation (rads)	Looper Radiation (rads)	Tracking Period (GMT day)	Cassette Radiation (rads)	Looper Radiation (rads)
072/073	3.50	4.00	110	5.25	5.50	142	7.00	7.00
075	3.50	4.50	111	5.50	5.50	143	7.00	7.00
078	3.75	4.50	112	5.50	6.00	144		
079	3.75	4.50	113/114	5.50	6.00	145	7.50	42.00
081	4.00	4.50	115/116	5.75	6.00	147	7.50	43.00
083	4.00	4.50	120	6.00	6.00	149	8.25	47.00
085/086	4.25	4.50	126	6.25	6.50	150		
087	4.25	5.00	128	6.25	6.50	151	8.50	48.50
089	4.25	5.00	129	6.25	6.50	152	8.50	48.50
092	4.50	5.00	129	6.25	6.50	153	8.50	48.50
094	4.75	5.00	130			155		
095	4.75	5.00	132	6.50	6.50	156		
097	4.75	5.00	133	6.50	6.50	158		
098/099	5.00	5.50	134	6.50	6.50	159	9.00	50.00
101/102	5.00	5.50	135	6.50	6.50	164	9.25	50.50
102/103	5.00	5.50	135	6.75	6.50	164	9.25	50.50
103	5.00	5.50	137			166/167		
104	5.25	5.50	138	6.75	7.00	167	9.50	50.50
106	5.25	5.50	139			168	9.50	51.00
107	5.25	5.50	141	7.00	7.00	169	9.50	51.00

Table 4-1 (continued)

Tracking Period (GMT day)	Cassette Radiation (rads)	Looper Radiation (rads)	Tracking Period (GMT day)	Cassette Radiation (rads)	Looper Radiation (rads)	Tracking Period (GMT day)	Cassette Radiation (rads)	Looper Radiation (rads)
171	9.50	51.00	221			246/247		
174	9.75	51.50	223	12.25	60.50	248/249	13.25	69.50
176	9.75	51.50	224			250	13.50	70.00
177			226	12.25	62.00	253	13.50	71.50
178			226	12.25	62.00	254/255	13.75	72.00
180	10.00	52.00	227	12.25	62.50	256/257	13.75	73.00
186	10.50	53.00	228			258/259	13.75	74.00
188	10.50	53.00	230	12.50	63.50	261/262	14.00	75.50
191	10.75	53.50	230			264/265	14.25	76.50
196	10.75	54.50	232			267	14.25	77.50
197/198	11.00	54.50	233	12.75	64.50	270	14.50	78.50
202	11.25	55.50	234	12.75	64.50	272		
205	11.25	56.00	235	12.75	64.50	273	14.50	79.00
209	11.50	57.00	236	12.75	65.00	274/275	14.75	79.50
210	11.50	57.00	237	12.75	65.50	275	14.75	79.50
215	11.75	59.00	239	13.00	66.00	276	14.75	79.50
216	11.75	59.00	240			277	15.00	80.00
217	12.00	59.50	241/242	13.00	67.00	278/279	15.00	80.00
219			242/243	13.00	67.00	281/282	15.00	80.50
220	12.00	60.00	244	13.25	68.00			

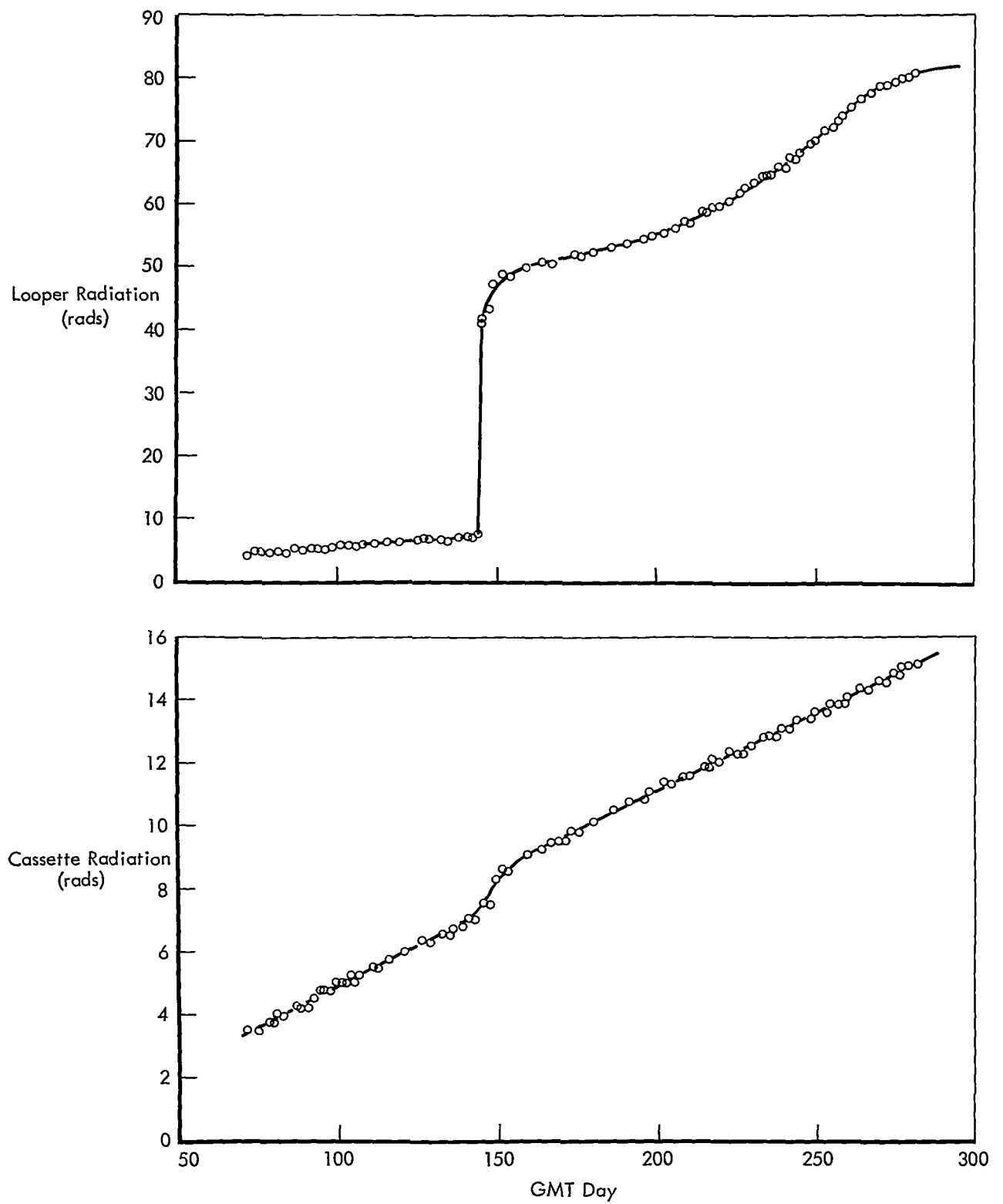


Figure 4-1: Radiation Data

ing stations, indicating the spacecraft high-gain antenna was properly oriented.

4.2.2 MSFN-AGNQ Support

The exercise was conducted to assist in qualifications of the MSFN tracking stations for use during Apollo missions. The MSFN activities for which the spacecraft was used included:

- Actively tracking the spacecraft at lunar distances using the MSFN USB tracking systems;
- Transmit tracking data to the MSC, Houston, Texas;
- Generation of antenna patterns to determine optimum focus position of the hyperbolic subreflectors;

- Preliminary qualification of the basic RTCC navigational concepts.

Table 4-3 is a summary of the tracking periods in support of this effort.

4.2.3 Ionosphere Experiment

The experiment, performed to determine the effect of the Earth's ionosphere on doppler and ranging data obtained by the spacecraft, consisted of obtaining two-way doppler and ranging data on eight horizon-to-horizon passes. Lunar Orbiter III was used for two of these tracking periods, on Day 092 from 09:53 to 19:00 GMT and on Days 101/102 from 15:00 to 03:30 GMT. The data were compiled and transmitted to the requesting agency, Jet Propulsion Laboratory, Pasadena, California.

Table 4-3: MSFN-AGNQ Tracking Summary

Day	Total Tracking Time (GMT)	MSFN Three-Way Tracking (GMT)	MSFN Two-Way Tracking (GMT)
072/3	19:33-04:10	19:48-03:57	
078	01:44-11:06	01:44-11:06	
085/6	15:37-01:21	16:30-01:15	
098/9	17:11-02:51	17:45-01:10	
254/5	10:10-15:15	10:10-21:30 14:33-15:15	21:30-13:45
261/2	05:46-13:28	05:46-15:55 04:56-05:00 10:05-10:30 12:16-13:28	16:48-04:56 05:43-09:22 10:30-11:32
264/5	03:35-09:00	03:35-13:00 07:57-09:00	13:00-07:57
278/9	08:41-11:00	08:41-09:10 14:41-00:20 10:22-11:00	09:10-14:41 00:20-09:34

The spacecraft communications subsystem was in the following condition:

- TWTA on;
- Ranging modulation on;
- High-gain antenna pointed at DSS-12.

Data were collected at DSS-12 by the requesting agency.

4.2.4 MSFN Ranging

The purpose of this experiment was to examine the feasibility of the MSFN tracking stations ranging with the spacecraft operating in Modulation Mode 4.

The test was conducted on Day 95 with satisfactory results. The MSFN stations and DSS-12 successfully ranged with the spacecraft in

Modulation Mode 4 with the data recorded in Table 4-4.

**Table 4-4: MSFN Ranging Test Data
Guidance Maneuvers**

Data	Modulation Mode	
	4	1
● Received signal strength (dbm)	-134.0	-138.2
● Correlation voltage	0.8	0.8
● Ranging receiver clock loop attenuator (db)	13	13
● Integration time setting	10	11

5.0 Spacecraft Subsystem Performance

Periodic monitoring of spacecraft telemetry data provided information that was used to determine subsystem performance. The data was analyzed to show performance trends in an attempt to establish detrimental effects on components or subsystems after their exposure to space environment. The data and results are presented in this section.

5.1 SUMMARY

Individual subsystem performance was generally within design requirements; there was very little evidence of subsystem or component degradation. The *attitude control subsystem* performed normally during the extended mission. The star tracker operated as planned; however, glint or background noise was a problem during the periods when Canopus was out of the field of view. Sufficient data was collected on other stars to maintain accurate roll reference. The star map signal degraded approximately 42% due to photomultiplier tube degradation; however, the signal was 50% above the lower recognition gate and did not affect the mission. The *communications subsystem* performed within specification requirements; however, the TWTA rf power output was temperature sensitive but had no adverse effect on the mission objectives. The *power subsystem* provided sufficient power at all times despite the predictable solar array degradation of 6.1% and battery capacity reduction of 29%.

The *photo subsystem* film advance mechanism was inoperable in the forward direction due to a failure of the film advance motor at the beginning of the extended mission. During a readout attempt, there was an apparent failure in the high-voltage-power supply. The V/H sensor was used to conduct a tracking limit exercise, and the subsystem heaters were used to provide electrical load during other tests. The environmental controls performed as required. The *velocity and reaction control subsystem* performed satisfactorily. Use of nitrogen was nominal. The subsystem was operated seven times, accumulating 752 seconds of engine burn time. Four velocity maneuvers were conducted

during the extended mission, accumulating 171.5 seconds of burn time. The final velocity maneuver to impact the spacecraft was conducted after 247 days of exposure to space environment.

Except for the EMD thermal coating, the *structure and mechanism subsystem* performed as predicted. Degradation of the thermal control coating occurred as anticipated, requiring that the spacecraft be oriented off-Sun to maintain proper spacecraft thermal control.

5.2 SUBSYSTEM PERFORMANCE

5.2.1 Attitude Control Subsystem

The attitude control subsystem consists of inertial reference, control assembly, star tracker, sun-sensor units, and a switching assembly. The inertial reference unit is a three-axis, strapdown gyro system with an accelerometer for differential velocity derivation. Inertial reference outputs consist of angular rates and position data about each of the spacecraft's three orthogonal axes, and spacecraft velocity change in line with the X axis. Subsystem control and integration are furnished by the control assembly, which consists of a memory core, a clock oscillator, a logic system, input circuitry, and closed-loop electronics. Its primary purpose is to command the spacecraft either from stored commands or real-time commands and, through the logic system and closed-loop electronics, control the position thrusters and the engine pointing angle. The star tracker contains a photomultiplier tube for sensing Canopus presence, a bright-object sensor to operate a sun shade for protection of the photomultiplier tube, light baffles and optics, and associated electronics. Its purpose is to furnish spatial roll axis references. The sun sensors are silicon solar cells that provide spatial yaw and pitch axis reference. The switching assembly contains high-power switching circuitry and is controlled by the control assembly (see Figure 5-1). A tabulation of extended-mission activities is given in Table 5-1. Table 5-2 categorizes the types of maneuvers.

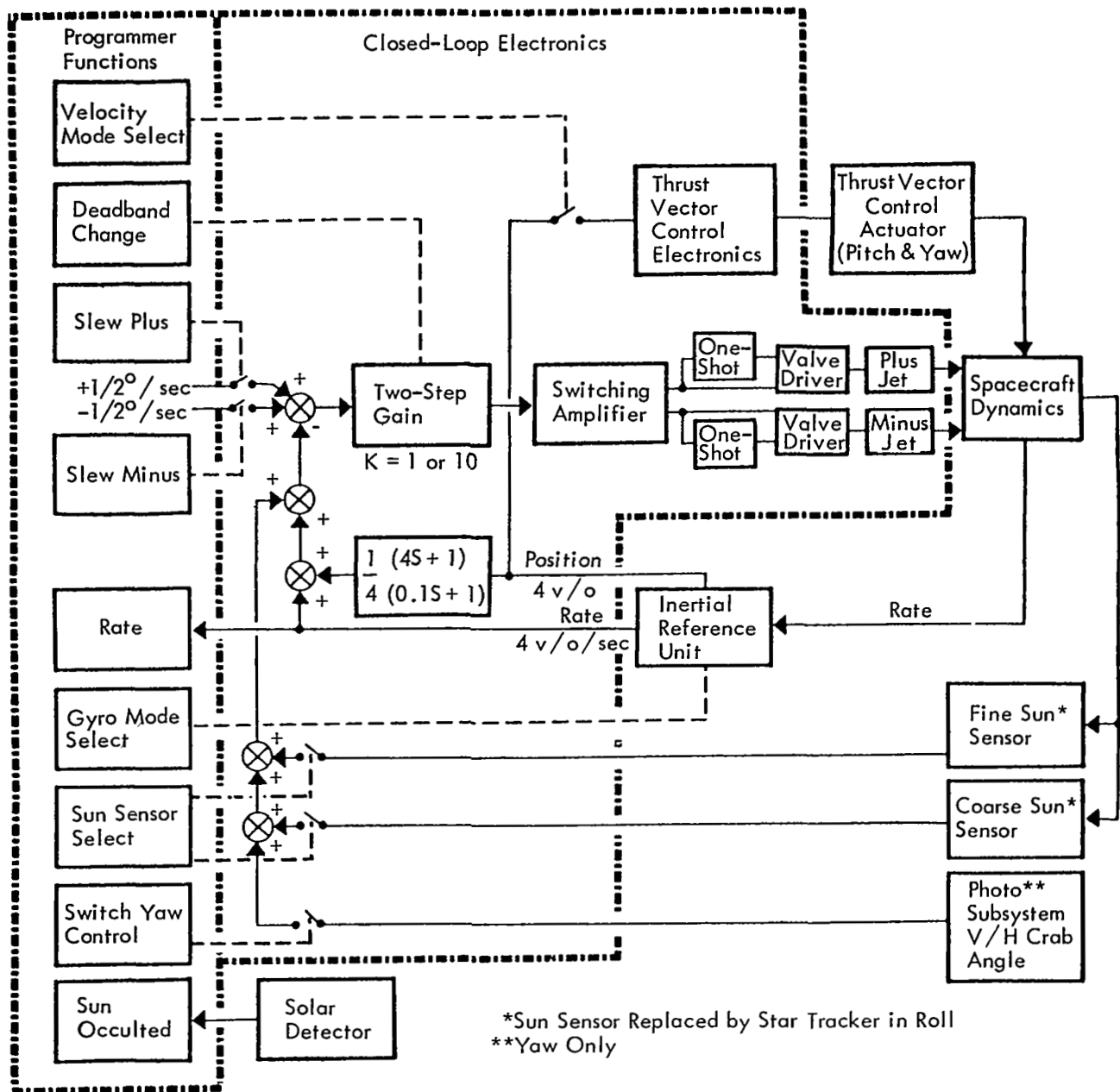


Figure 5-1: Attitude Control Subsystem

5.2.1.1 Inertial Reference Unit (IRU)

Performance of the IRU throughout the external mission was normal with no anomalies noted. The performance data did not deviate significantly from that collected during the photographic mission and prelaunch testing. Total operating time was 5904 hours.

Mission duration depends on the amount and use rate of attitude control gas used. Because of

this, gyro drift rate becomes a critical factor during the extended mission. Since the spacecraft is normally pitched off-Sun for thermal control with the attitude control subsystem in inertial hold gyro drift rate determines the rate attitude control gas is used. Figure 5-2 shows the prelaunch testing gyro drift history, Figures 5-3 and -4 show flight gyro drift history in comparison with Missions I and II. Table 5-3 shows drift rate and rate of change of drift rate during

Table 5-1: Extended-Mission Activities

GMT day:hr:min	Event	GMT day:hr:min	Event
067:14:24	Yaw and roll maneuver accuracy test	196:05:58	Star map to provide reference for velocity change. Star Acrux (α CRU) identified and tracked
068:15:40	Canopus tracker test-simulation of Mission IV lighting conditions at apolune	198:01:22	Velocity change of 47.2 feet per second
069:01:35	Pitch maneuver accuracy test	198:01:30	Maintain off-Sun attitude pitched minus approximately 60 degrees
069:03:11	Maintain off-Sun attitude, pitched minus approximately 50 degrees	241:20:47	Partial antenna map and star map to provide reference for velocity change. Vega located and tracked
075:04:15	Velocity over height (V/H) sensor high roll test	242:19:39	Velocity change of minus 198.3 feet per second
078:01:46	Stanford Experiment No. 1	242:20:00	Maintain off-Sun attitude pitched minus approximately 55 degrees
081:16:00	Canopus star tracker degradation test	254:10:10	Maintain off-Sun attitude pitched minus 43 to 53 degrees and maintain roll reference for MSFN tests
085:15:36	Canopus star tracker glint conditions test near PM terminator during period of full Moon	282:02:07	Star Map to provide reference for velocity change. Canopus located and tracked
101:16:36	Star map to provide reference for phasing velocity change. Vega (α Lyr) was identified and tracked	282:09:33	Velocity change of 172.6 feet per second to impact on Moon
101:20:24	Nitrogen isolation squib interaction test	282:09:38	Loss of data
102:17:40	Velocity change maneuver of minus 18 feet per second		
114:09:20	Lunar eclipse		
114:18:25	Maintain off-Sun attitude pitched minus approximately 55 degrees		
164:17:26	Maintain off-Sun attitude pitched minus approximately 60 degrees		

Table 5-2: Maneuver Summary

<u>Maneuver</u>	0.2 Degree Deadband		2.0 Degree Deadband	
	<u>Quantity</u>	<u>Typical Rate</u>	<u>Quantity</u>	<u>Typical Rate</u>
Roll	47	0.55 ± 0.05 deg/sec	20	0.053 deg/sec
Pitch	35	0.55 ± 0.05	104	0.057 to 0.113
Yaw	11	0.55 ± 0.05	4	0.048 to 0.057
ASU (acquire Sun)	19		90	
ACA (acquire Canopus)	16		2	
ACP (acquire Canopus plus)	1		0	
CDZ* (Change to 0.2 deadband)			10	
CDZ (change to 2.0 deadband)	11			
VEL (Velocity)			4	

prelaunch and flight conditions. The improved drift rate and drift stability from Mission III over Missions I and II is attributed to the construction of the gyros. Note that drift rates and rate of change of drift is very low and stable. These factors permitted the off-Sun angle to be maintained for an average 2.5 days without acquiring a celestial reference to update the gyros, which resulted in a considerable savings in attitude control gas.

Limit cycle was normal both in the rate and inertial hold modes. The rates developed averaged between 21 and 1.5 degrees per hour for a typical orbit. The high rates were due to disturbances such as sunrise and antenna pointing. Except for these, the average rate was considerably lower than the design goal of 9

degrees per hour and significantly less than the mission design requirements of 36 degrees per hour. Figure 5-5 shows a typical limit cycle during an orbit for the 2.0 degree dead band in the inertial hold mode. Deadband limits for the inertial hold mode in the 0.2 degree and 2.0 degree deadbands are shown in Table 5-4.

Attitude control subsystem operation in the maneuver made was normal. The maneuver rates and accuracies were within design tolerances (Tables 5-5 and 5-6).

IRU temperature control was normal, and follows the EMD temperature. No temperature oscillations were observed, indicating that the IRU temperature circuitry was never saturated. There are no abrupt changes in wheel current, indicating that the gyros were operating nor-

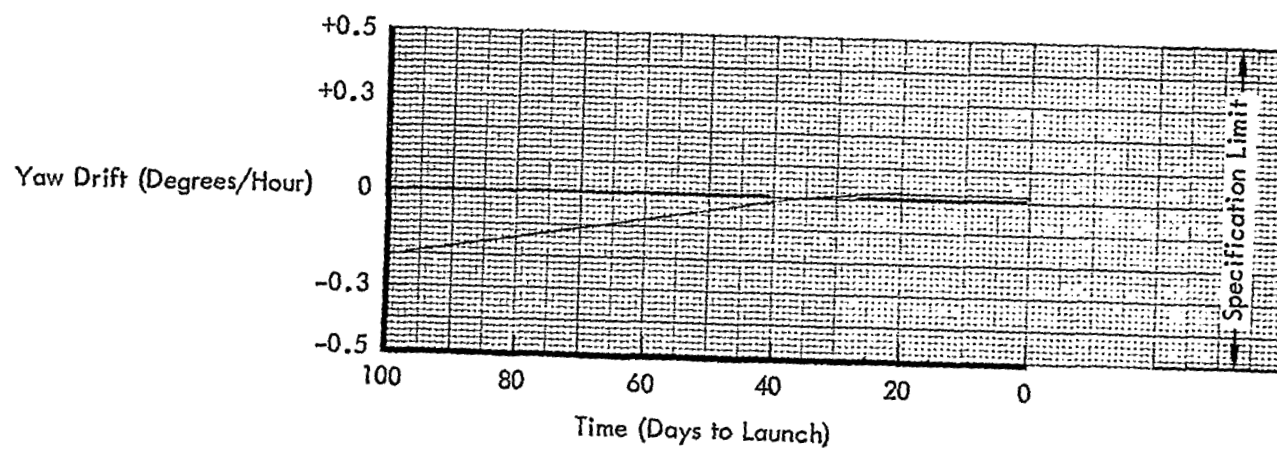
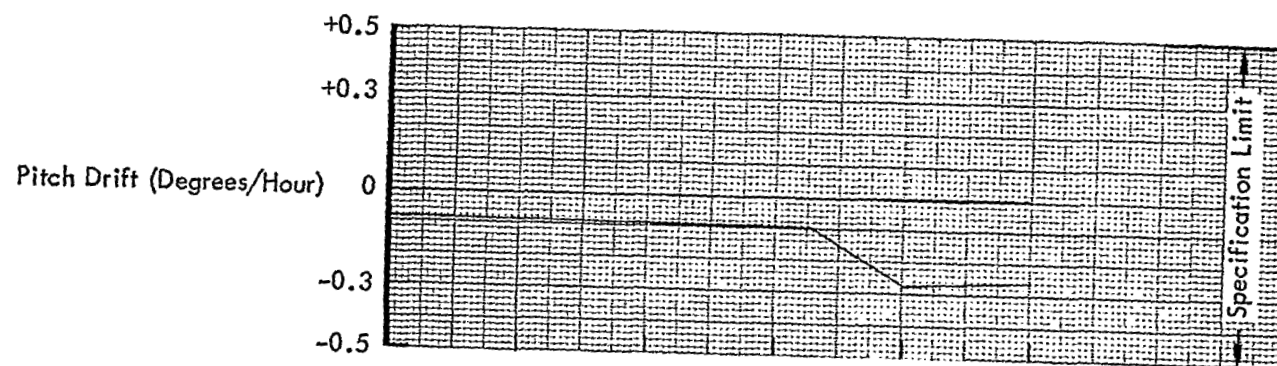
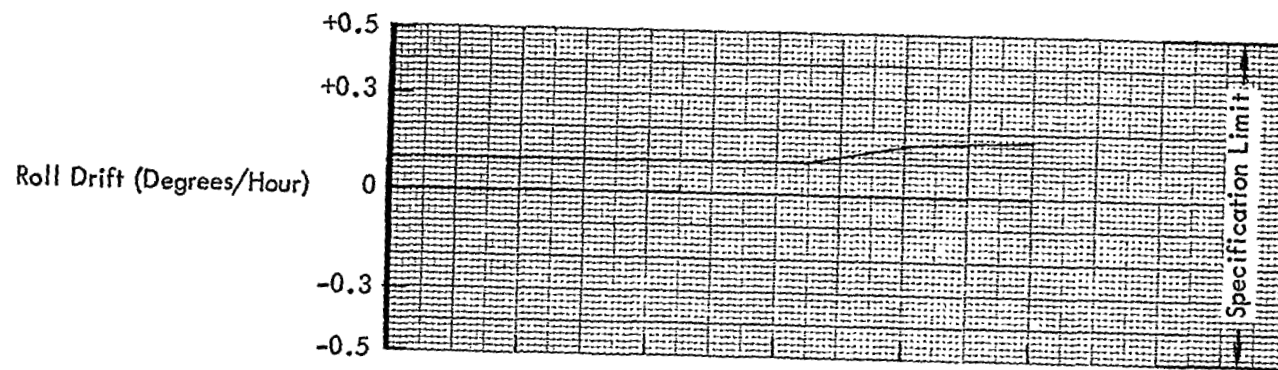


Figure 5-2: Prelaunch Gyro Drift Data

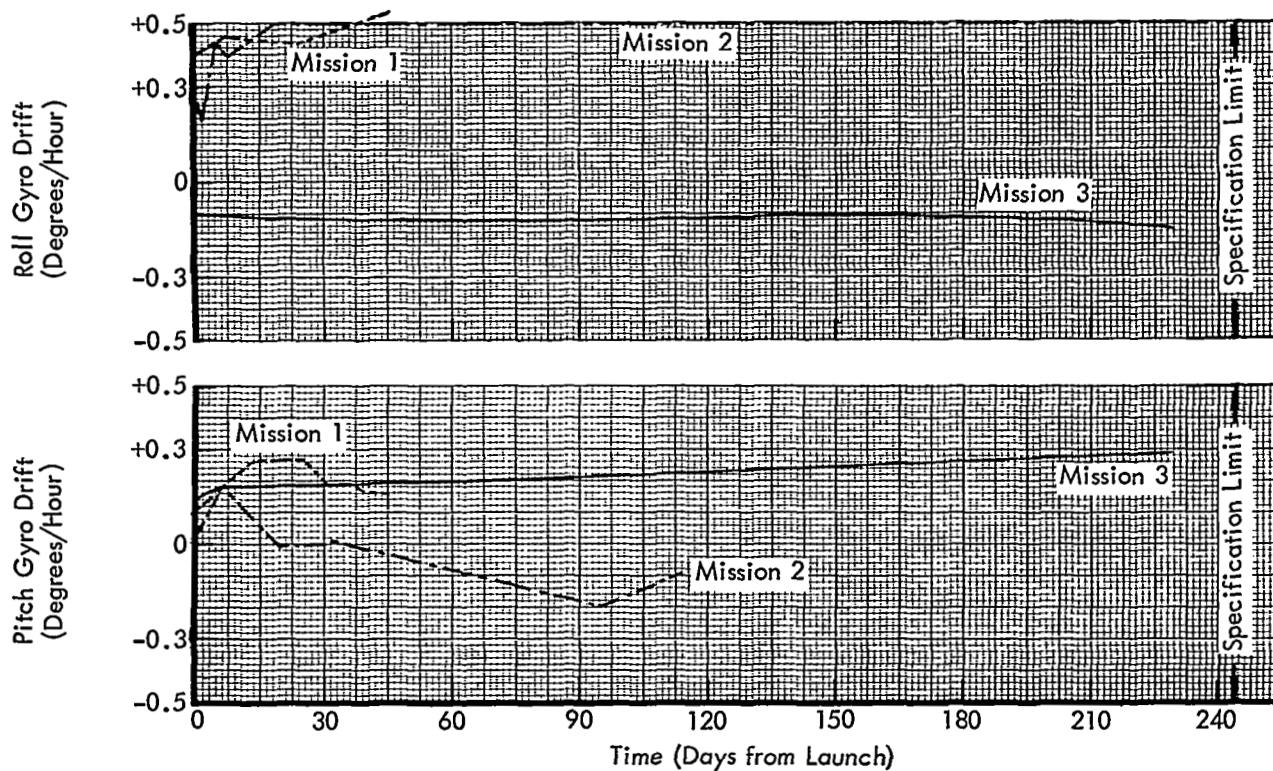


Figure 5-3: Flight Gyro Drift History

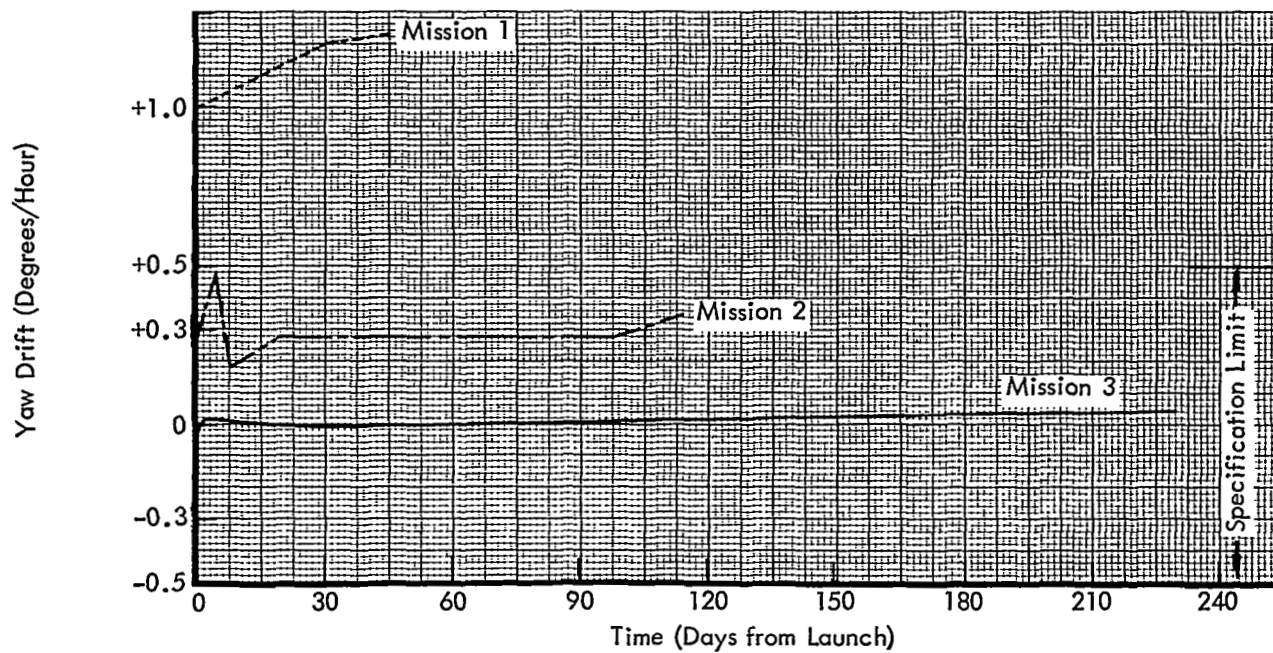


Figure 5-4: Flight Gyro Drift History

Table 5-3: Gyro Drift Data

Prelaunch Data
Average *

	Drift (deg/hr)	Change (deg/day)
Roll	+ 0.056	4×10^{-4}
Pitch	- 0.75	1×10^{-3}
Yaw	+ 0.02	1.1×10^{-3}

Flight Data
Average

	Drift (deg/hr)	Change (deg/day)
Roll	-0.14	5×10^{-4}
Pitch	+0.21	7×10^{-4}
Yaw	-0.01	6×10^{-4}

* Sign of ground data is reversed from flight data due to testing method.

Table 5-4: Deadband Limits

0.2 Deadband

	Design	+ Side	- Side
Roll	$\pm 0.18 \pm 0.03$	0.162	0.175
Pitch	$\pm 0.18 \pm 0.03$	0.163	0.172
Yaw	$\pm 0.18 \pm 0.03$	0.164	0.176

2.0 Deadband

	Design	+ Side	-Side
Roll	$\pm 2.0 \pm 0.3$	1.968	1.980
Pitch	$\pm 2.0 \pm 0.3$	1.957	2.019
Yaw	$\pm 2.0 \pm 0.3$	1.965	2.020

Table 5-5: Maneuver Rate Summary

0.2 Deadband				2.0 Deadband			
Axis	Number Completed	Plus (deg/sec)	Minus (deg/sec)		Number Completed	Plus (deg/sec)	Minus (deg/sec)
Roll	47	0.509 to 0.526	0.466 to 0.523	Roll	20	0.051 to 0.061	---
Pitch	35	0.507 to 0.513	0.509 to 0.518	Pitch	104	---	0.052 to 0.065
Yaw	11	0.491 to 0.513	0.488 to 0.518	Yaw	4	0.048 to 0.057	---

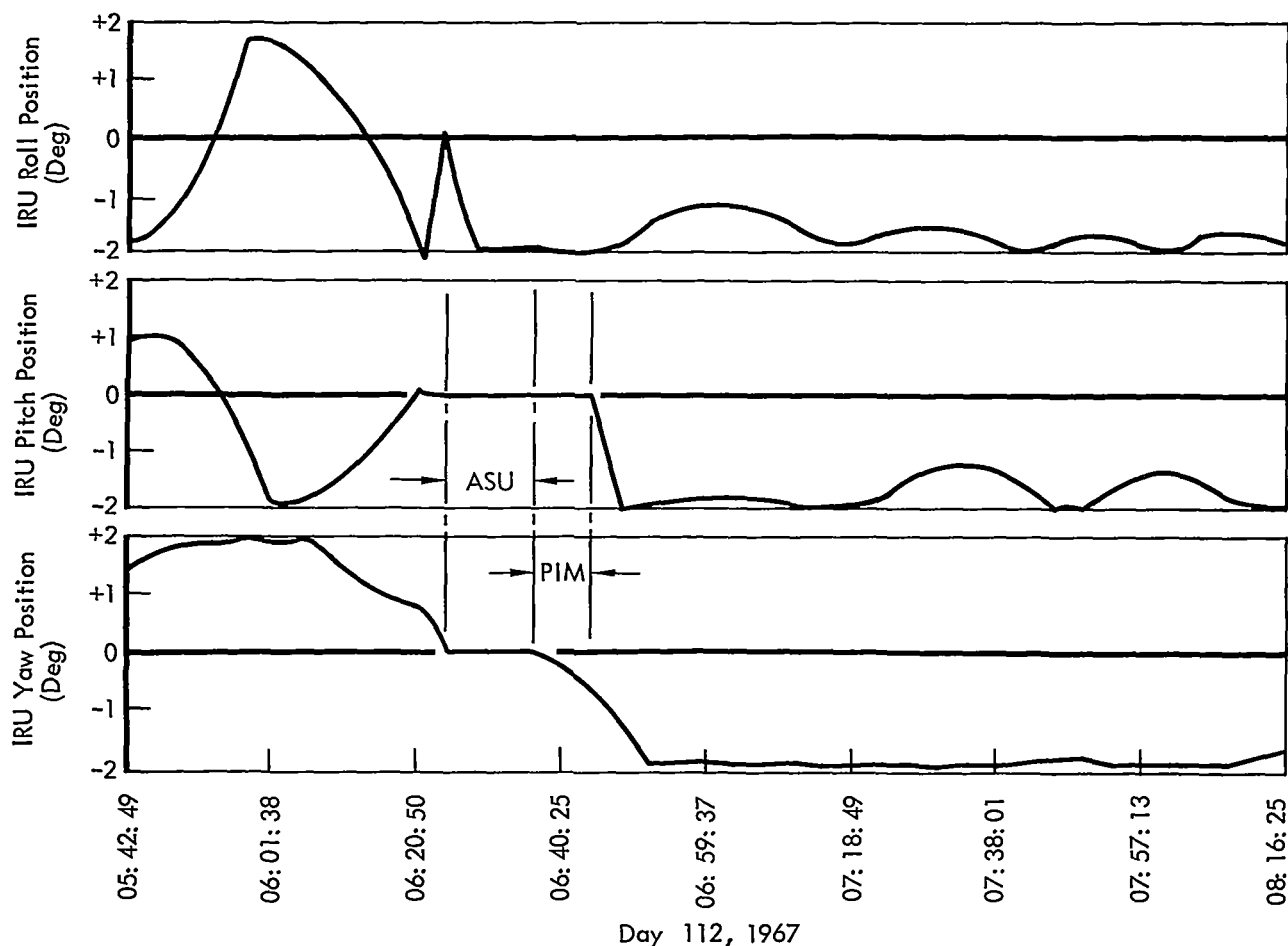


Figure 5-5: Typical Limit Cycle

mally and did not experience bearing or pivot problems. There was noted a small decrease in wheel current during the mission due to an apparent relaxation in bearing "preload" caused by wear. Figures 5-6 and 5-7 show the wheel currents, gyro temperature, and deck temperature versus time for the start (Day 078) and end (Day 262) of the extended mission.

Tracking and orbit determination data indicated that accelerometer performance was normal and as programmed. Table 5-7 shows the programmed trajectory and achieved trajectory for Extended-Mission orbital changes.

5.2.1.2 Star Tracker

The Canopus star tracker continued to operate satisfactorily throughout the extended mission. The total operating time accumulated during

the life of the spacecraft was 118 hours with 229 on-off cycles. Extended-mission operating time was 28 hours with 84 on-off cycles. The BOS operated as designed on the occasions when the tracker was exposed to sunlight; however, the star map voltage degraded from 3.2 to 1.8 volts. Figures 5-8 and 5-9 show star map voltage as a function of time.

Canopus was out of the star tracker yaw field of view when the spacecraft was on the sunline from Day 098 to Day 202; consequently, other stars were used for roll reference. Star maps were generated on Days 101, 196, and 202. The data observed is shown in Figures 5-11, -13, and -15. Figures 5-10, -12, and -14 show the *a priori* star maps generated from the computer program SIDL for Days 101, 196, and 202. Note the close correlation between the *a priori* and observed values, indicating a properly functioning tracker.

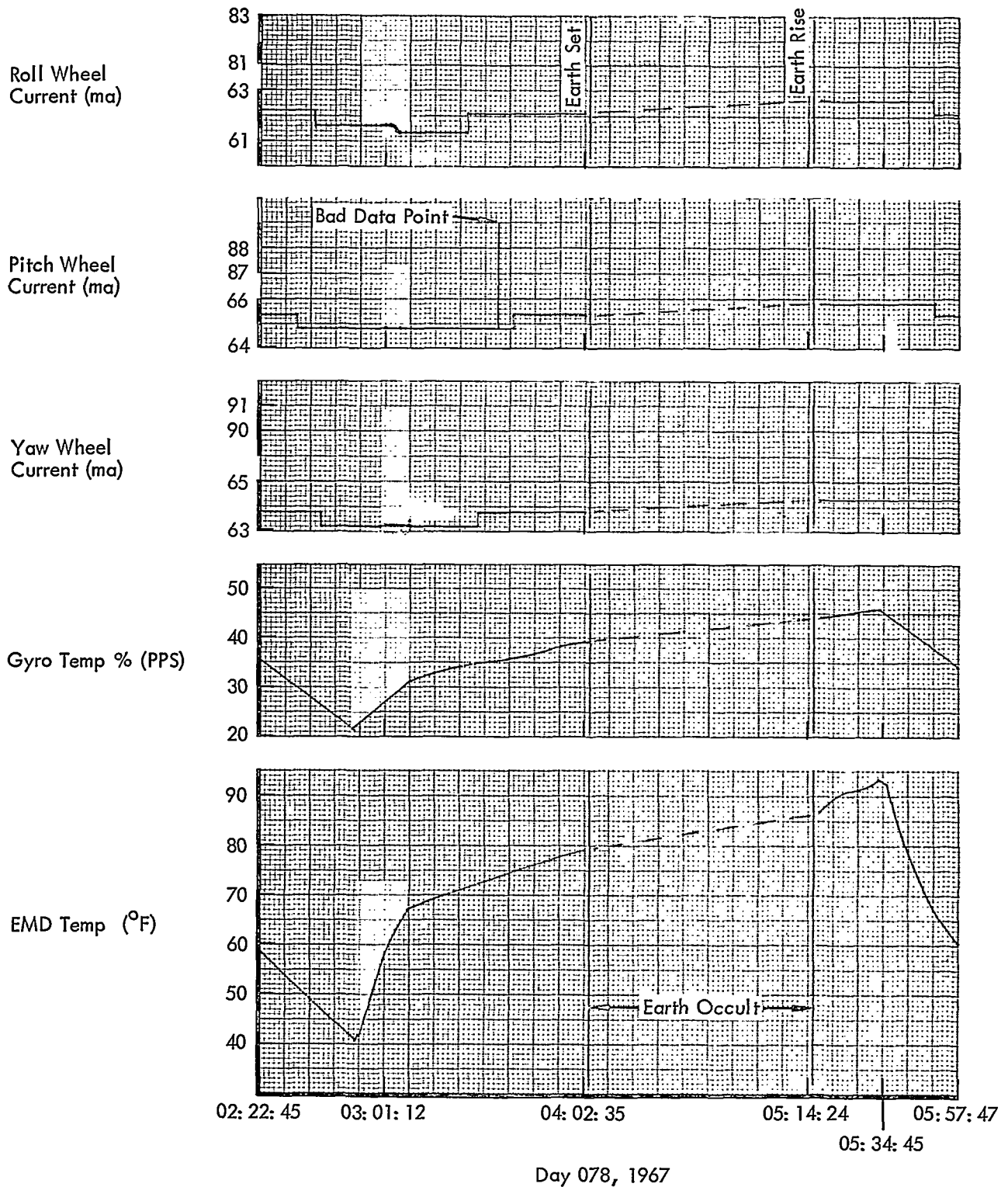


Figure 5-6: Gyro Wheel Current and Temperature

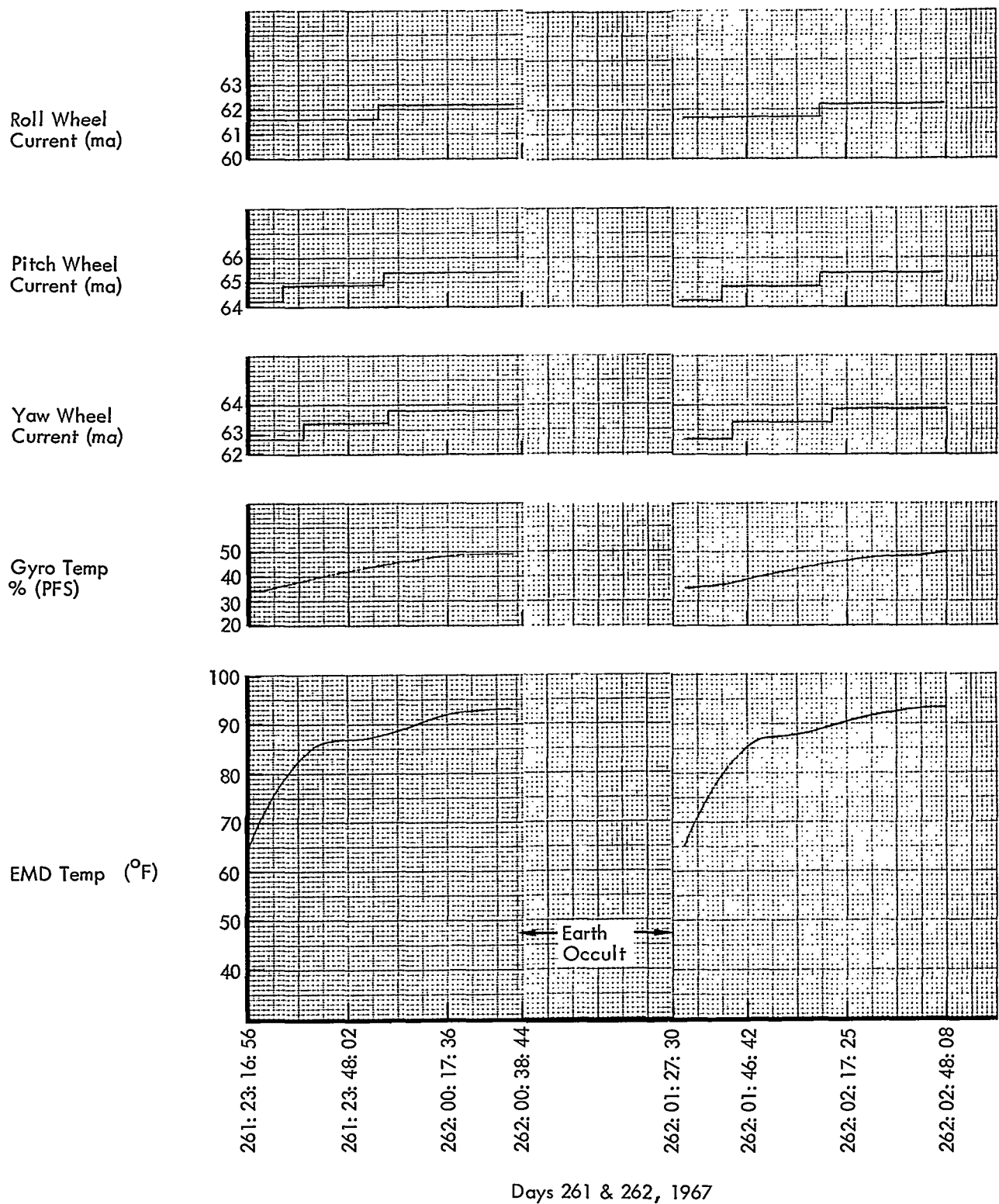


Figure 5-7: Gyro Wheel Current and Temperature

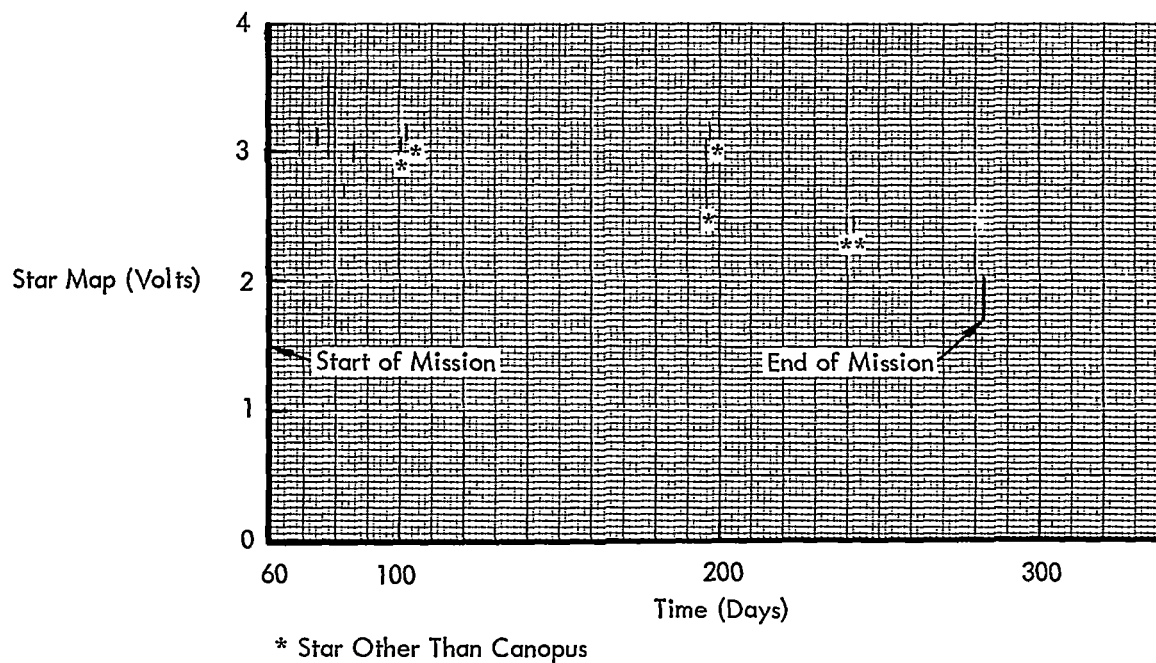


Figure 5-8: Star Map Voltage

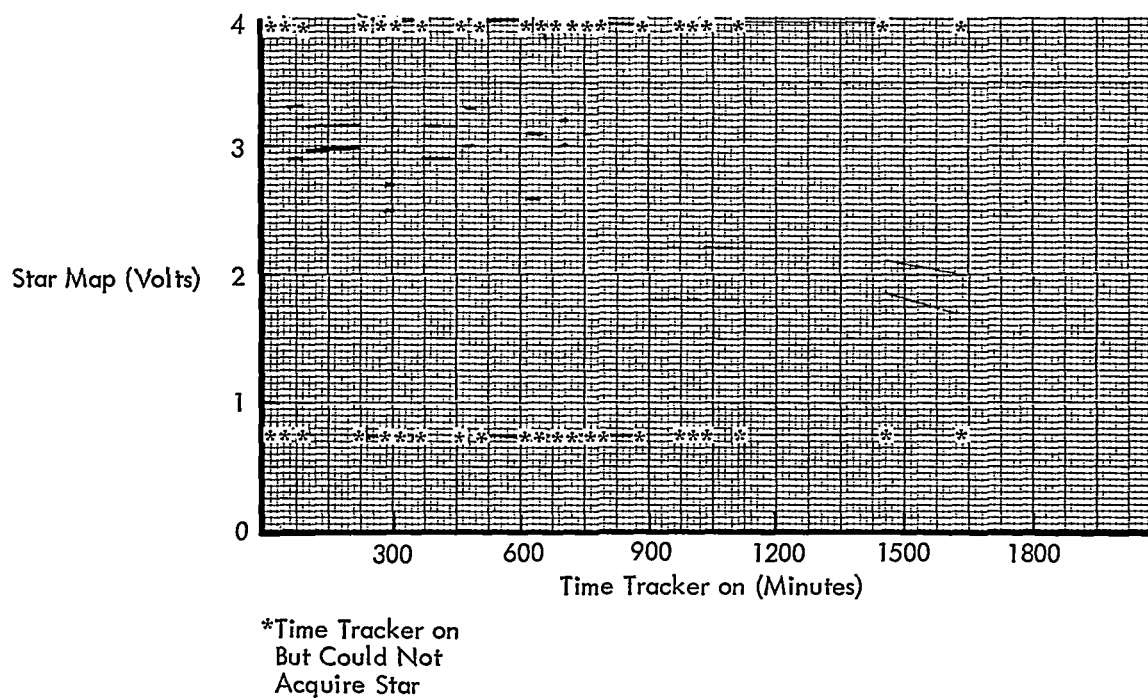


Figure 5-9: Star Map Voltage

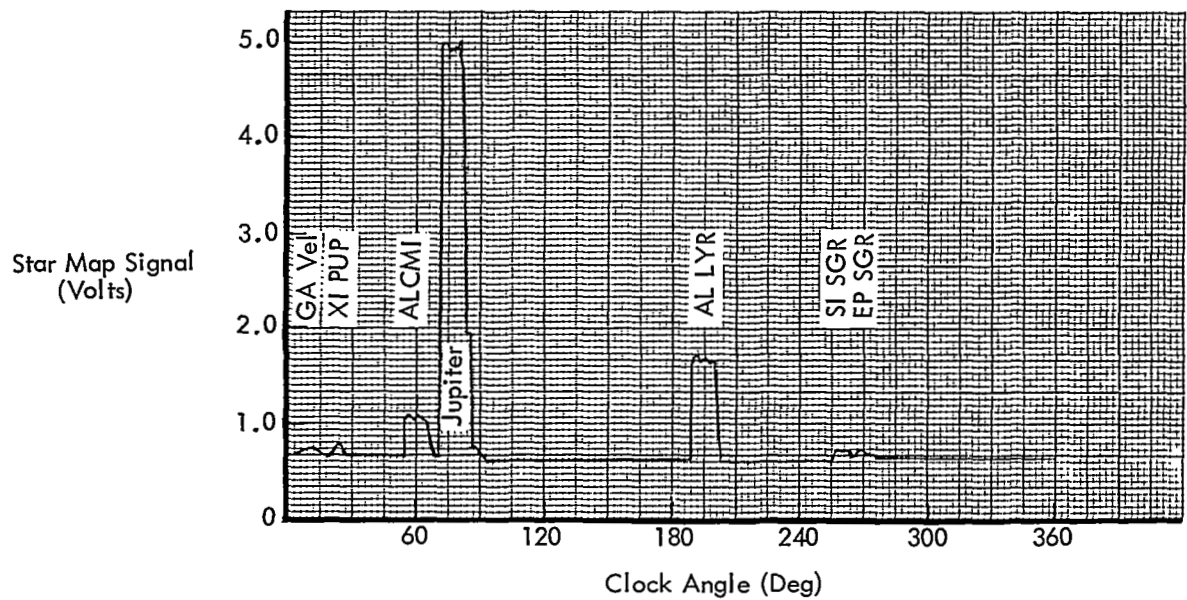


Figure 5-10: A Priori Star Map Day 101

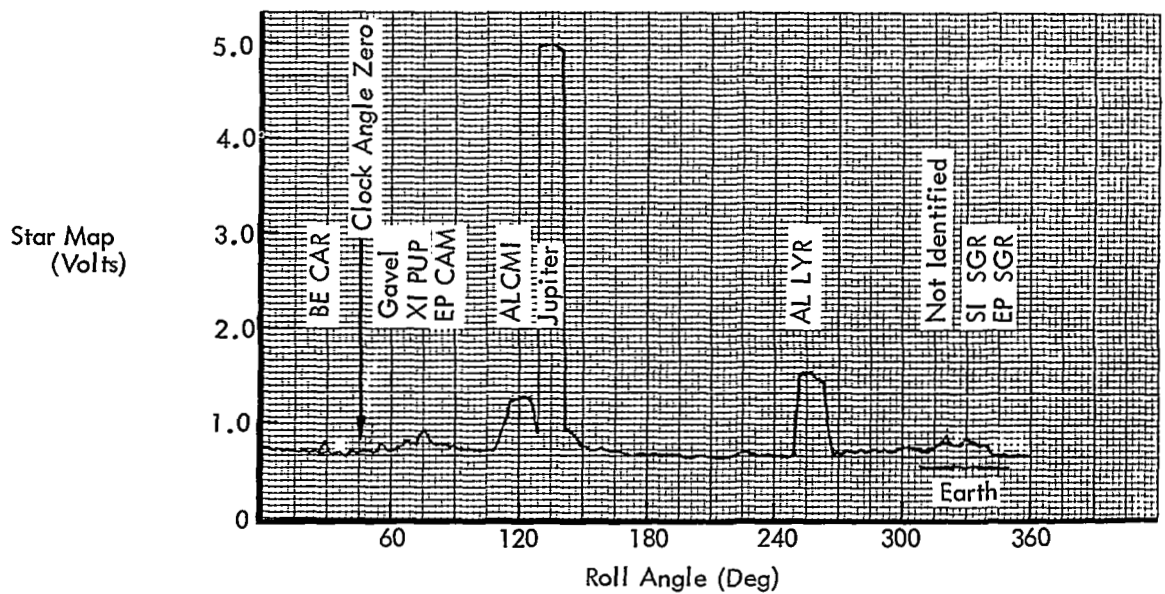


Figure 5-11: Observed Star Map Day 101

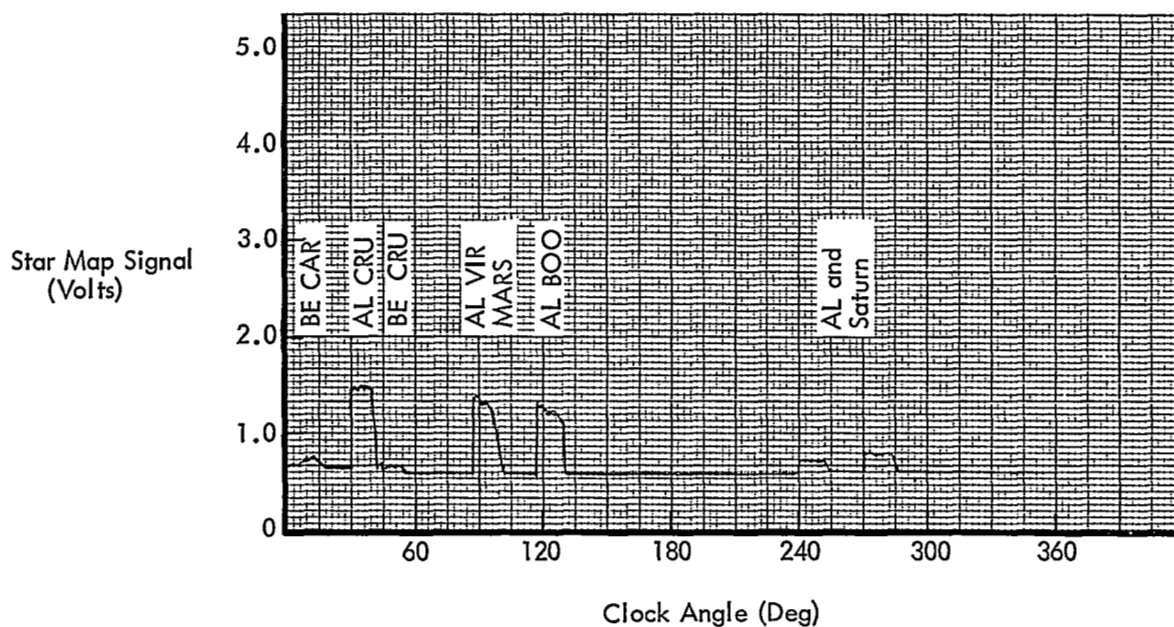


Figure 5-12: A Priori Star Map Day 196

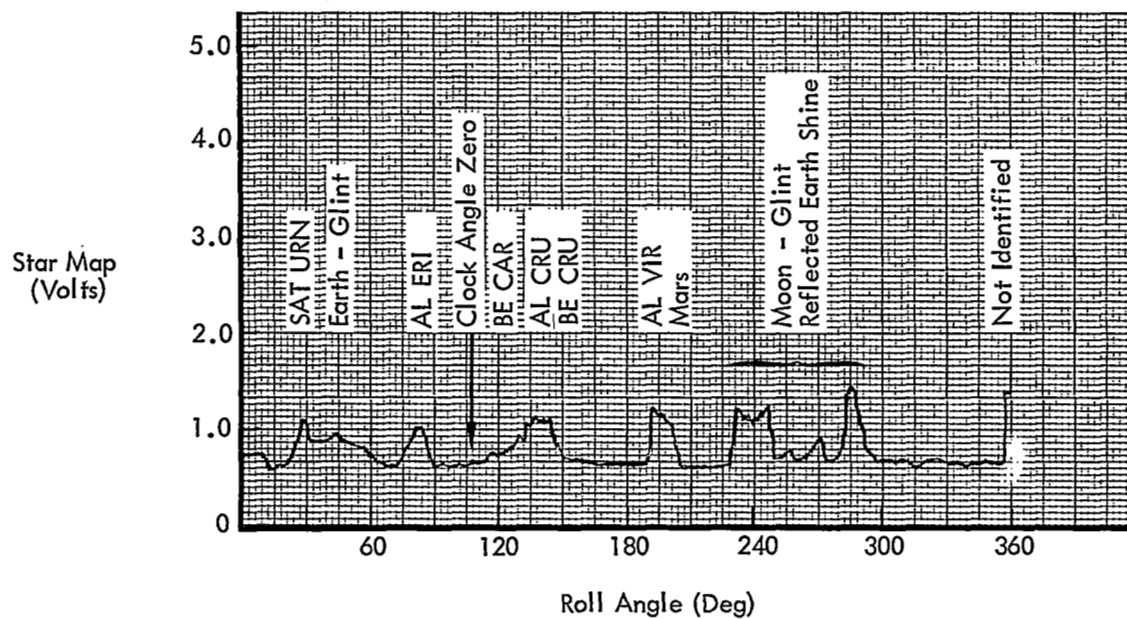


Figure 5-13: Observed Star Map Day 196

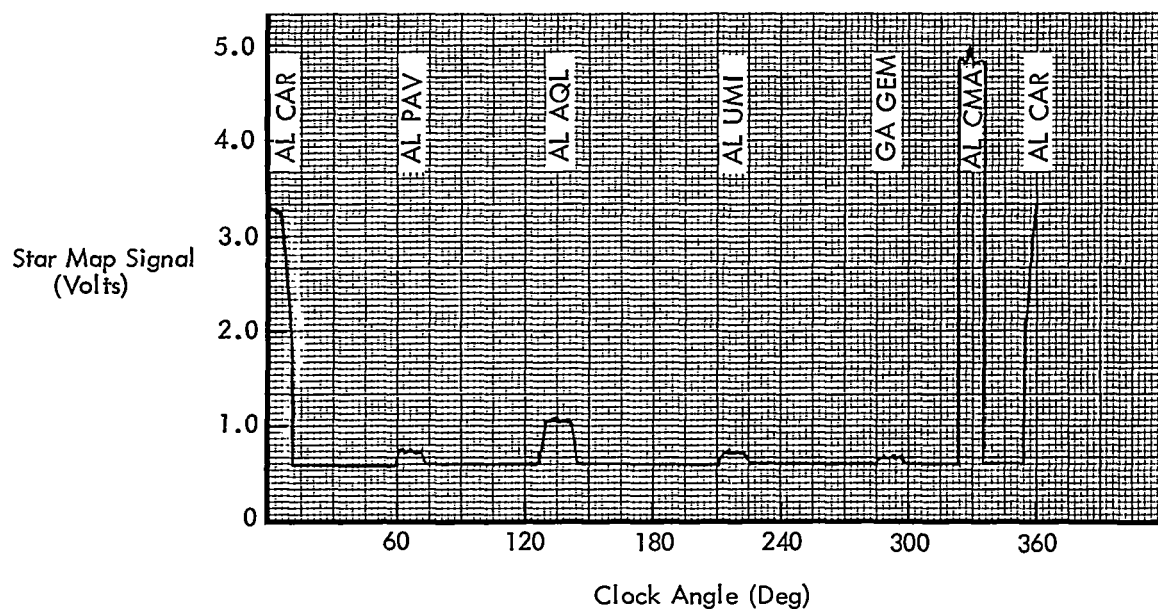


Figure 5-14: *A Priori* Star Map Day 202

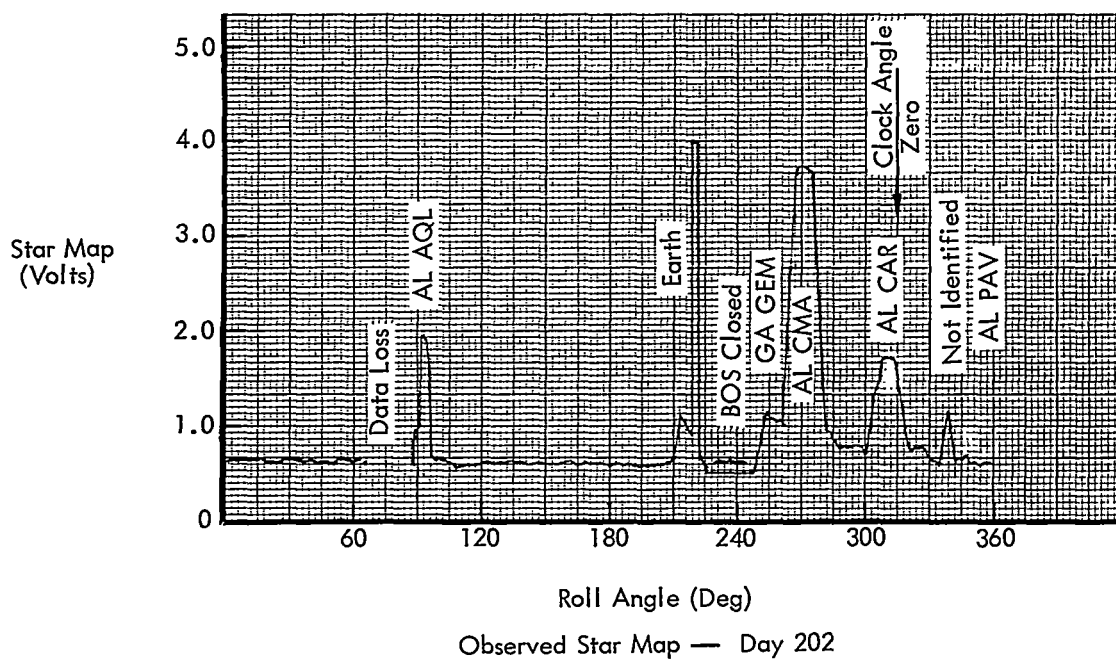


Figure 5-15: Observed Star Map Day 202

Table 5-6: Maneuver Accuracy Summary

Actual Magnitude	Maneuver Error	Percent Error
Roll plus 360 360.19	-1.19	+0.05
Roll minus 360 -359.74	-0.26	-0.07
Pitch plus 360 360.45	+0.45	+0.13
Yaw plus 360 360.56	+0.56	+0.16
Yaw minus 360 -359.89	-0.11	-0.03

In order to save attitude control gas, a pitch minus 360-degree maneuver was not attempted.

Table 5-7: Velocity Maneuver Summary

Orbit Change Date	Orbit Altitude	Desired Trajectory	Actual Trajectory
Day 102	Rp	3562.66 km	3562.45 km
	Ra	1797.35 km	1797.59 km
Day 198	Rp	3564.83 km	3562.14 km
	Ra	1878.34 km	1881.72 km
Day 242	Rp	2054.07 km	3562.14 km
	Ra	1881.65 km	1882.55 km

Table 5-8 tabulates the SIDL data for the star maps generated showing the correlation between predicted and actual star map voltages at predicted and actual clock angles.

5.2.1.3 Switching Assembly

The switching assembly was not used during the extended mission except for velocity maneuvers, firing of the nitrogen isolation squib, and propellant tank heater operation. Performance was normal. No anomalies were observed in the spacecraft telemetry data that would indicate a switching assembly problem.

5.2.1.4 Closed-Loop Electronics

The closed-loop electronics performed satisfac-

torily throughout the extended mission. No anomalies were noted. The minimum-impulse circuit, or "one shot," used to establish minimum jet thruster actuation time appeared to operate between 11 and 14 milliseconds throughout the extended mission (this was the same as observed in Missions I and II). The nominal minimum-impulse value is 11 milliseconds. The minimum-impulse circuit allowed single pulses for approximately 50%, and 20% of the time for the roll, pitch, and yaw axes, respectively. The average limit cycle rate was approximately ± 0.001 degree per second for all axes. The minimum rate increment theoretically possible was 0.0005, 0.001, and 0.001 degree per second for the roll, pitch and yaw axes, respectively.

Compensation networks for the thrust vector control circuitry and the inertial hold circuitry performed correctly. Table 5-9 shows the range of actuator position in degrees controlled through the thrust vector control circuitry.

Table 5-9: Actuator Position Range

GMT Day	Pitch Range (degrees)	Yaw Range (degrees)
102	0.121 - 0.306	0.165 - 0.076
198	0.213 - 0.328	0.098 - 0.142
242	0.167 - 0.236	0.120 - 0.410
282	0.167 - 0.259	0.187 - 0.254

5.2.1.5 Sun Sensors

The yaw sun sensor output voltage at a pitch angle of 40 degrees was approximately 42% of the voltage when oriented on the Sun. Theoretical calculations indicate the change should be 25%. The difference between the actual and calculated is due to shadowing caused by construction of the sun sensor. Moonlight falling on the coarse sun sensors caused shifts in error output at various portions of the orbit but had no detrimental effect on mission performance.

Table 5-8: SIDL Data

GMT Day 101					
SIDL No., Name	Clock A Priori	Angle Observed	Canopus Flux Ratio	Map A Priori	Voltage Observed
27 BE CAR Miaplacidus	343	342	0.09	*	0.74
23 GA VEL	0.7	8	0.01	0.7	0.75
39 XI PUP Naos	15	16	0.1	0.7	0.8
17 EP CMA Adhara	25	25	0.13	0.8	0.94
69 DE CMA Wezen	27	28	0.06	*	0.82
10 AL CMI Procyon	60	62	0.37	1.1	1.2
502 Jupiter	77	75	1.76	Sat.	Sat.
3 AL LYR Vega	194	205	0.44	1.7	1.5
UNKNOWN	*	255	*	*	0.8
34 SI SGR Nunki	259	260	0.12	0.7	0.9
32 EP SGR Kaus Australia	267	264	0.09	0.7	0.86

*Data not available

**Predicted to be 0.4 degree outside yaw field of view

GMT Day 196					
SIDL No., Name	Clock A Priori	Angle Observed	Canopus Flux Ratio	Map A Priori	Voltage Observed
503 SATURN	275	278	0.11	0.8	1.1
601 EARTH "Glint"	272	300	NA	NA	NA
5 AL ERI Achernar	337	341	0.43	**	1.0
28 BE CAR Miaplacidus	19	21	0.09	0.75	0.78
8 AL CRU Acrux	37	37	0.38	1.5	1.3
13 BE CRU Nemosa	42	41	0.16	1.5	1.1
9 AL VIR Spica	90	91	0.35	1.4	1.3
501 MARS	91	91	0.21	1.4	1.3

GMT Day 202					
12 AL AQL Altair	134	136	0.25	1.1	1.8
601 EARTH	278	275	5×10^{-16}	---	---
36 GA GEM Alhena	291	295	0.07	0.8	1.2
1 AL CMA Sirius	324	324	2.33	5.0	3.6
2 AL CAR Canopus	0	0	1.0	3.5	1.8

Spacecraft operation in the celestial hold limit cycle produced deadband data shown in Table 5-10. There was little or no degradation nor any detectable null shift in sun sensor output during the extended mission (see Table 5-11). Test measurements indicated that the five sun sensors would cause a null offset of +0.05 degree in pitch and +0.06 degree in yaw. Table 5-12 confirms these values.

Table 5-10: Deadband Data

0.2 Deadband			
Axis	Design	+Edge	-Edge
Pitch	$\pm 0.18 \pm 0.03$	0.174	0.169
Yaw	$\pm 0.18 \pm 0.03$	0.178	0.189
2.0 Deadband			
	Design	+Edge	-Edge
Pitch	$\pm 2 \pm 0.3$	1.829	1.883
Yaw	$\pm 2 \pm 0.3$	1.881	1.902

Table 5-11: Sun Sensor Null Output (degrees)

	Pitch	Yaw
<u>Fine</u>		
Ground Test	-0.093 to +0.097	-0.140 to +0.052
Start of Ext. Mission	+0.002	-0.044
End of Ext. Mission	-0.005	-0.042
<u>Coarse</u>		
Ground Test	-0.395 to +0.750	-0.343 to +0.814
Start of Ext. Mission	-0.11	+0.24
End of Ext. Mission	-0.21	+0.20

Table 5-12: Sun Sensor Null Offset

PITCH (deg)		
	Ground Test	Flight
Fine	+0.002 to +0.100	+0.051
Coarse	-0.053 to +0.537	+0.24
YAW (deg)		
	Ground Test	Flight
Fine	-0.034 to +0.061	+0.061
Coarse	+0.126 to +0.690	+0.41 to +0.69

5.2.1.6 Control Assembly

During the extended mission the control assembly responded correctly to every received and stored-program command.

A total of 2,553 commands were transmitted and executed during the extended mission. Since many of these were repetitive, the programmer actually executed some 5,444 commands. Moreover, the programmer cycled 2 billion times and accumulated 200 million clock incrementations while directing spacecraft operation. The total clock error as of Day 282 was minus 2.68 seconds for a slope of 0.4 millisecond per hour. This drift is well within the design tolerance of 3.4 milliseconds per hour.

5.2.2 Communications Subsystem

The communications subsystem (see Figure 5-16) consists of the equipment which: (1) receives information from the ground via an rf link and converts this information to a form suitable for use by the spacecraft; (2) receives information from the spacecraft (telemetry and video), converts this information to modulation on an rf carrier, and transmits this modulated rf carrier

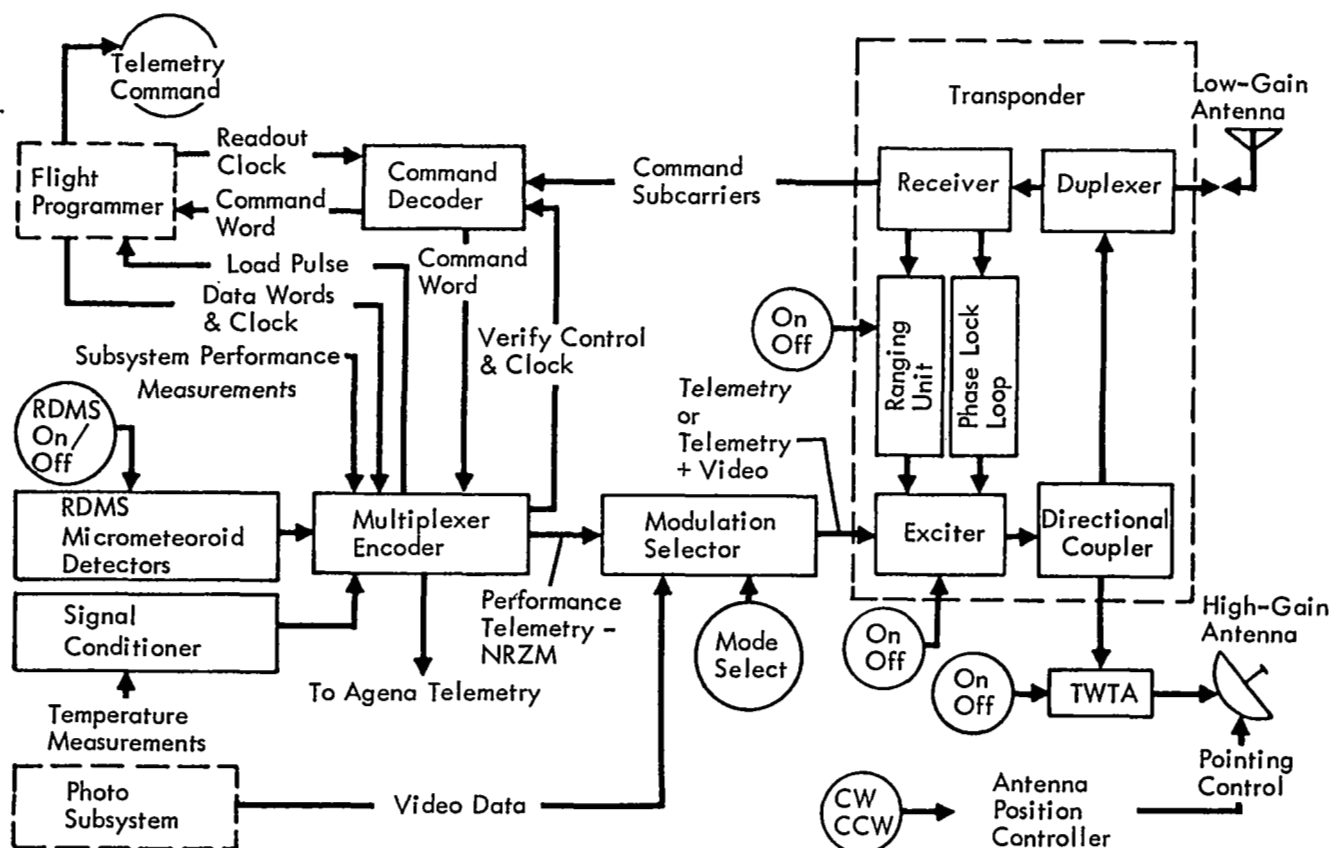


Figure 5-16: Communications Subsystem

to the ground; (3) receives ranging information from the ground via rf link, modulates this information on an rf carrier, and retransmits this to the ground for use in range determination; and (4) establishes a specific ratio between the received rf frequency from the ground and the spacecraft-transmitted frequency for accurate determination of the spacecraft velocity using doppler information.

The communications subsystem operated nominally throughout the extended mission while performing the following functions.

Command Capability – The command loop received, verified, and executed 1,080 RTC's and 1,473 SPCS commands without error; the use of command decoder redundant command register was never required. The communications subsystem responded to all operational commands as directed. Three spurious commands were executed by the Mission III flight

programmer during Mission IV and three more were executed during Mission V (refer to Sections 3.1.1, "Command Activity," and 5.3.5, "Transponder Threshold").

Spacecraft Performance Information – Telemetry data from all spacecraft subsystem transducers were compiled and transmitted with desired accuracy.

Lunar Environment Information – As a primary objective of the extended mission, radiation and micrometeoroid data were provided by the communications subsystem throughout the extended mission.

Photographic Information – Although the communications subsystem maintained this capability, no video data were transmitted during the extended mission.

Selenodetic Information – Ranging and co-

herent doppler data with one and two tracking stations were successfully provided throughout the extended mission. Time correlation between tracking stations was accomplished using the ranging system.

5.2.2.1 Transponder

The transponder was "on" and operated satisfactorily throughout the extended mission. Telemetry indication of transponder rf power output variations with transponder temperature and equipment mounting deck temperature is shown in Figures 5-17 and 5-18, respectively. The decrease in power output with increasing temperature is normal and compares favorably with the FAT data. Actual power output variation is only about one-third to one-half that indicated by telemetry because of the temperature sensitivity of the transponder power output signal sampler. Figure 5-19 portrays typical transponder rf power output versus transponder temperature during the extended mission. Exceptional correlation exists between telemetry-indicated power output and temperature.

For constant uplink rf carrier power with no command or ranging modulation present, transponder automatic gain control remained within ± 2 dbm. The transponder ranging module was "on" throughout the extended mission and approximately 80 hours of ranging data were obtained.

No problems were encountered with ground-received signal strength and the transponder fulfilled all design requirements while operating for 247 days.

5.2.2.2 Traveling-Wave-Tube Amplifier

The TWTA was used to provide a high-power signal for the extended-mission exercises and for tracking by the manned spaceflight network stations. The TWTA was cycled on and off 64 times and had accumulated an operating time of 41.92 hours. At the completion of Extended Mission III on Day 282, the TWTA had been cycled on and off for a total of 178 times and operated 196.92 hours from launch.

Except for the telemetry indication of rf power output being excessively temperature sensitive, TWTA operation throughout the extended mission was nominal, as indicated by Figure 5-20. Actual rf power output was within the normal 10- to 12-watt range, as evidenced by proper ground-received signal strength. The telemetered voltage is obtained from a diode power monitor in the filter/monitor assembly located within the TWTA. An adjustable probe extracts a small amount of the S-band energy present at the filter input. The rf signal is rectified by two Type IN831A point-contact diodes connected in series across the probe to ground. The most probable cause of the error in telemetry indication of rf power output was a gradual shift in the diode rectification characteristics with temperature. The problem was unique to the Mission III TWTA.

5.2.2.3 Command Decoder

The command decoder performed as planned throughout the extended mission; there were no errors in any of the verified words that were executed into the flight programmer.

5.2.2.4 Modulation Selector

Operation of the modulation selector was satisfactory. No problems or anomalies were encountered. The subcarrier telemetry frequencies were well within specification requirements.

5.2.2.5 High- and Low-Gain Antennas

Both the high- and low-gain antennas performed satisfactorily throughout the extended mission. Based on DSS-received signal levels, the gain and directivity of both antennas were nominal as expected.

5.2.2.6 High-Gain Antenna Position Controller

The antenna position controller responded successfully to all rotation commands and the encoder that telemetered rotation angle functioned correctly. During exposure to outer space environment, the antenna was rotated a total of 654 degrees to the left and 1,261 degrees to the right. The portion of this total rotation accumulated during the extended mission was 448 degrees left and 746 degrees right.

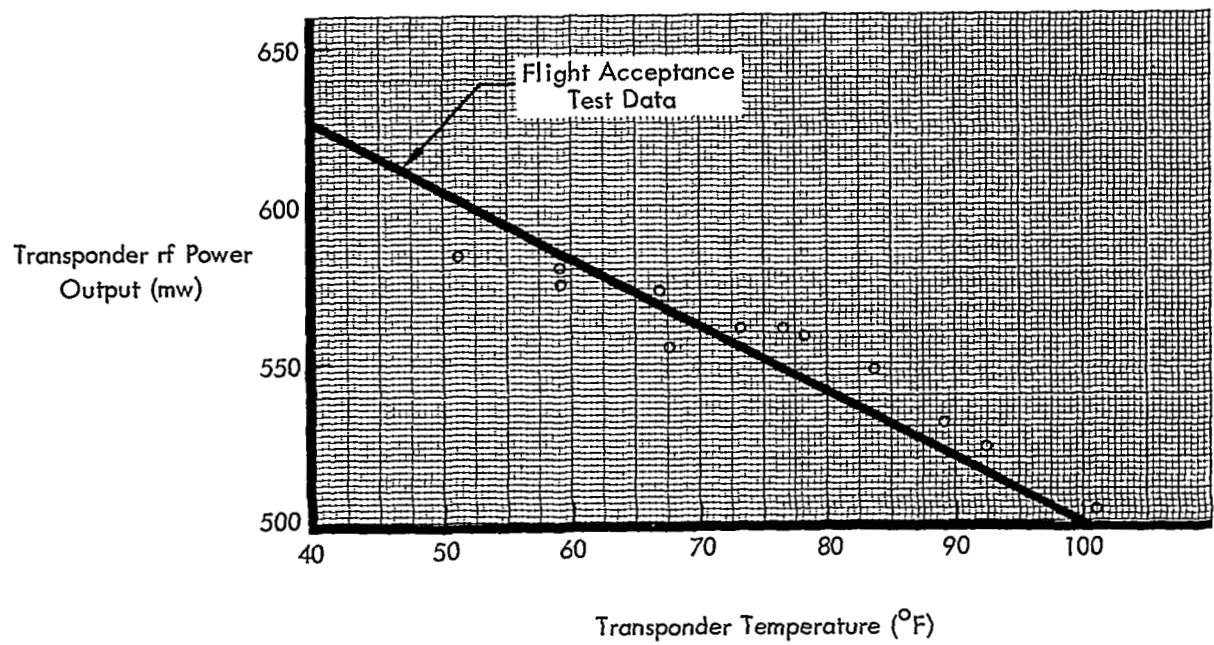


Figure 5-17: Transponder Temperature versus Power Output

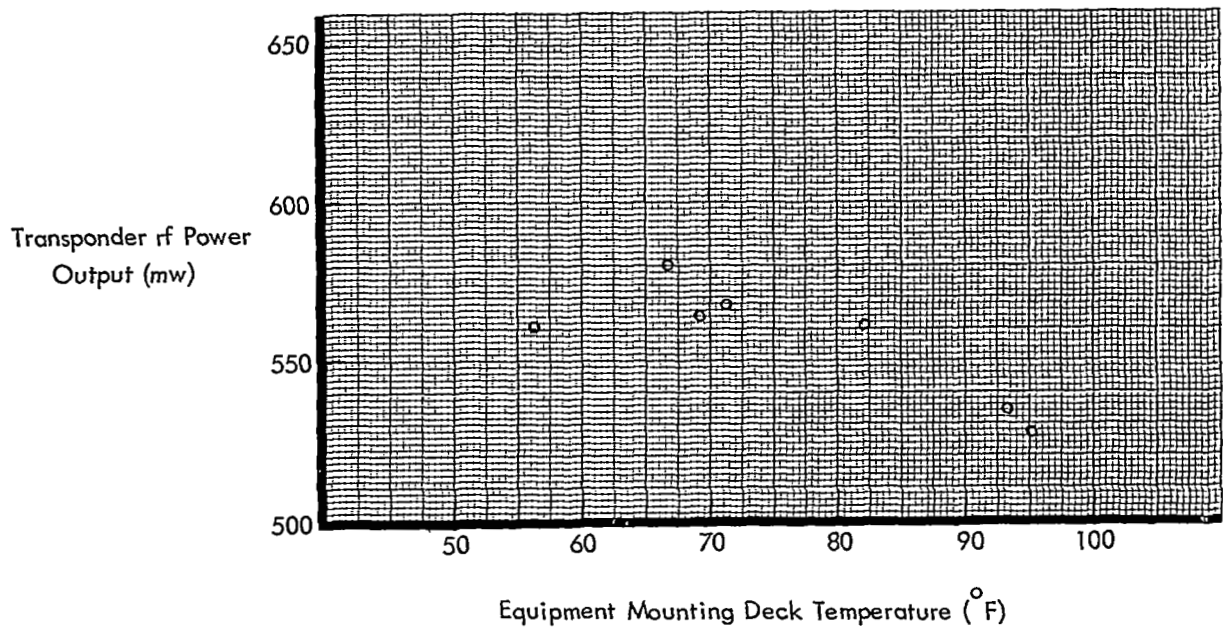


Figure 5-18: EMD Temperature versus Transponder Power Output

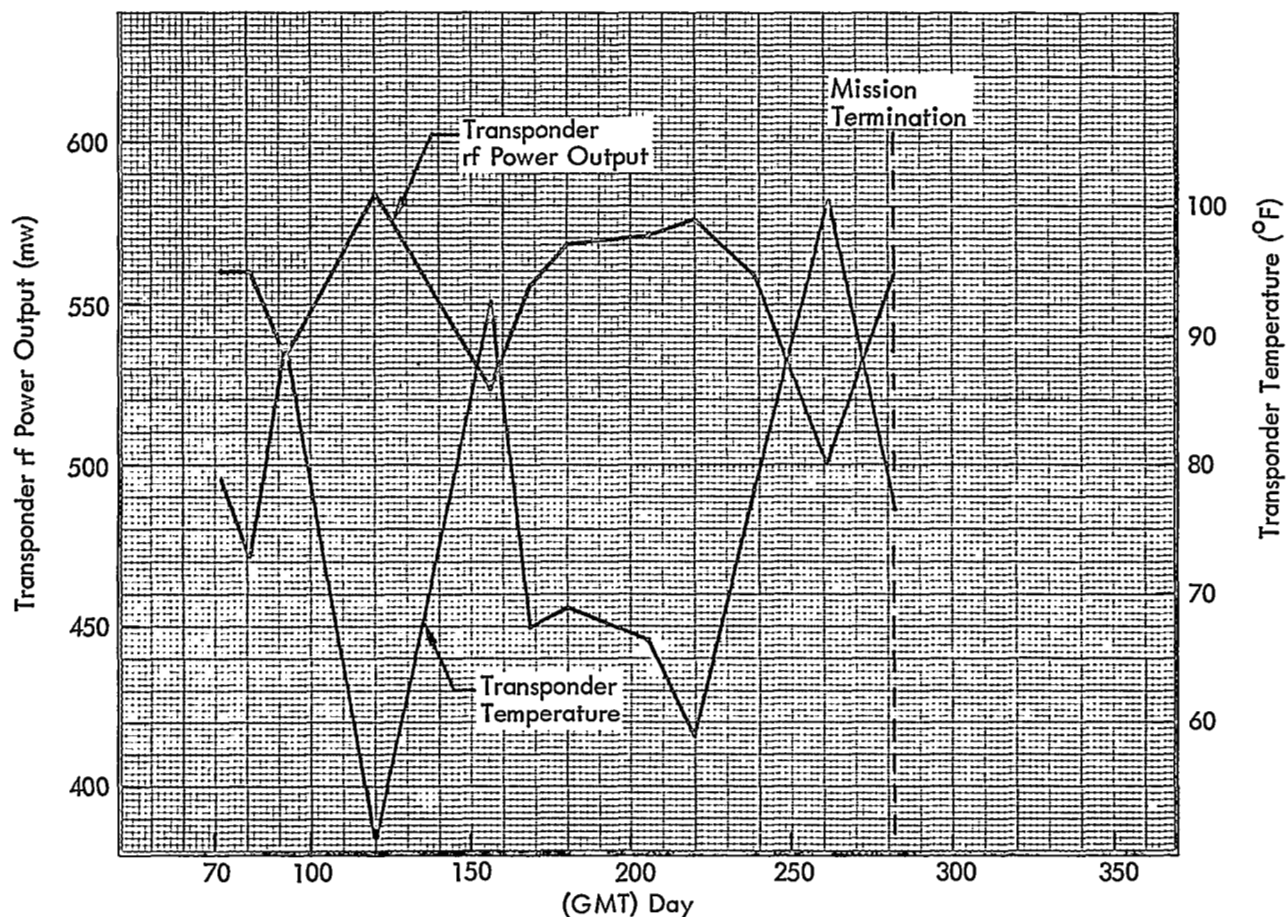


Figure 5-19: Transponder Performance

5.2.2.7 Radiation Dosage Measurement System (RDMS)

The RDMS continued to function normally during the extended mission.

5.2.2.8 Micrometeoroid Data

At the initiation of the extended mission, one micrometeoroid hit had been recorded by Detector 17; four additional micrometeoroid hits were experienced by the spacecraft detectors.

5.2.3 Power Subsystem

The electrical power subsystem is the sole source of all electrical power used by the spacecraft as it performs all phases of its space mission. Radiant solar energy is collected by 2,714 N-on-P solar cells mounted on each of four solar panels and is converted into electrical energy. This energy supplies all spacecraft

loads, power subsystem losses, and charging current to the nickel-cadmium battery. The shunt regulator dissipates excessive electrical energy in power-dissipating elements mounted externally to the spacecraft thermal shield. The shunt regulator also limits the bus voltage to less than 31 volts. A charge controller protects the battery from overvoltage and overtemperature conditions by regulating the charging current. The 12-ampere-hour battery provides electrical power to the spacecraft loads during periods of Sun occultation. Refer to Figure 5-21 for a functional schematic of the subsystem.

5.2.3.1 Solar Array

The solar array operated normally throughout the extended mission. Sufficient power was provided to maintain a constant bus voltage of 30.56 volts when in the sunlight. Solar panel degradation was minimal. Total solar panel out-

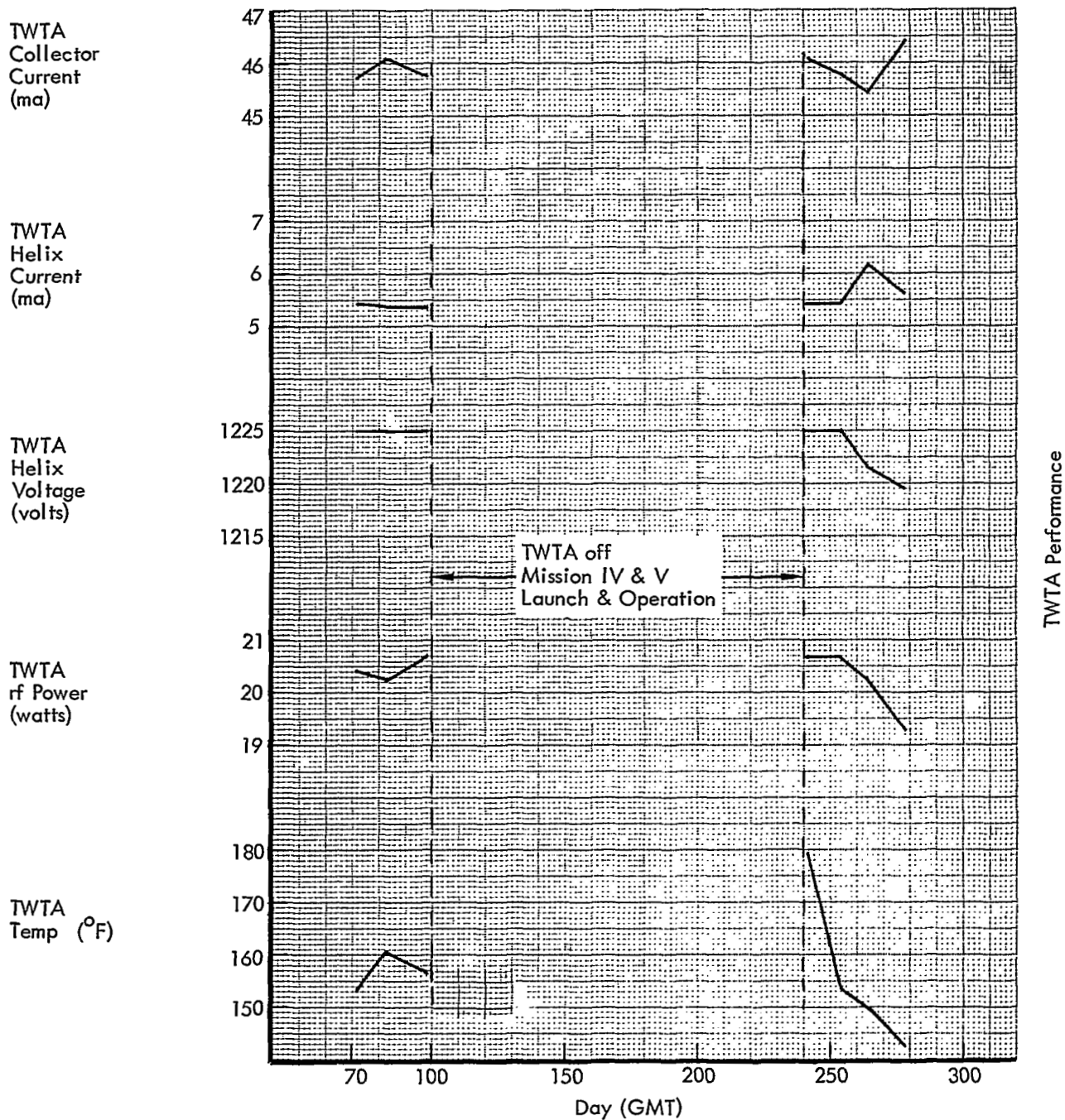


Figure 5-20: TWTA Performance

put power at Lunar Orbiter IV launch was 13.30 amperes at 30.56 volts. As the mission progressed, the output power varied with time as a function of solar-cell degradation and the

changing solar constant (see Figure 5-22); the curves are adjusted to an equal solar constant. By the end of the extended mission, performance degradation was 6.1%.

5.2.3.2 Shunt Regulator

The shunt regulator started exhibiting an irregular mode of operation on GMT Day 226. It drew current when the bus voltage was below

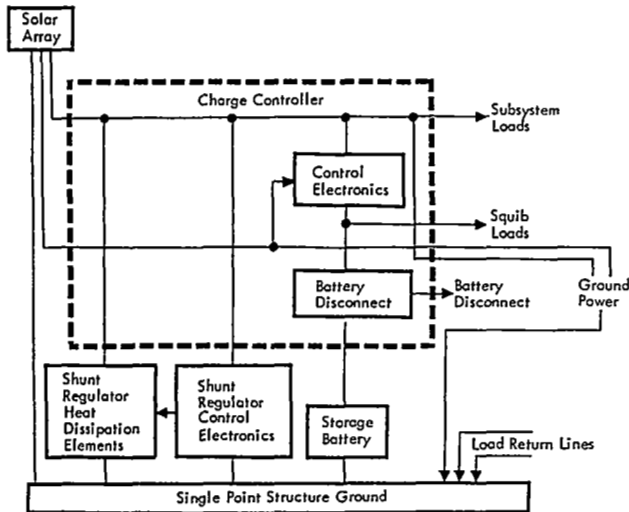


Figure 5-21: Power Subsystem

30.0 volts, which occurred randomly both during periods of battery discharge and periods of battery charge during large solar-array off-Sun angles when no current should have been shunted. The shunted currents under these conditions ranged from 0.13 to 0.56 ampere. A leakage current was proportional to bus voltage. This new operational mode did not affect the quality of the power supplied to the spacecraft. Insufficient information is available from telemetry data to develop an explanation for this phenomenon. The characteristics do not parallel the failure mode experienced earlier on the Lunar Orbiter I power transistor assembly.

5.2.3.3 Charge Controller

Charge controller performance was normal throughout the primary and extended mission. The charge rate, which is a function of battery temperature and voltage, was controlled to the proper level at all times. No charge controller anomalies were observed.

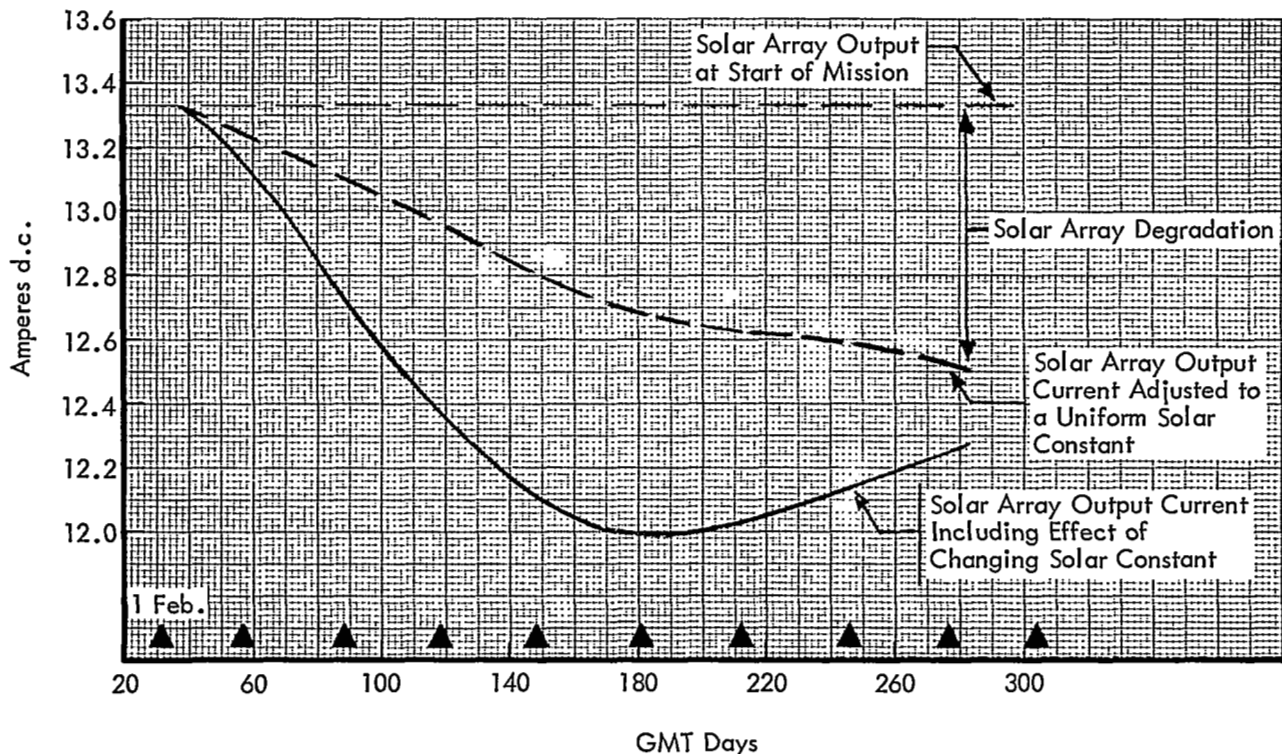


Figure 5-22: Solar Array Degradation

5.2.3.4 Battery Performance

Battery performance was normal throughout the primary and extended missions. Adequate electrical power was provided to the spacecraft during all off-Sun maneuvers and Sun occult periods, including the April 24, 1967 eclipse. Battery temperatures were higher than desired and the battery may have sustained some memory effect; Figure 5-23 shows the battery end-of-discharge parameters observed. Load and temperature variations caused by spacecraft activities and the limited number of orbits monitored preclude obtaining a good battery end-of-discharge voltage trend. The dashed line represents an approximation of the end-of-discharge voltage decay, which indicates that a small degree of memory may have been present.

Battery deep-discharge tests were conducted on Days 112 and 274 to erase possible battery memory effects. Complete correction of memory requires removing all energy from the battery, but since this was not possible, only a partial erasure of memory was attempted. A typical Sun occult discharge curve is shown in Figure 5-24 and a deep discharge characteristic is shown in Figure 5-25. The normal discharge removed 2.79 ampere-hours and the deep discharge removed 5.47 ampere-hours of energy.

After sustaining 1,747 charge-discharge cycles, the battery was subjected to a deep discharge over a period of four Sun occults by increasing the load, extending the discharge period, and not fully recharging the battery between suc-

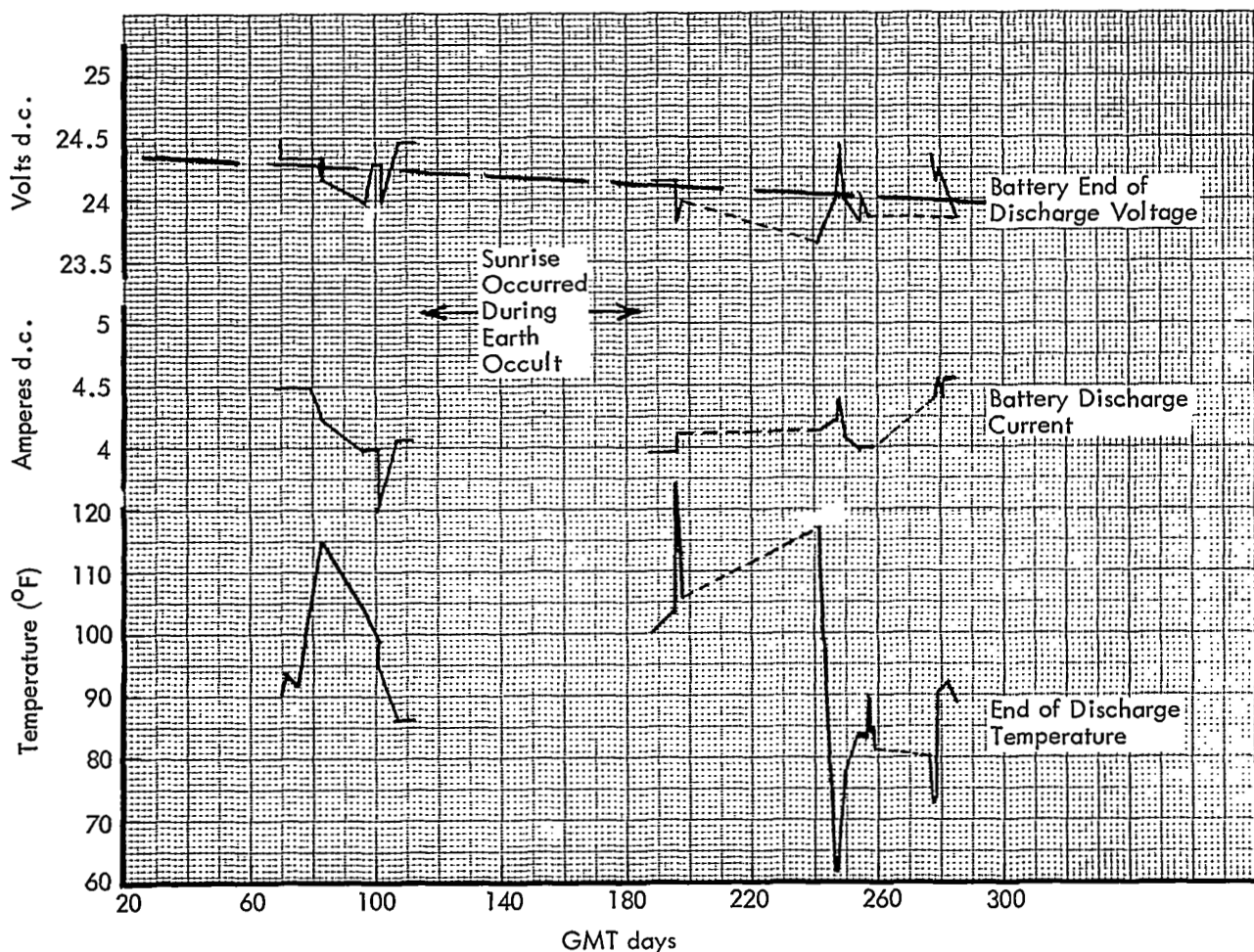
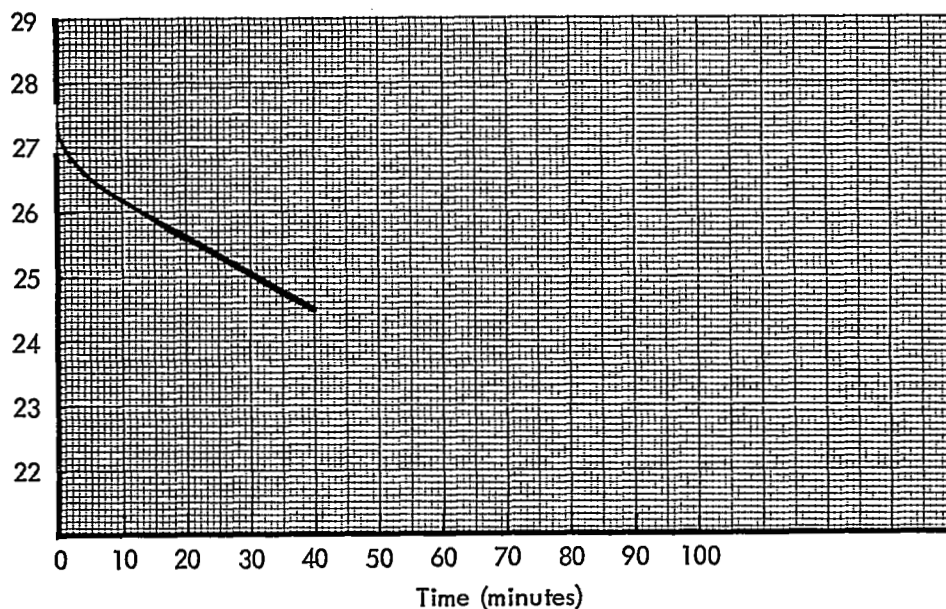


Figure 5-23: Battery Performance Characteristics

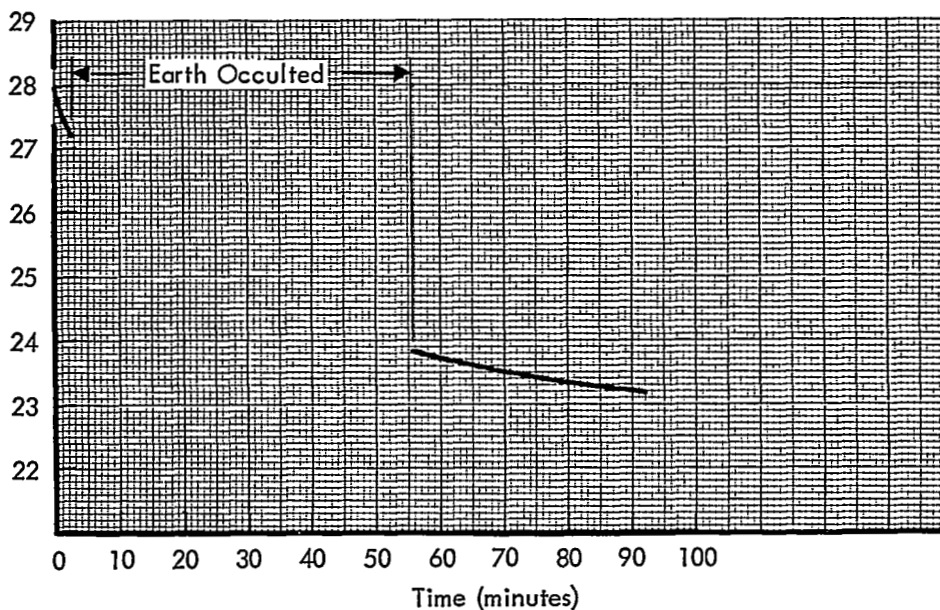
Battery Voltage
(volts d.c.)



Battery normal discharge starting on GMT 107:11:02,
Orbit 458. Average current = 3.93 amperes.
Energy removed = 2.79 ampere-hours.
Battery temperature ranged from 91.2 to 83.9°F.

Figure 5-24: Battery Performance Characteristics

Battery Voltage
(volts d.c.)



Battery deep discharge starting on GMT 112:04:49,
Orbit 498. Estimated average current was 4.0 amperes.
Estimated energy removed = 5.47 ampere-hours.
Battery temperature ranged from 62 to 79°F.

Figure 5-25: Battery Performance Characteristics

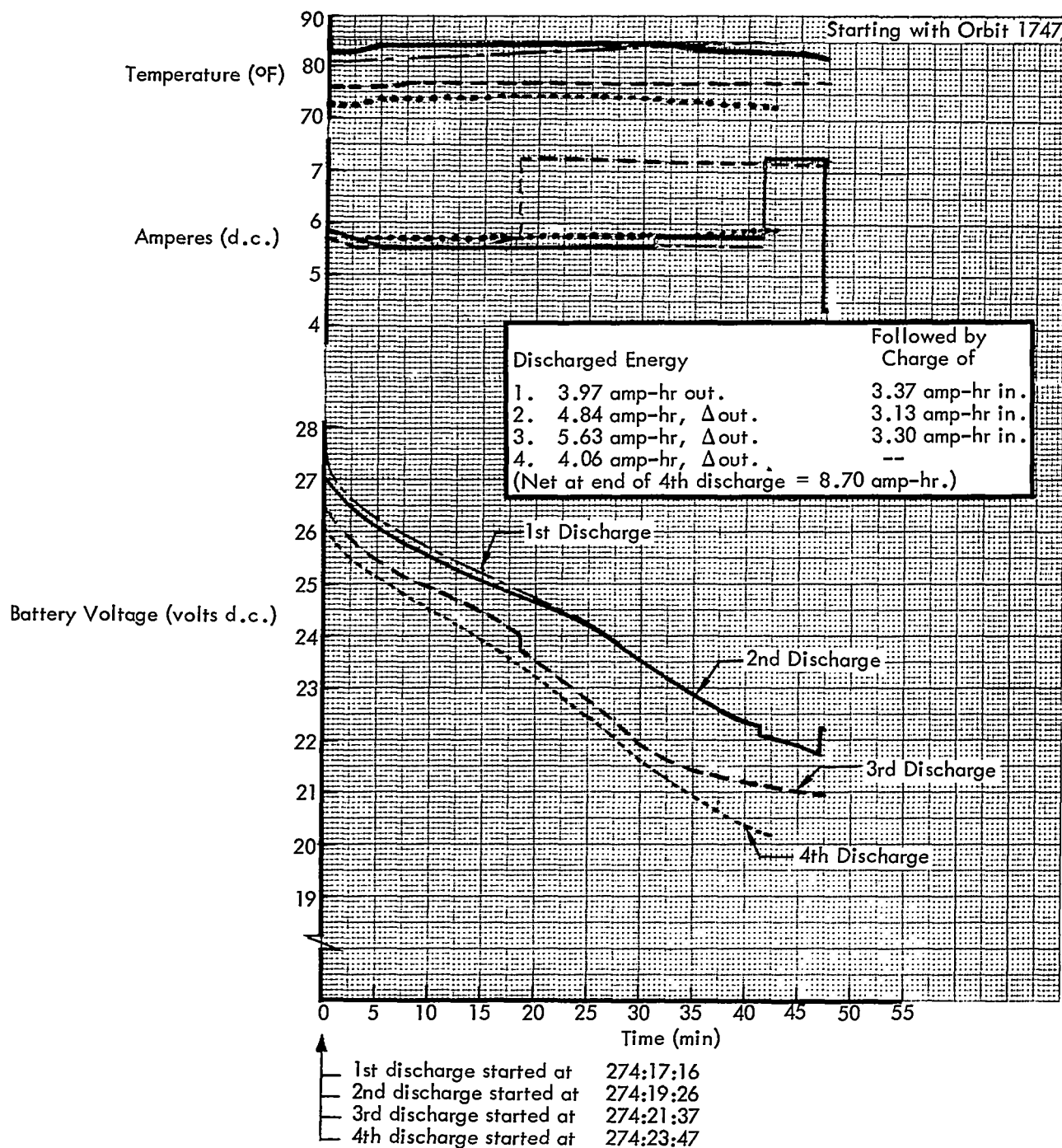


Figure 5-26: Battery Discharge Performance

cessive deep discharges. This method permitted approaching the desired depth of discharge gradually. In addition to healing memory effect, the objective was to evaluate the condition of the battery to determine if it could carry the

spacecraft through the October 18 eclipse. Figure 5-26 shows that the battery capacity after 1,747 cycles was between 8.5 and 9 ampere-hours at approximately the 2-hour rate of discharge. These deep-discharge data were

included in the data reviewed by the contractor and the customer when the decision was made to crash the spacecraft prior to the eclipse.

The temperatures plotted on Figure 5-23 reflect the end-of-discharge temperatures. Seventeen higher temperatures reached during battery charge periods that contributed to the 6.1% degradation are given in Table 5-13.

Table 5-13: Battery Temperature Data

<u>GMT Day</u>	<u>Battery Temperature</u>
78	110.8°F
83	115.0°F
85	117.7°F
86	126.0°F
92	113.4°F
94	101.1°F
95	115.3°F
102	104.2°F
114	105.1°F
132	114.0°F
196	106.0°F
197	109.7°F
198	109.7°F
241	130.5°F
242	130.8°F
279	96.4°F
267	97.5°F

5.2.4 Photo Subsystem

The photo subsystem is housed in a pressurized,

thermally controlled container, and includes the camera, lens, film, and film handling, film processor, and readout equipment and environmental controls (see Figure 5-27). The subsystem is designed to expose, develop, and read out images for transmission to Earth via the communications subsystem.

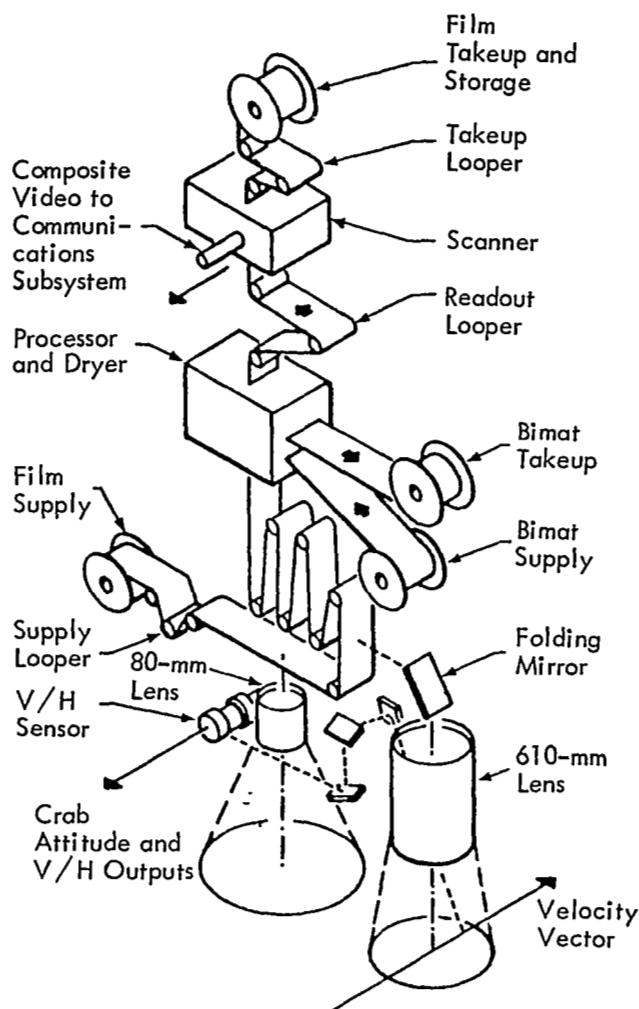


Figure 5-27: Photo Subsystem

Status of the various subsystems during the extended mission (from Day 68 on) follows.

5.2.4.1 Camera and Lens

There was no activity during the extended mission because all photography was completed on Day 53. The V/H sensor was operated in support of the special exercises described in Section 5.3. The shutter was set from 1/100 to 1/25 second on Day 112 to facilitate detection of a preset pulse

and/or photo subsystem logic changes. The photo subsystem responded nominally to all commands involved in this shutter setting sequence.

5.2.4.2 Film Processor

There was no film processor activity during the extended mission because processing and Bimat cut were completed on Day 53.

5.2.4.3 Film Handling

Failure of the film advance motor during the regular mission precluded further film handling in either the wind-forward direction (supply spool to takeup spool) or final-readout direction (readout looper to supply spool). However, film could be, and was, transported from the takeup to the readout looper (in the final readout mode) until the readout looper was filled. This film was then returned to the takeup reel by entering the wind-forward mode with a "camera on" command.

At the start of the extended mission, with the readout looper full, the readout index was 70.00.

Prior to the squib firing sequence conducted prior to the orbit phasing maneuver on Day 101, the photo subsystem was placed in the readout standby mode and its performance monitored for any logic changes produced by the shock of firing. No logic changes were noted. The command sequence (Table 5-14) was used in conjunction with the squib firing sequence, with responses as noted.

Table 5-14:
Photo Subsystem Command Sequence

Time (GMT)	Command	Response
101:20:12	"Solar eclipse off"	Command verified.
20:15	"Camera on"	Readout looper emptied normally and the shutter began repetitive operation.
20:18	"Bimat cut"	Command verified.
20:24:38	"Squib firing sequence"	Logic condition remained unchanged during sequence.
20:27	"Solar eclipse on"	Camera turned off.

The responses noted were expected since the film advance motor failure prevented completion of a picture taking sequence, thus allowing continuous shutter operation until termination by non-normal means.

5.2.4.4 Readout Equipment

A readout sequence was initiated on Day 101 in an attempt to fill the readout looper which had been emptied by the command sequence table prior to the squib firing sequence earlier. Since the film to be moved into the looper had been read out previously, the TWTA was not turned on. Telemetry indicated that, when "readout electronics on" was commanded, the high voltage reached a peak of 15.84 kv rather than a normal value of 20 kv, dropped to 1.54 kv in approximately 4 minutes, and then varied between 1.54 and 3.90 kv. In approximately the same period, the peak video indication increased to a normal value of 4.85 volts and then decayed to zero. During the time that the electronics was on, the LST cathode current remained constant, and normal, at 19.95 microamperes. An abnormal increase in spacecraft load current was noted at the time of electronics turn on. Photomultiplier power supply voltage increased to and remained at normal value of 1,800 volts during the attempted readout sequence. Readout looper contents increased normally. Analysis of these events indicated a high-voltage power supply failure.

On Day 114, another readout sequence was attempted with the TWTA on. At this time the previous indicated failure was confirmed; i.e., high-voltage and peak video voltage remained essentially zero after "readout electronics on." No attempt was made to advance film into the readout looper, the readout sequence being terminated by a "readout drive off" command as soon as the continued presence of the failure was confirmed.

Analysis of the failure, based on the telemetry and previous test experience, led to the conclusion that the most probable cause of failure was a short circuit on the secondary of the high-voltage supply. This short most likely was produced by breakdown of one of the following.

- High-voltage lead;
- Secondary windings of either one of two high-voltage transformers;
- Line scan tube anode.

Since only an incomplete analysis was possible with available data, and since this was the first high-voltage failure at the photo subsystem level, either in test or in flight, it was considered to be an isolated event for which no corrective action was possible.

5.2.4.5 Environmental Controls

Environmental conditions during the extended mission were normal. A gradual decrease in internal photo subsystem pressure was noted, but not to the point that makeup nitrogen from the internal pressurization system was required. The variations in nitrogen bottle pressure were considered to be normal, corresponding to variations in photo subsystem temperatures. Table 5-15 shows representative photo subsystem pressures and temperatures throughout the extended mission.

Photo subsystem heaters were inhibited on Day 095 and were not enabled until Day 274, at which time they were successfully enabled for two periods of 5 minutes and 32 minutes, respectively, to provide additional loads during the battery discharge test.

5.2.5 Structures and Mechanisms Subsystem

The structures and mechanisms subsystem consists of the support structure, thermal control coatings, thermal barrier, engine deck heat shield, solar panel and antenna deployment mechanisms, camera thermal door, rocket engine gimbal, bipropellant tank heaters, and the interconnecting electrical wiring.

With the exception of the camera thermal door (CTD) and the rocket engine gimbal, this subsystem is in a passive state during the extended mission. Only the thermal control coating performance is discussed since the remainder of the subsystem performed as anticipated.

5.2.5.1 EMD Thermal Control Coating

The Mission III EMD thermal control coating was the same as Mission II (2 mils of S13G over 8 mils of B1056). This coating, combined with orienting the spacecraft "off-Sun," provided adequate thermal control during Mission II. Since the solar intensity for Mission II was the maximum that would be encountered, it demonstrated that this coating would provide satisfactory thermal control for Mission III. During the extended mission the spacecraft was oriented

Table 5-15:
Photo Subsystem Temperatures and Pressures

GMT Day	Internal Pressure (psia)	Nitrogen Bottle Pressure (psi)	Readout Thermal Fin Temp. (°F)	Lower Environ. Temp. (°F)	Upper Environ. Temp. (°F)
111	1.28	2,098	46.6	45.2	45.6
197	1.20	2,186	66.5	63.6	64.2
243	1.20	2,215	67.1	68.2	68.9
255	1.04	2,215	72.6	67.4	66.7
264	1.12	2,215	65.5	61.7	65.0
282	1.12	2,230	80.7	73.1	72.6

approximately 45 degrees off-Sun for thermal control. Figures 5-28 through 5-35 show the EMD temperatures and approximate spacecraft angle "off-Sun." The extent to which the thermal control coating degraded cannot be determined

because the spacecraft attitude was not maintained constant for a sufficient period of time to allow the EMD temperature to stabilize during tracking periods.

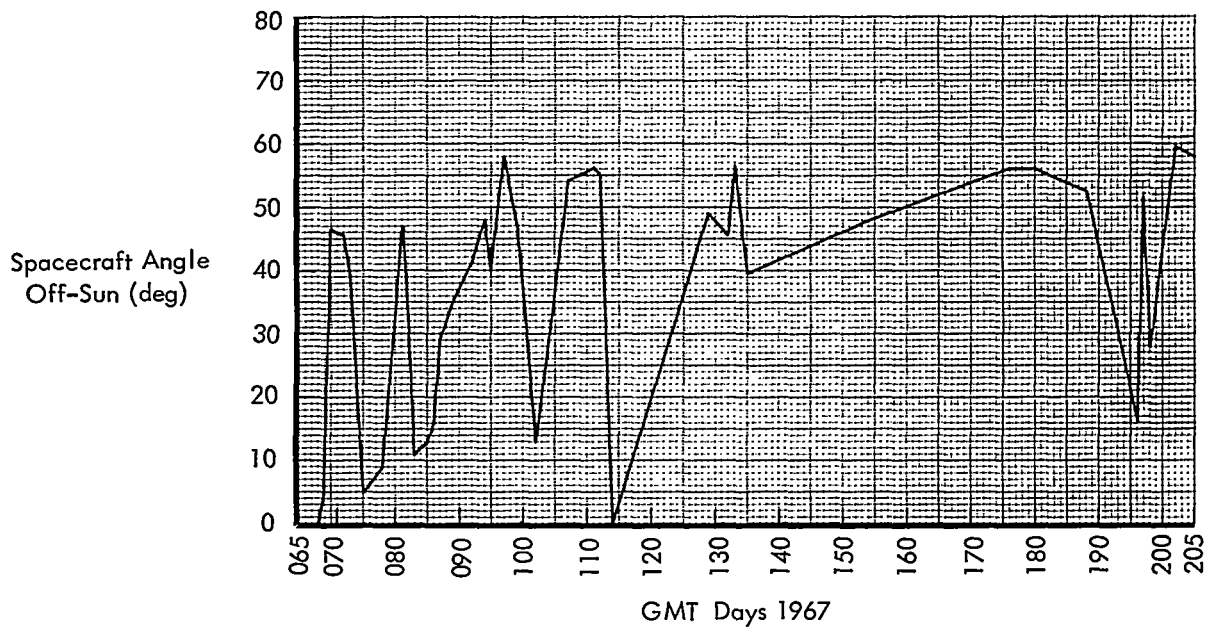


Figure 5-28: Pitch Angle History

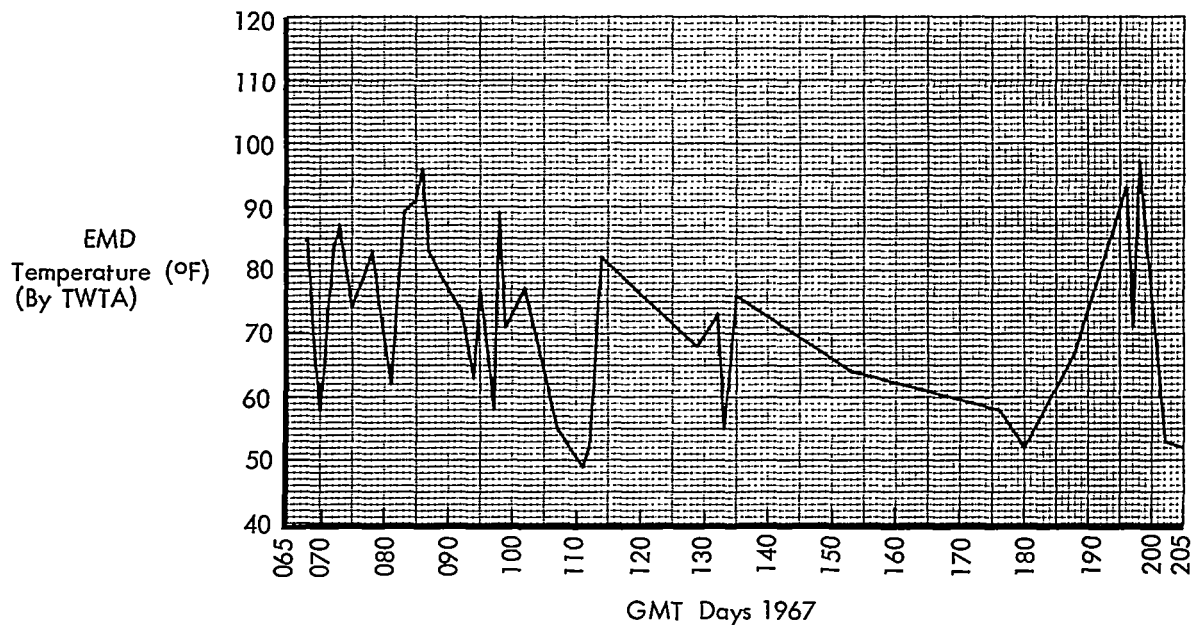


Figure 5-29: EMD Temperature History (TWTA)

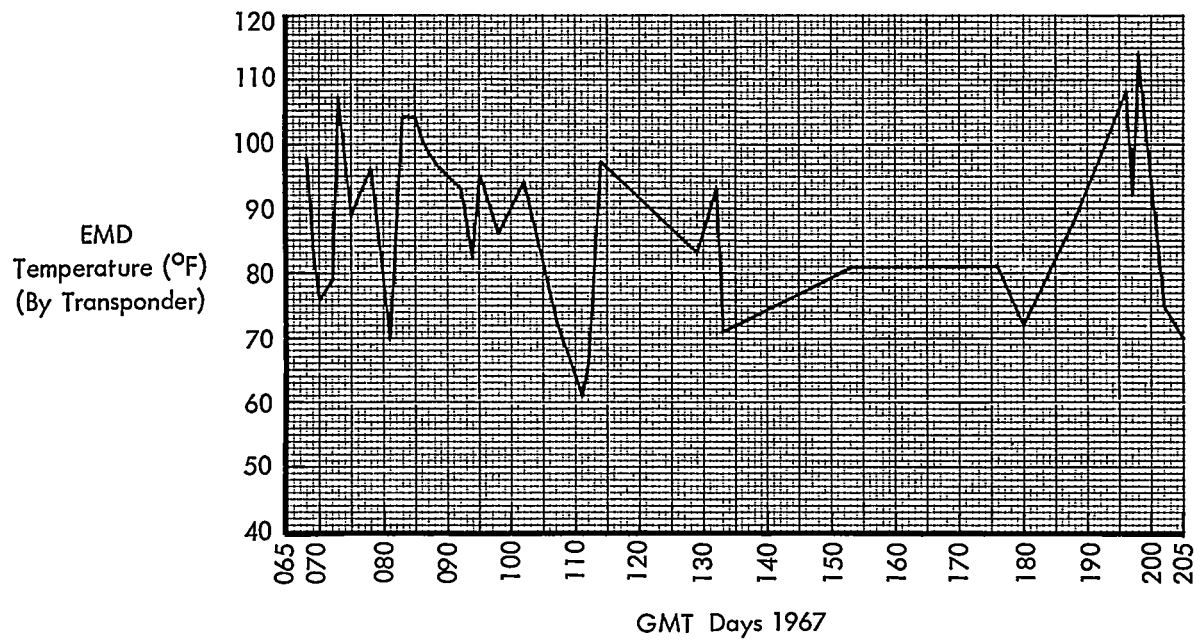


Figure 5-30: EMD Temperature History (Transponder)

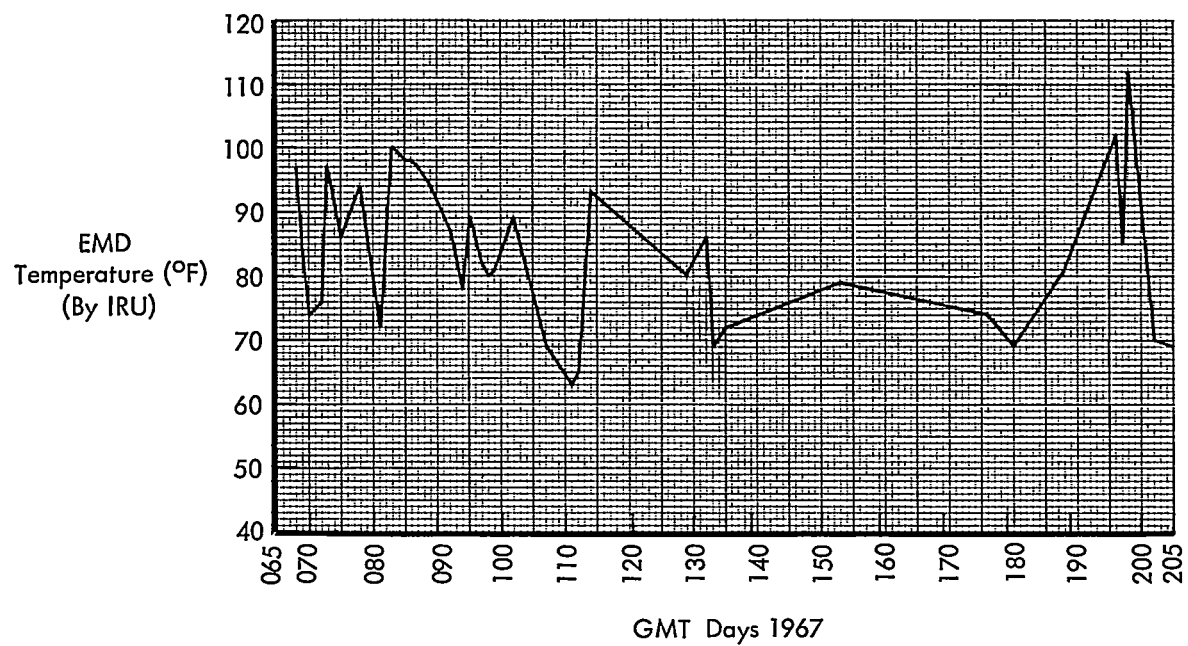


Figure 5-31: EMD Temperature History (IRU)

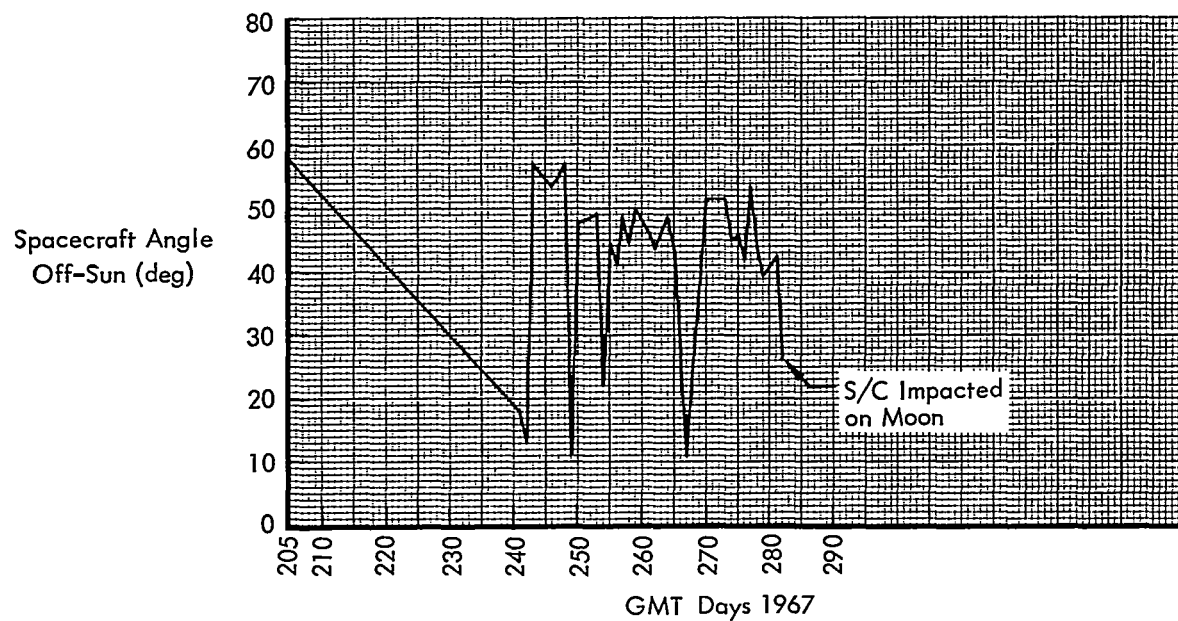


Figure 5-32: Pitch Angle History

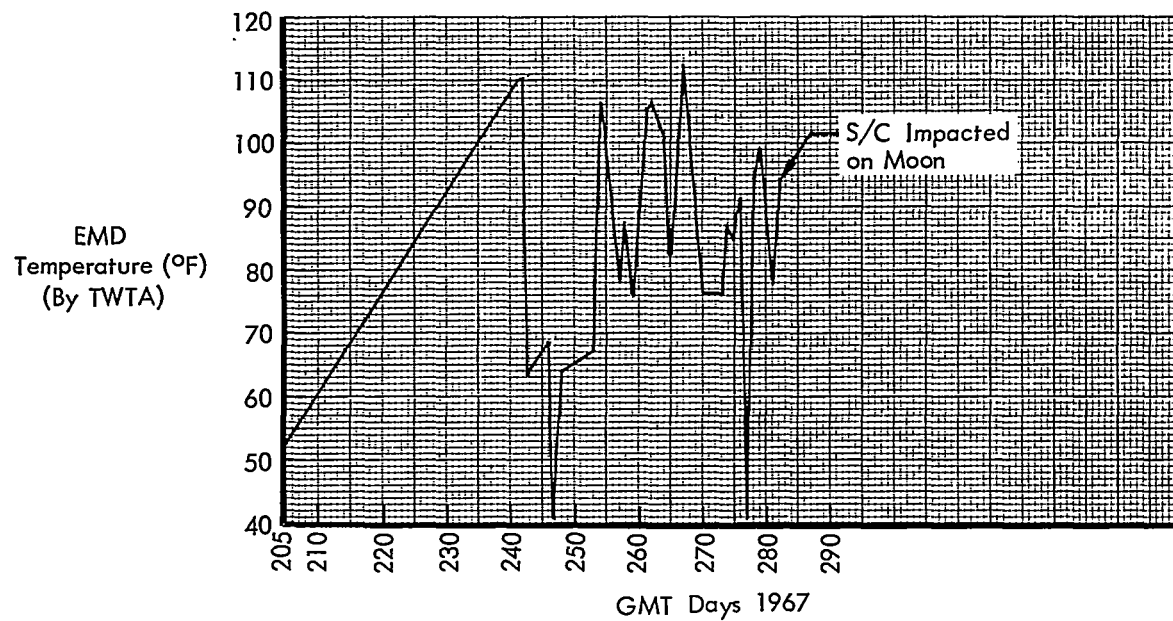


Figure 5-33: EMD Temperature History (TWTA)

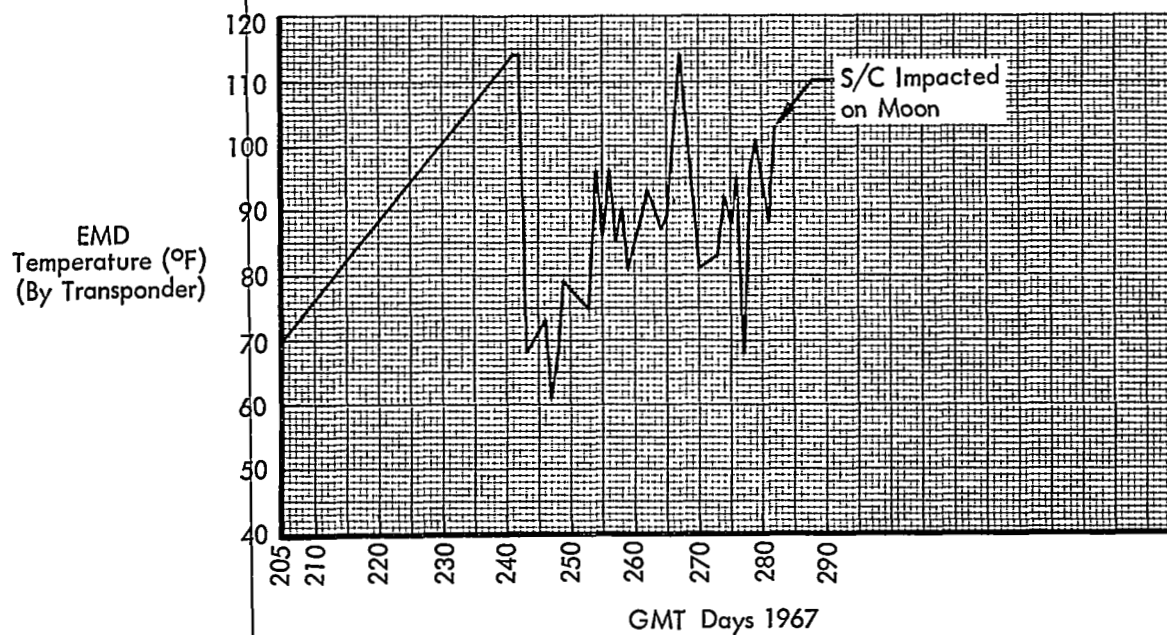


Figure 5-34: EMD Temperature History (Transponder)

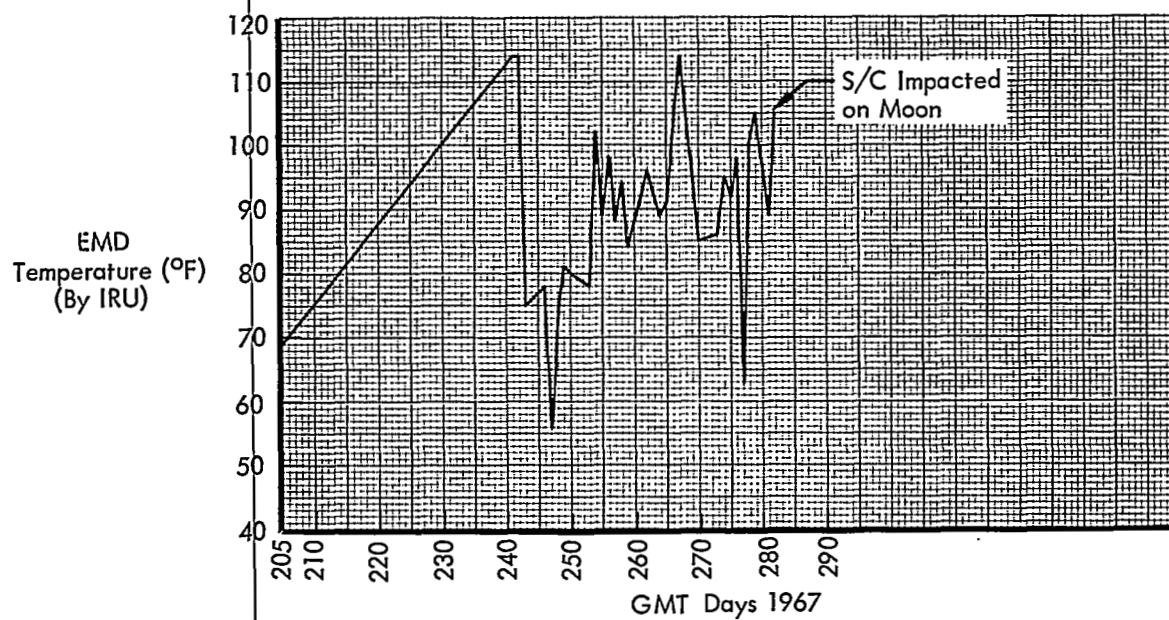


Figure 5-35: EMD Temperature History (IRU)

5.2.5.2 Thermal Control Coating Coupons

The Mission III spacecraft was instrumented with a paint coupon assembly to provide flight data on selected thermal control coatings by measuring the temperature of the individual coupons. The following paint coupons were used.

<u>Paint Coupon</u>	<u>Paint Description</u>
● S13G over B1056 (Measurement ST09)	B1056 is zinc oxide with RTV 602 binder and SRC05 catalyst.
● S13G (Measurement ST10)	S13G is zinc oxide with a potassium-silicate treatment, RTV 602 binder, and SRC05 catalyst
● Surveyor White (Measurement ST11)	Titanium oxide with potassium-silicate treatment, RTV 602 binder, and TMG catalyst.
● B1060 (Measurement STR)	Same as S13G, except that a TMG catalyst is substituted for the SRC-05 catalyst.

The coupon assembly design was modified from that used on Mission II to improve thermal isolation of the individual coupons. The coupon was recessed so that the surface of the coupon was flush with the surface of the mounting plate, thus shielding the edge of the coupon from reflected and/or radiated thermal energy. The mounting plate was coated with B1056 paint and the separation between the coupon and the mounting plate (around the perimeter of the coupon) was filled with B1056 paint.

This design, as in Mission II, also failed to provide meaningful thermal data for determining thermal degradation owing to the following conditions.

- The mass of the mounting plate was large compared to the mass of the coupons.

- The B1056 paint on the mounting plate degraded rapidly, as observed during Mission I.
- The B1056 paint filling the gap around the edge of the coupon provided a direct thermal conductive path from the mounting plate to the coupon.

These conditions caused each of the samples to be driven essentially to the temperature of the mounting plate, which masked the individual characteristics.

The coupon assembly design was changed for Missions IV and V to achieve thermal isolation. Valuable degradation data was obtained on the samples selected.

5.2.6 Velocity and Reaction Control Subsystem

The velocity control subsystem (Figure 5-36) consists of the propellant pressurization equipment, propellant storage tanks and feed system, bipropellant rocket engine, and thrust vector

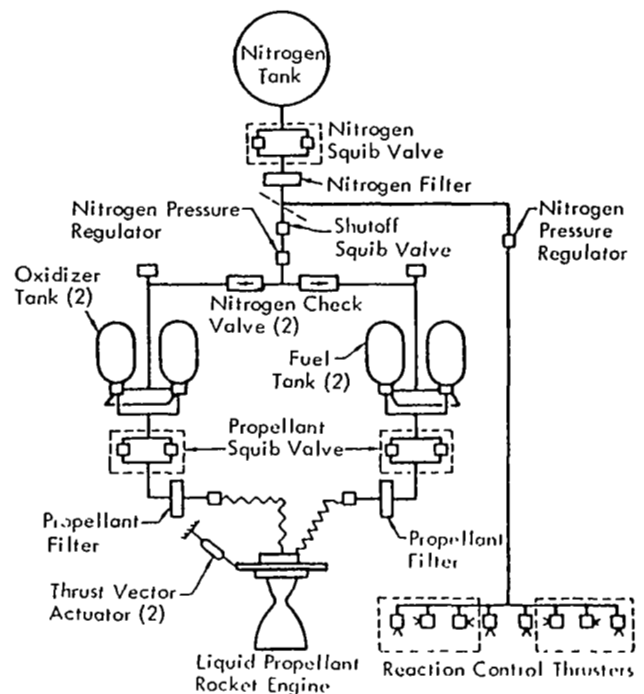


Figure 5-36:
Velocity and Reaction Control Subsystem

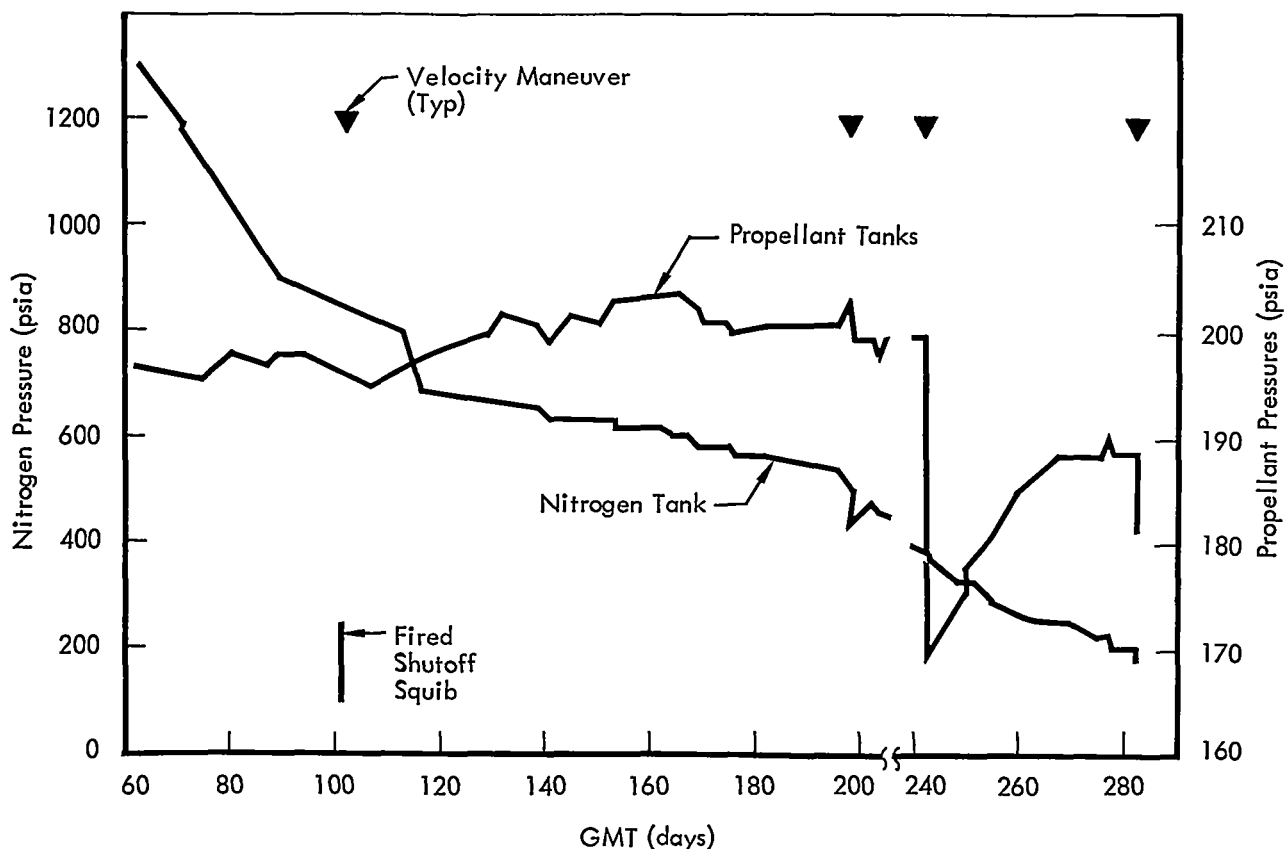


Figure 5-37: Spacecraft Tankage Pressure Profile

control (TVC) actuators. The reaction control subsystem includes the nitrogen storage tank (which is common to the velocity control subsystem), thrusters and interconnecting plumbing, filter, and regulator. The reaction control subsystem provides the impulsive force to maintain attitude control and perform attitude maneuvers about the pitch, roll, and yaw axes of the spacecraft.

5.2.6.1 Reaction Control Subsystem

The reaction control subsystem performed satisfactorily throughout the extended mission, maintaining spacecraft attitude control in wide (2-degree) deadband while in inertial hold in all three axes during the major part of the extended mission. Maneuvers were generally limited to those required for updating of the spacecraft pitch and yaw position for thermal control and for special tests. To minimize nitrogen consumption, most maneuvers were performed with the attitude control subsystem operating in wide deadband. The time histories

of nitrogen tank pressure and temperature are shown in Figures 5-37 and 5-38, respectively. Figure 5-39 shows nitrogen tank temperature variations for an Apollo-type orbit. The temperature environment for the thrusters was from 5 to 10 degrees lower than the temperature of the nitrogen tank.

Reaction control performance was evaluated on the basis of nitrogen gas consumption for attitude control and thruster performance. It was concluded that reaction control subsystem performance was nominal throughout the extended mission, with no evidence of degradation from that of the primary mission.

Nitrogen Utilization — Nitrogen usage is calculated from the telemetered nitrogen storage bottle pressure and temperature, and the volume of the high-pressure system. Predicted usage rate calculations are based on the maneuvers performed, the spacecraft moment of inertia about each axis, estimated limit cycle usage

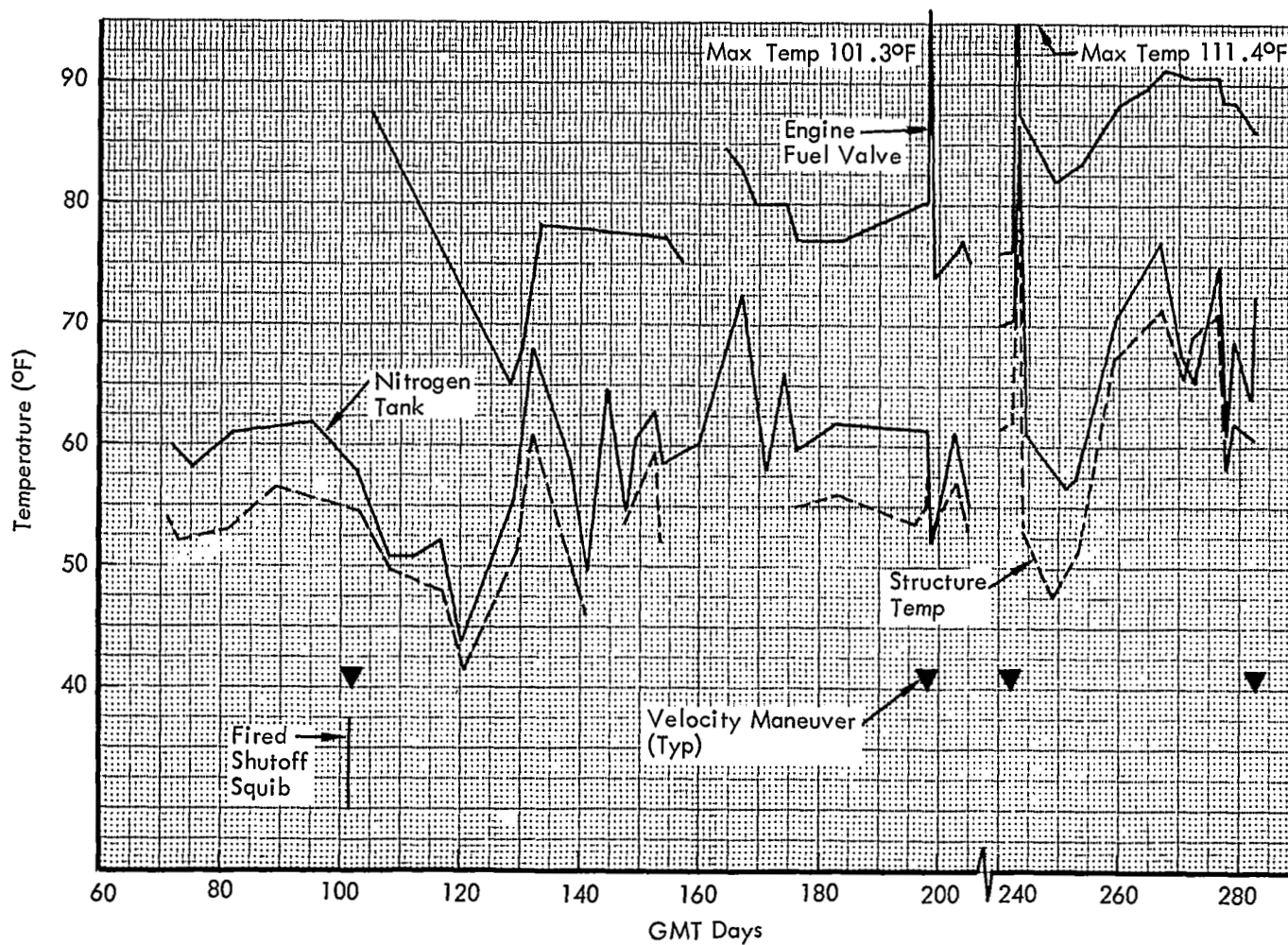


Figure 5-38: Velocity and Reaction Control Temperatures Profile

Temperature (°F)

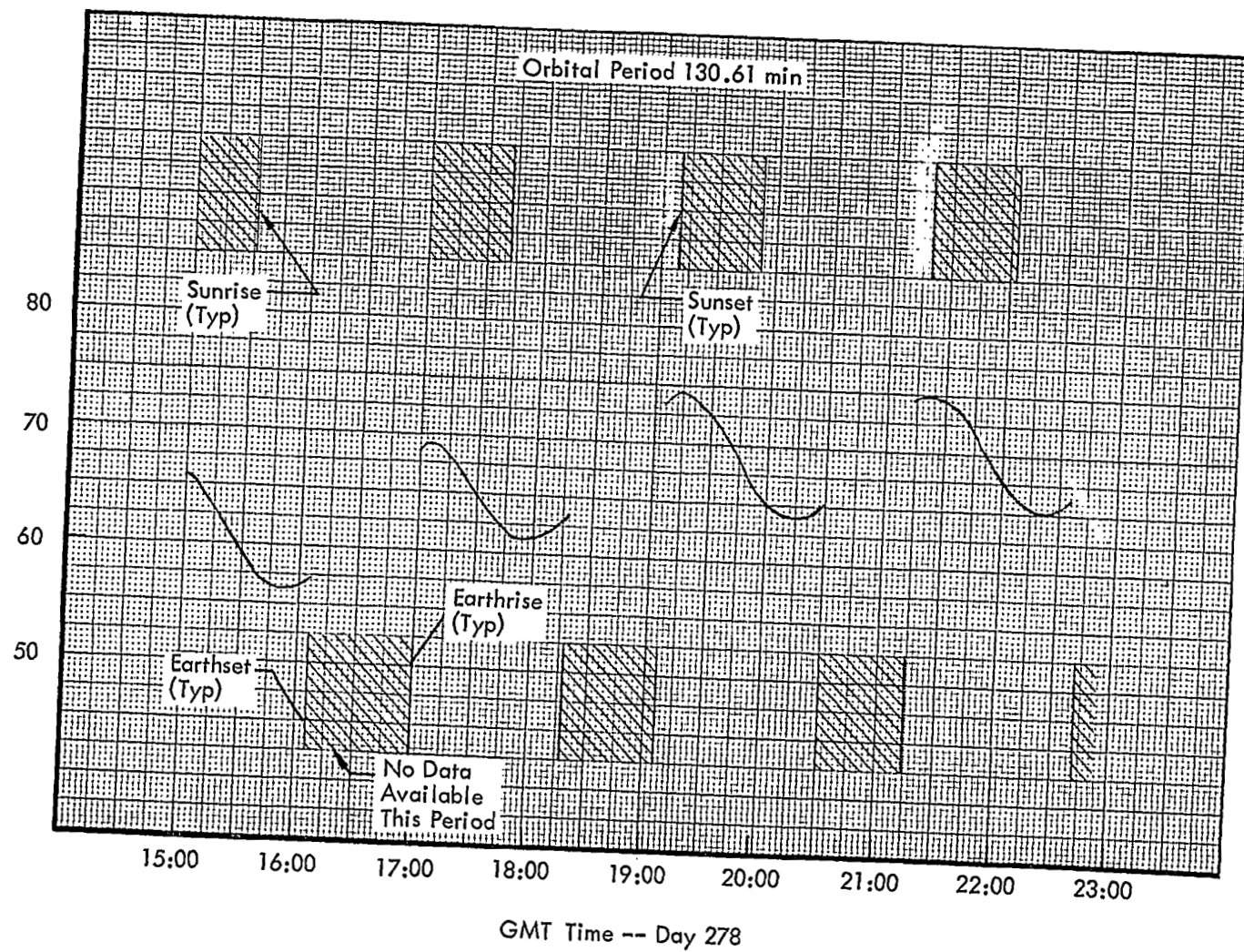


Figure 5-39: Nitrogen Tank Temperature Variation for Apollo-Type Orbit

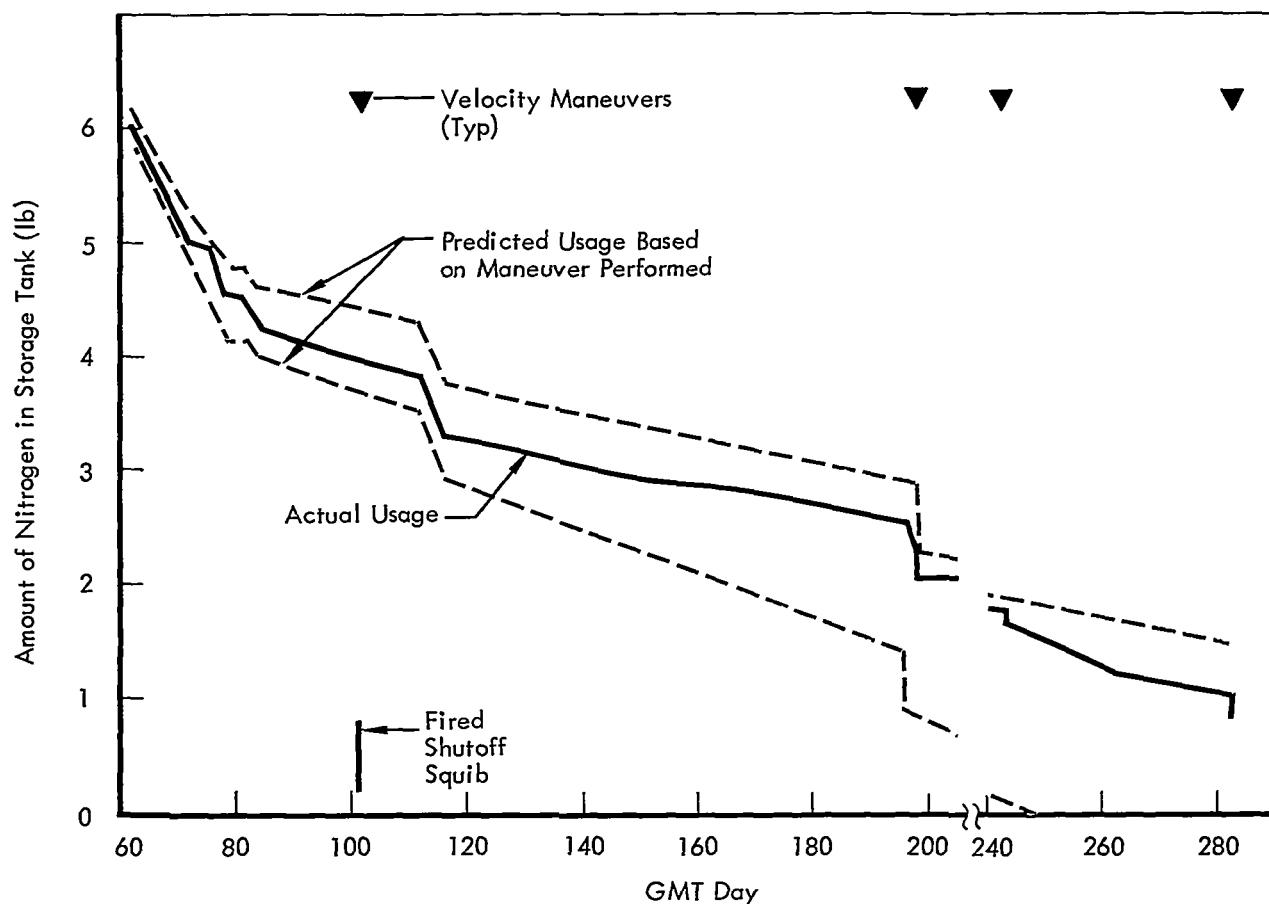


Figure 5-40: Nitrogen Gas Usage History

rates, and estimated disturbances. Minimum predicted nitrogen usage is based on minimum 12-millisecond single pulses of the thrusters during limit cycle operation. The maximum usage limit is based on pulse durations for limit cycle operation that result in 0.0025 degree-per-second angular rates in each axis. To obtain such angular rates, the equivalent pulse duration would be 35 milliseconds in pitch and yaw and 65 milliseconds in roll. Predicted usage rates for maneuvers (including Sun and Canopus acquisitions) and disturbances are the same for the minimum and maximum limits.

Actual nitrogen gas usage for the extended mission is shown in Figure 5-40. Major events that caused the higher usage rates are summarized in Table 5-16. Nitrogen usage for the first 120 days of the normal extended-mission mode of operation, which includes thermal maneuvers and ± 2.0 -degree limit cycling, ranged from

0.0106 to 0.007 pound per day, with an average of 0.0087 pound per day. Following the transfer to an Apollo-type orbit, the average nitrogen usage was 0.0119 pound per day for a 40-day period, with suitable adjustments for leakage of the nitrogen shutoff valve into the propellant tanks. The change in consumption rate is attributed to the greater gravity gradient effects of the lower orbit. Typical variations in spacecraft attitude while operating in an Apollo-type orbit are shown in Figure 5-41. The maximum and minimum predicted rates for the initial orbit were 0.018 and 0.010 pound per day, respectively.

Although thruster performance cannot be directly determined from flight data, the compatibility between predicted and actual thruster operating modes and nitrogen usage verifies that the specific impulse in flight is very close to predicted values established from ground testing. The specific impulse used for predicting nitrogen

usage was 68 seconds for limit cycle mode and 71 seconds for maneuvers.

5.2.6.2 Velocity Control Subsystem

Velocity control subsystem performance was analyzed on the basis of telemetered propellant tank pressures, actuator position, and incremental velocity change. The velocity control subsystem was operated four times during the extended mission, each time successfully, with no evidence of degradation.

Propellant tank pressures and system temperatures during the extended mission are shown in

Figures 5-37 and -38, respectively. Fuel and oxidizer tank pressures held essentially constant from the start of the extended mission until the shutoff squib valve was fired on Day 101 at 20:25, indicating that there was no significant lockup leakage of the velocity control regulator. Similarly, there was no evidence of external leakage from the velocity control subsystem, since propellant tank pressures did not decrease following actuation of the shutoff squib valve. Tank pressures actually increased from 195 to 203 psia in the next 96-day period while the general thermal environment increased about 10°F.

Table 5-16: Major Events Using Nitrogen Gas

<u>Time Period (GMT days)</u>	<u>Description of Events</u>
62 to 72	Canopus tracker glint tests Maneuver accuracy tests Antenna mapping
75	V/H high roll angle test
81 to 85	Canopus tracker degradation test Radar mapping (Stanford) exp. V/H high roll angle test
85 to 101	Extended-mission mode of operation
101	Star map Squib interaction test
102	Orbit-phasing maneuver
112 to 117	Mission IV training
118 to 198	Extended-mission mode of operation
198	Perilune transfer maneuver
199 to 242	Extended-mission mode of operation
242	Apolune transfer maneuver
243 to 282	Extended-mission mode of operation in Apollo-type orbit
282	Impact orbit-transfer maneuver

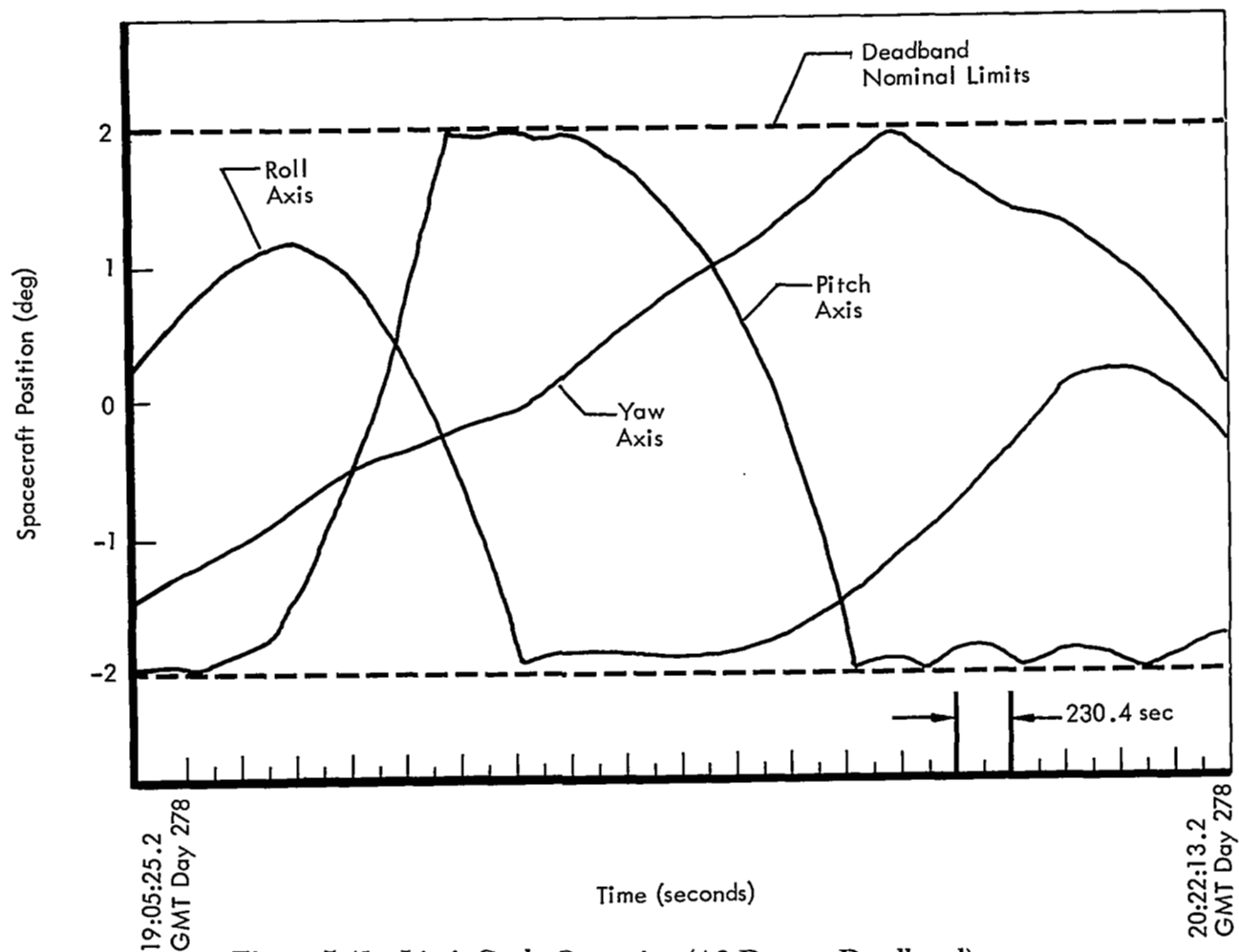


Figure 5-41: Limit Cycle Operation (± 2 -Degree Deadband) – Apollo-Type Orbit Maneuver

Immediately following the velocity maneuver of Day 242, a nitrogen shutoff valve leak occurred of sufficient magnitude to drive the propellant tank pressures from 170 to 189 psia in 23 days. This represents a leak of approximately 157cc/hr. The pressures then remained at 189 psia, the regulator lockup pressure, until the next engine ignition on Day 282.

The details of each velocity maneuver performed during the extended mission are discussed below.

Phasing Maneuver for April 1967 Eclipse – On Day 102 at 17:40 GMT, a velocity maneuver was performed to decrease the orbital period to optimize the phasing for the Day 114 eclipse. The maneuver was required to impart a velocity

change of 5.5 meters per second, which was calculated to require a burn time of 3.5 seconds. Because of the short duration of the burn as compared to the data sampling rate, it was not possible to confirm engine-burn time or thrust level (estimated to be 102.8 pounds). The maneuver did terminate exactly as programmed based on telemetered velocity data, and the magnitude was verified by tracking data. The engine burn was short enough to preclude any extensive decay of the propellant tank pressures, which decreased only 1 psi even though operated in the blowdown mode. The nitrogen gas supply pressure remained constant (the shutoff squib valve had been actuated).

Performance of the thrust vector control system was satisfactory, as shown in Figure 5-42.

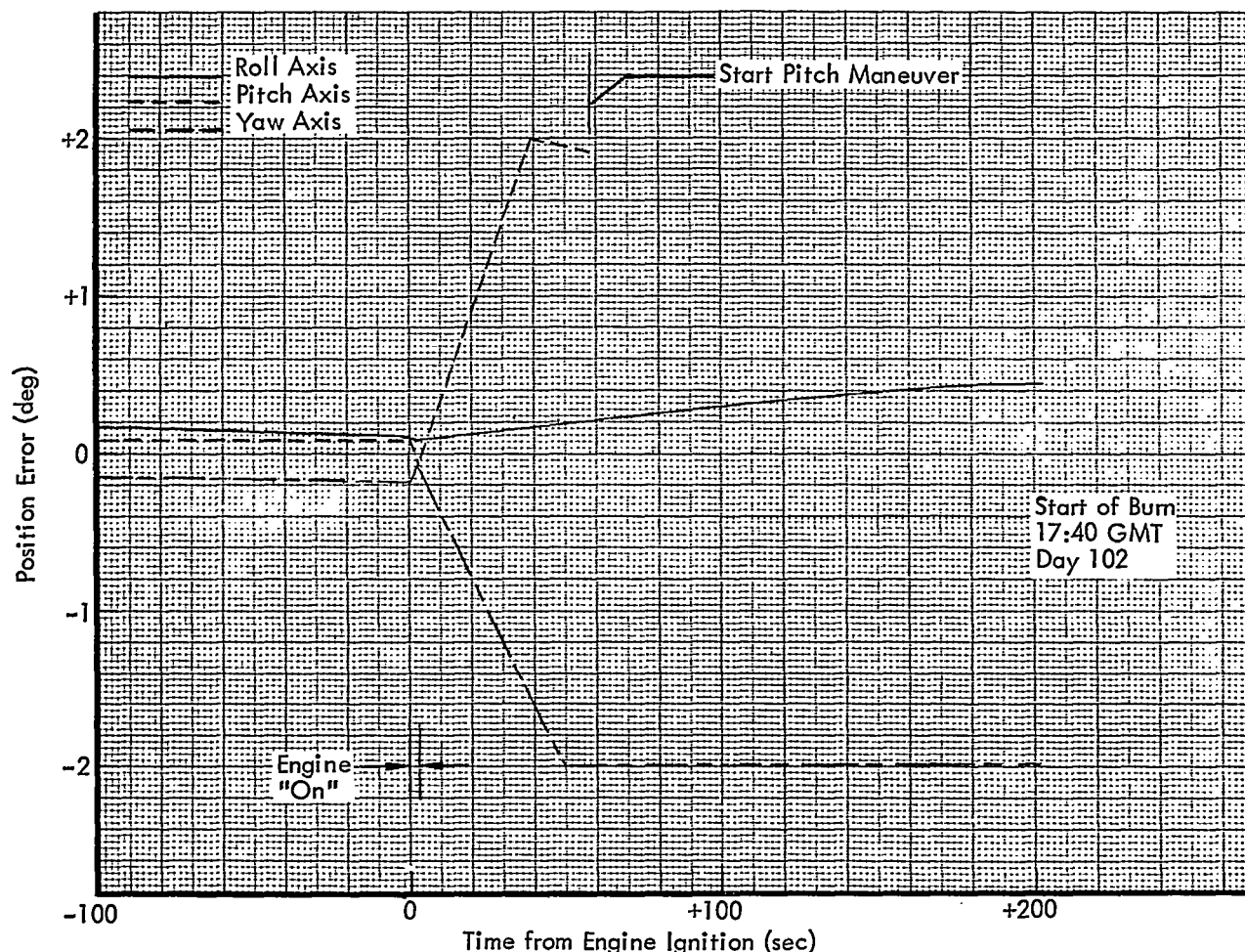


Figure 5-42: Spacecraft Position Error – Orbital Lifetime Adjust Maneuver

Orbital Lifetime Adjust Maneuver – On Day 198 at 01:22 GMT, a velocity change maneuver was performed to raise the orbit perilune from approximately 52 to 140 kilometers to preclude lunar impact due to orbit decay. The maneuver provided a velocity change of 14.4 meters per second, which is shown as a function of time in Figure 5-43. Average thrust during the burn was 104.6 pounds, as computed from spacecraft weight and acceleration. The nitrogen gas supply pressure remained constant (the nitrogen shutoff squib valve had been previously fired) while propellant feed system pressures decayed 4 psi to 198.8 psia, which is consistent with the duration of the burn. Thrust vector control system performance was satisfactory throughout the burn, as shown in Figure 5-44.

Maneuver Into Apollo-Type Orbit – On Day 242 at 19:39 GMT, a velocity change maneuver was performed to change the orbit apolune from 1,824 to 315 kilometers (approximate values) to simulate an Apollo-type orbit. This orbit transfer decreased the orbit period from 212 to 130 minutes. The maneuver provided a velocity change to the spacecraft of 198.3 meters per second, which is shown as a function of time in Figure 5-45. The average thrust during the burn was 96.93 pounds, as computed from spacecraft weight and acceleration data. Engine-burn time established from telemetry data was 127.1 seconds. Propellant feed system pressures for the maneuver are shown as a function of time in Figure 5-46. Fuel and oxidizer tank pressures were consistent with predicted values for system

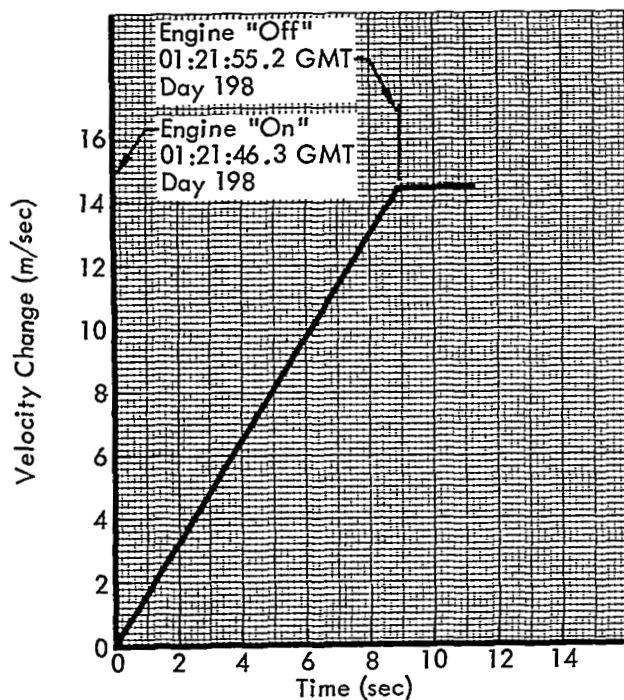


Figure 5-43:

Orbital Lifetime Adjust Maneuver (ΔV)

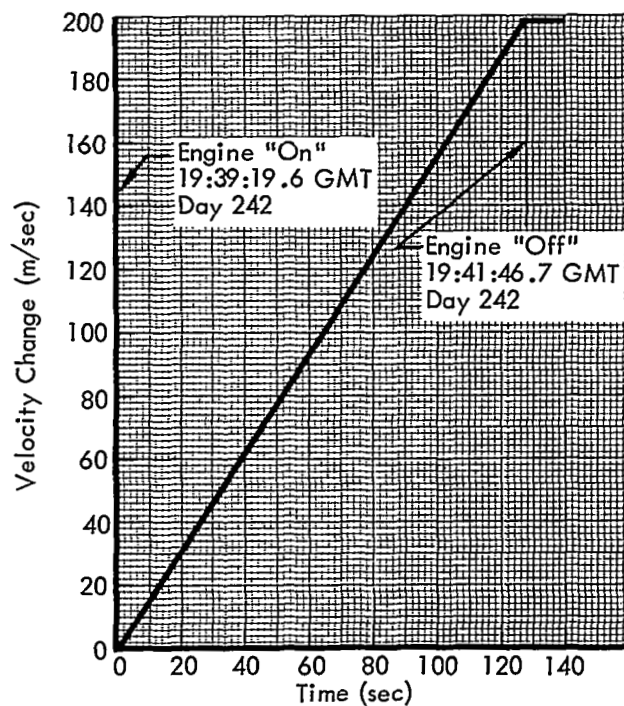


Figure 5-45:

Apollo-Type Orbit Maneuver (ΔV)

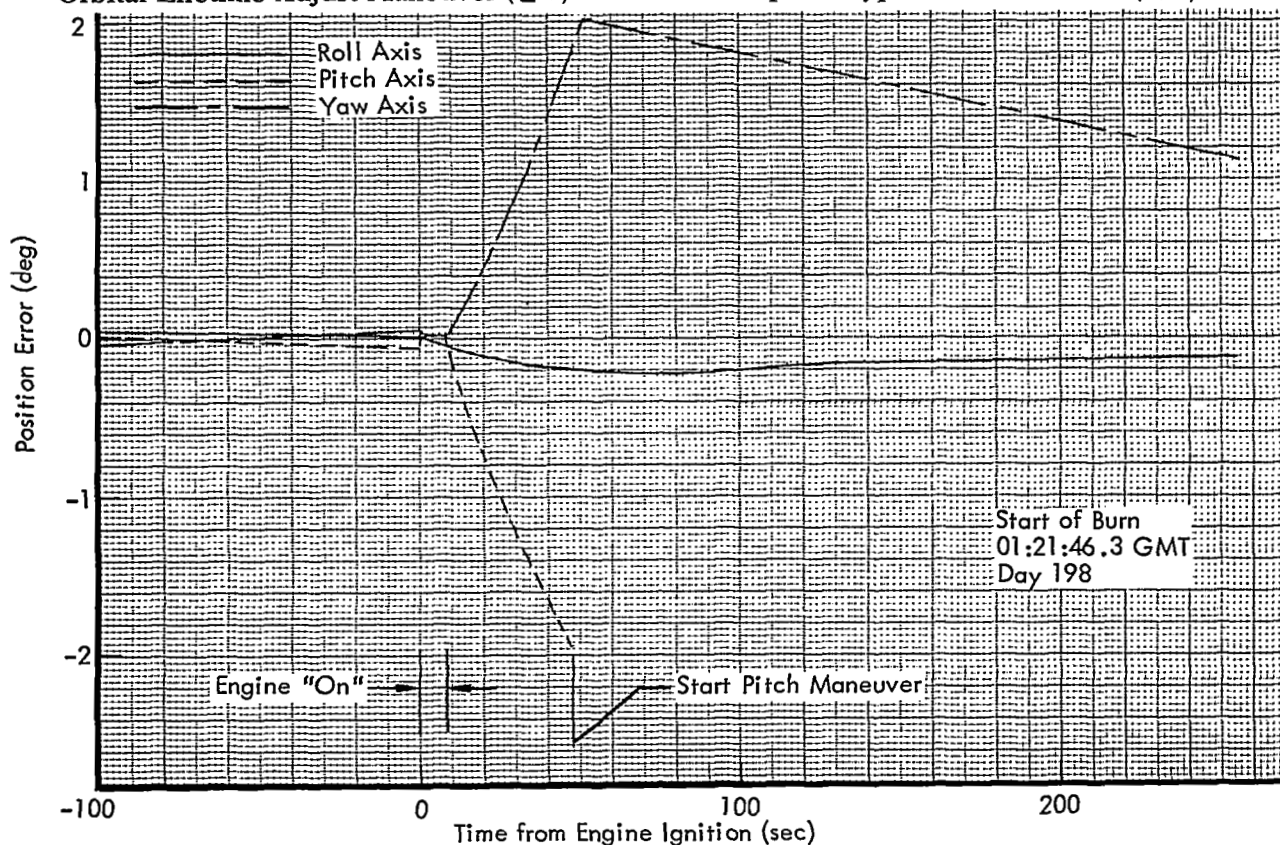


Figure 5-44: Spacecraft Position Error – Orbital Lifetime Adjust Maneuver

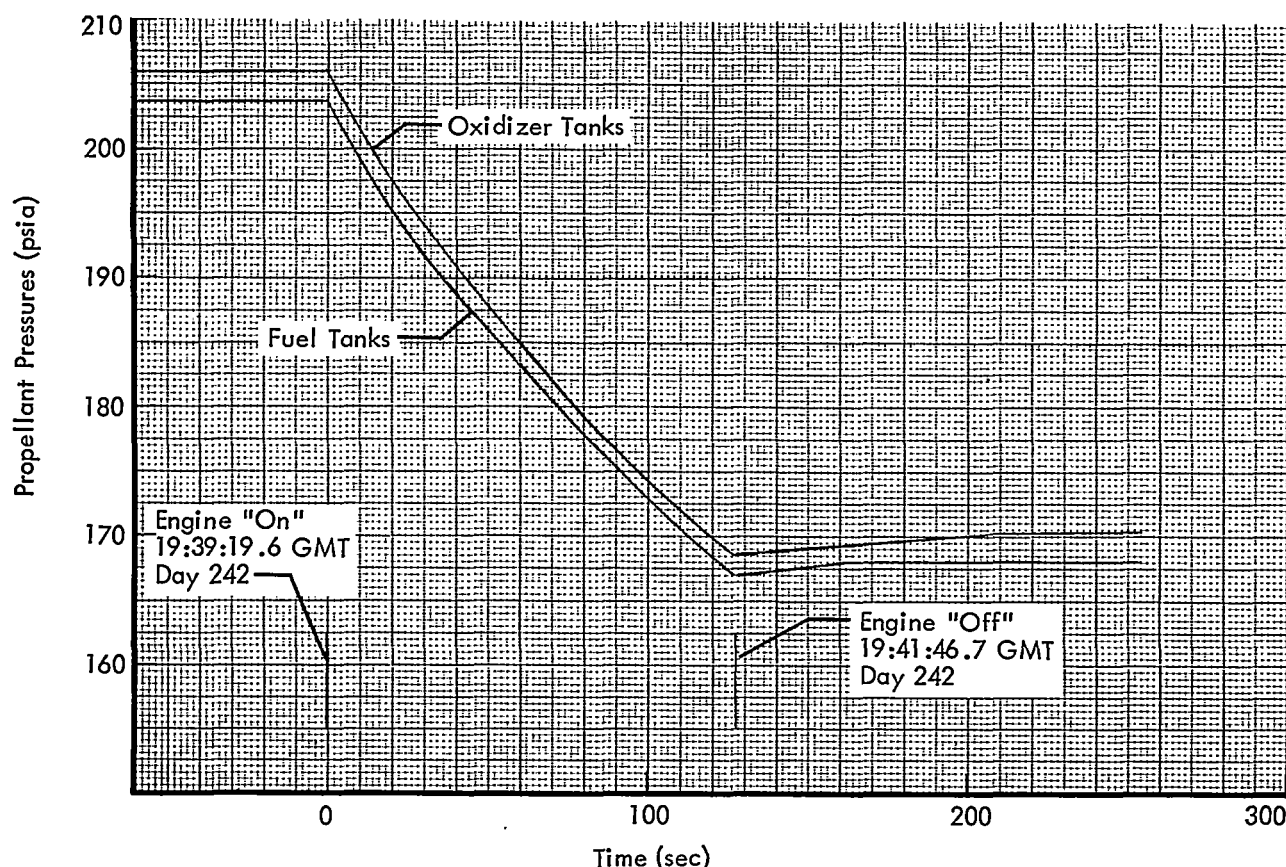


Figure 5-46: Propellant Pressures — Apollo-Type Orbit Maneuver

operation in the blowdown mode. The nitrogen gas supply pressure remained constant.

Performance of the thrust vector control system was satisfactory throughout the burn, as shown by Figure 5-47. No excursions in spacecraft attitude beyond 0.12 degree were observed from telemetry data during the time the thrust vector control system had control capability. The engine position data shown in Figure 5-48 confirm the stability of the system during the velocity maneuver. The engine position data also show that the spacecraft center of gravity location relative to the engine pointing angle experienced a shift of 0.12 degree in the yaw plane. The allowable shift is 0.5 degree. Figure 5-49 presents the engine fuel valve time/temperature relationship following the engine burn.

Terminal Transfer Maneuver — On Day 282 at 09:33 GMT, a velocity change maneuver was

performed to place the spacecraft in an orbit which would impact the lunar surface. This maneuver, programmed to expel 99% of the oxidizer loaded, provided a velocity change of 52.6 meters per second, sufficient to impact on the lunar surface approximately 54 minutes after engine ignition. A plot of the velocity change as a function of time is shown in Figure 5-50. Average thrust during the burn was 97.5 pounds, as computed from spacecraft weight and acceleration data. Engine burn time, as established by telemetry data, was 32 seconds. Propellant system pressures are shown as a function of time in Figure 5-51, and are consistent with predicted values for system operation in the blowdown mode. The nitrogen gas supply pressure remained constant.

Performance of the thrust vector control system was satisfactory throughout the burn, as shown by Figure 5-52, with the largest spacecraft attitude excursion, as shown by telemetry data, less than 0.1 degree.

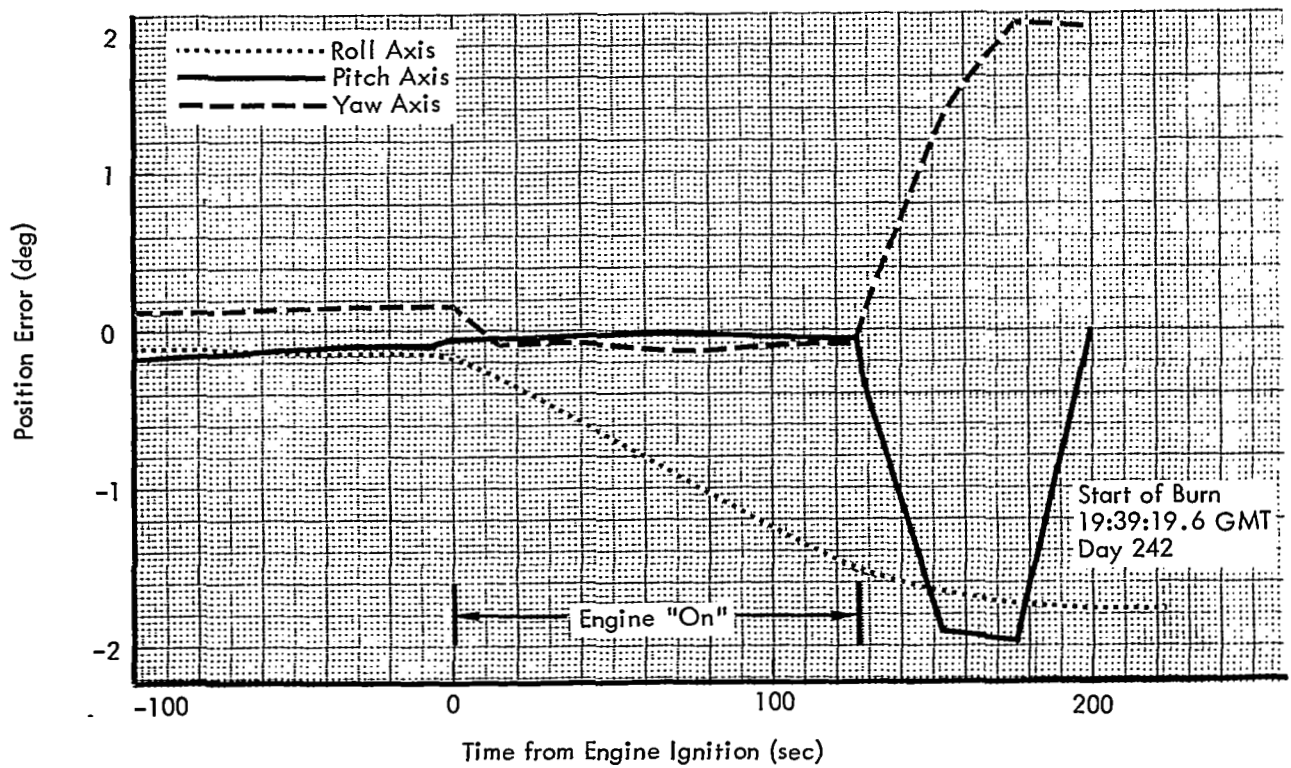


Figure 5-47: Spacecraft Position Error – Apollo-Type Orbit Maneuver

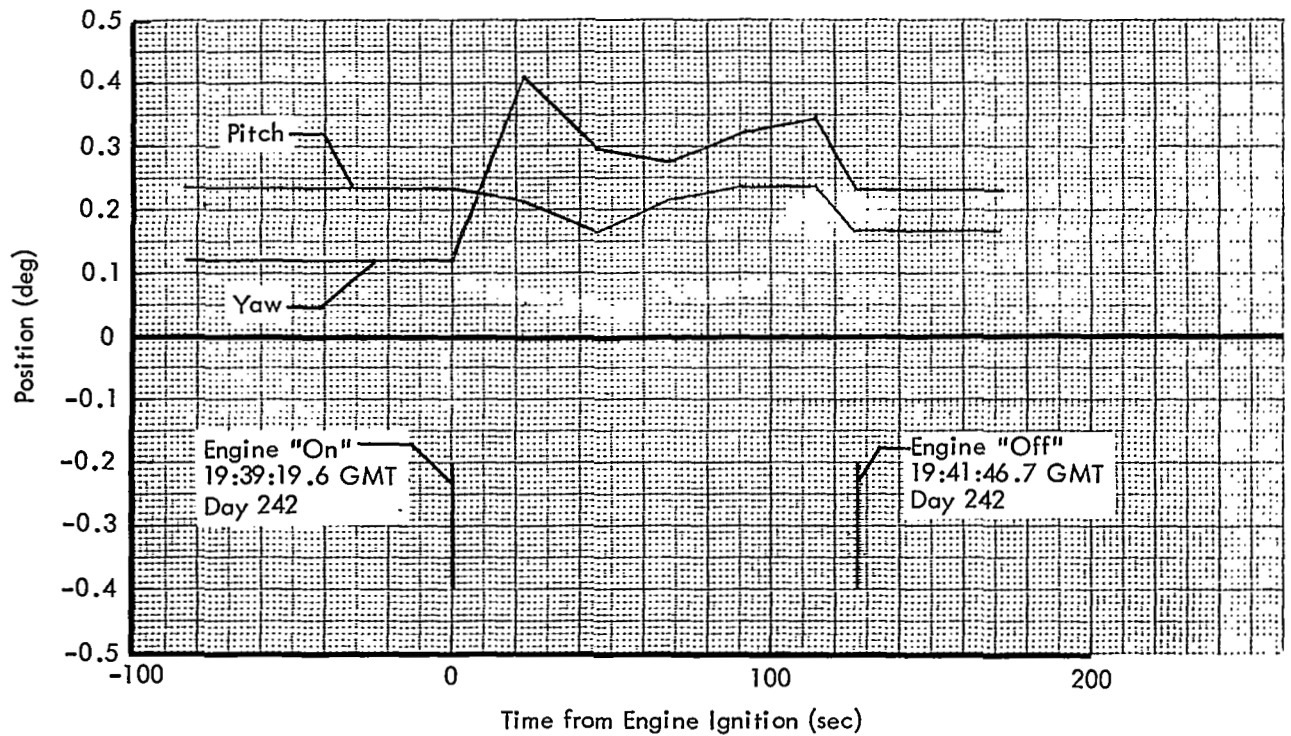


Figure 5-48: TVC Actuator Position – Apollo-Type Orbit Maneuver

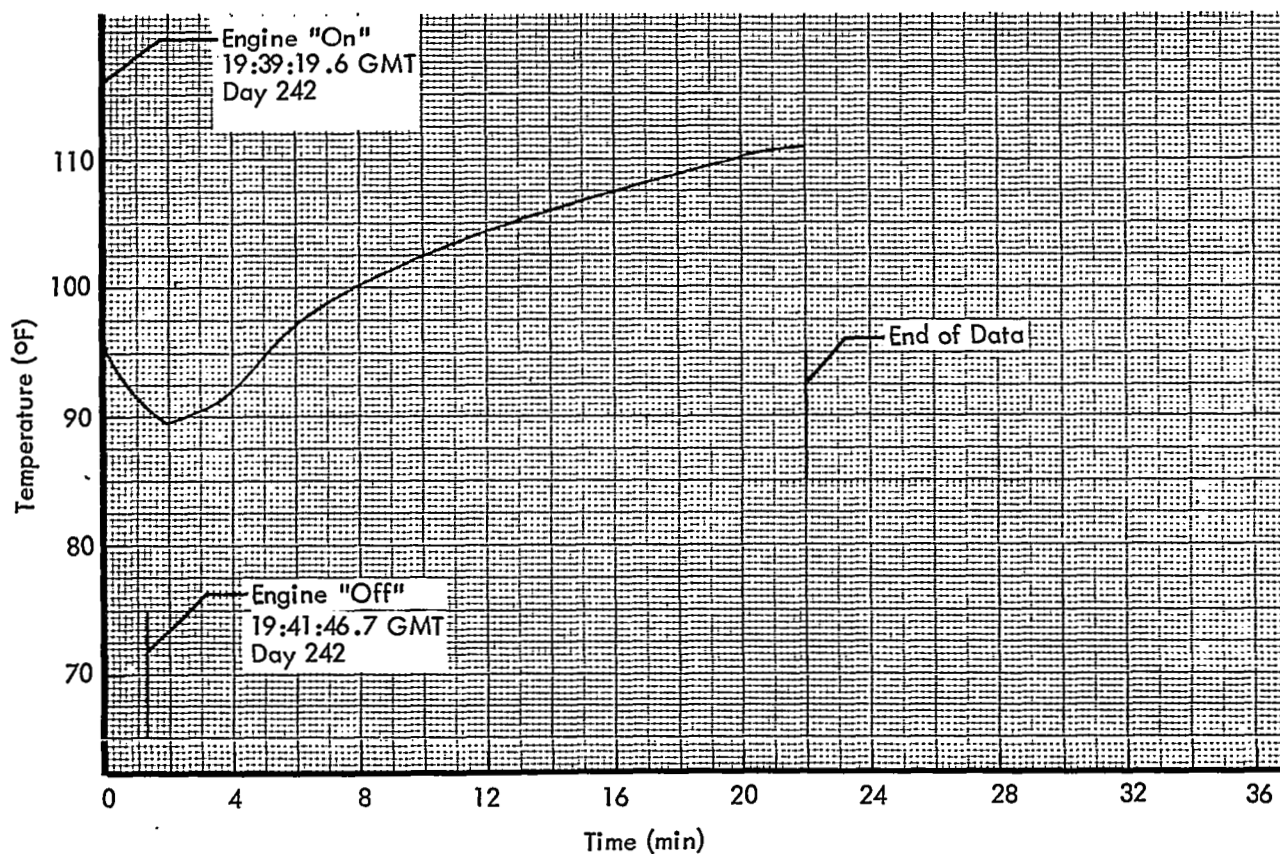


Figure 5-49: Engine Valve Temperature Characteristics—Apollo-Type Orbit Maneuver

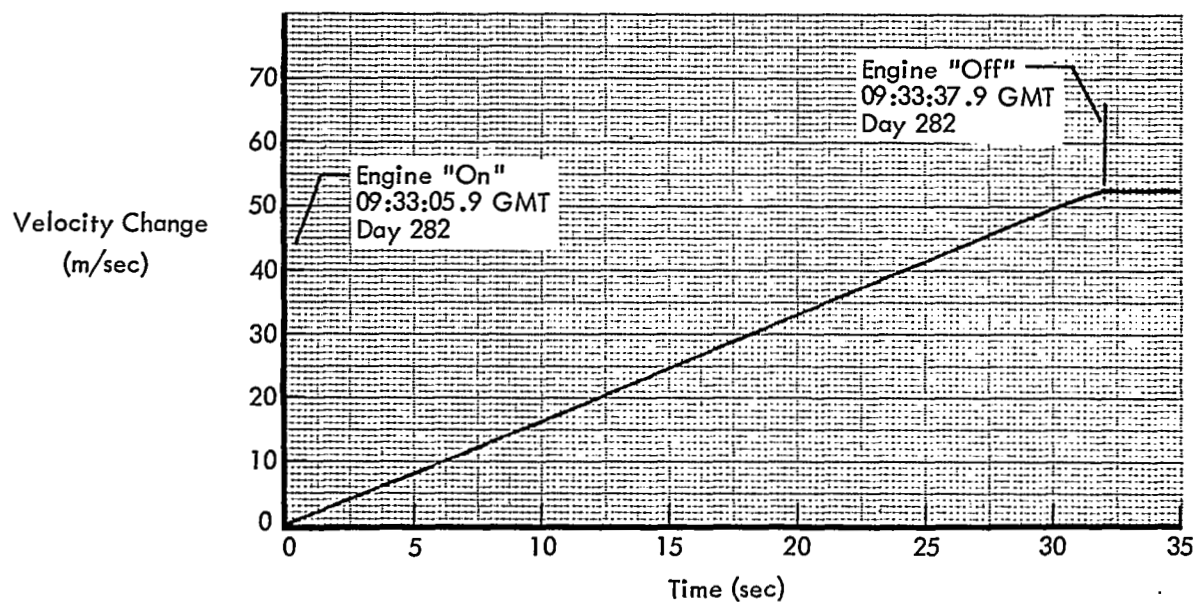


Figure 5-50: Terminal Transfer Maneuver (ΔV)

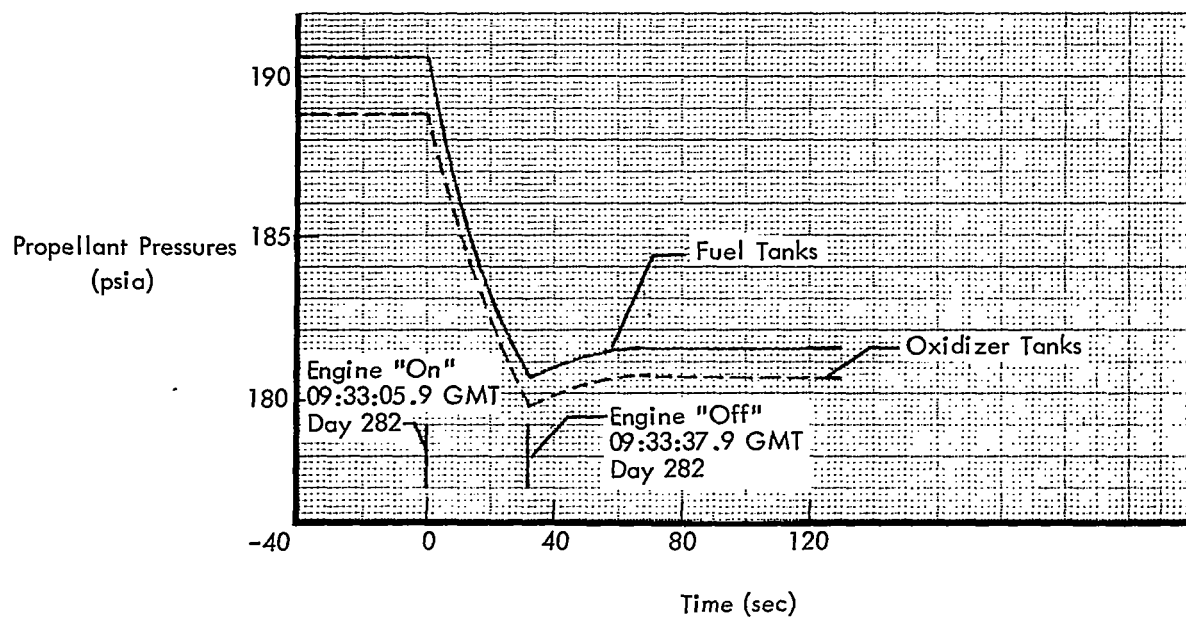


Figure 5-51: Propellant Pressure – Terminal Transfer Maneuver

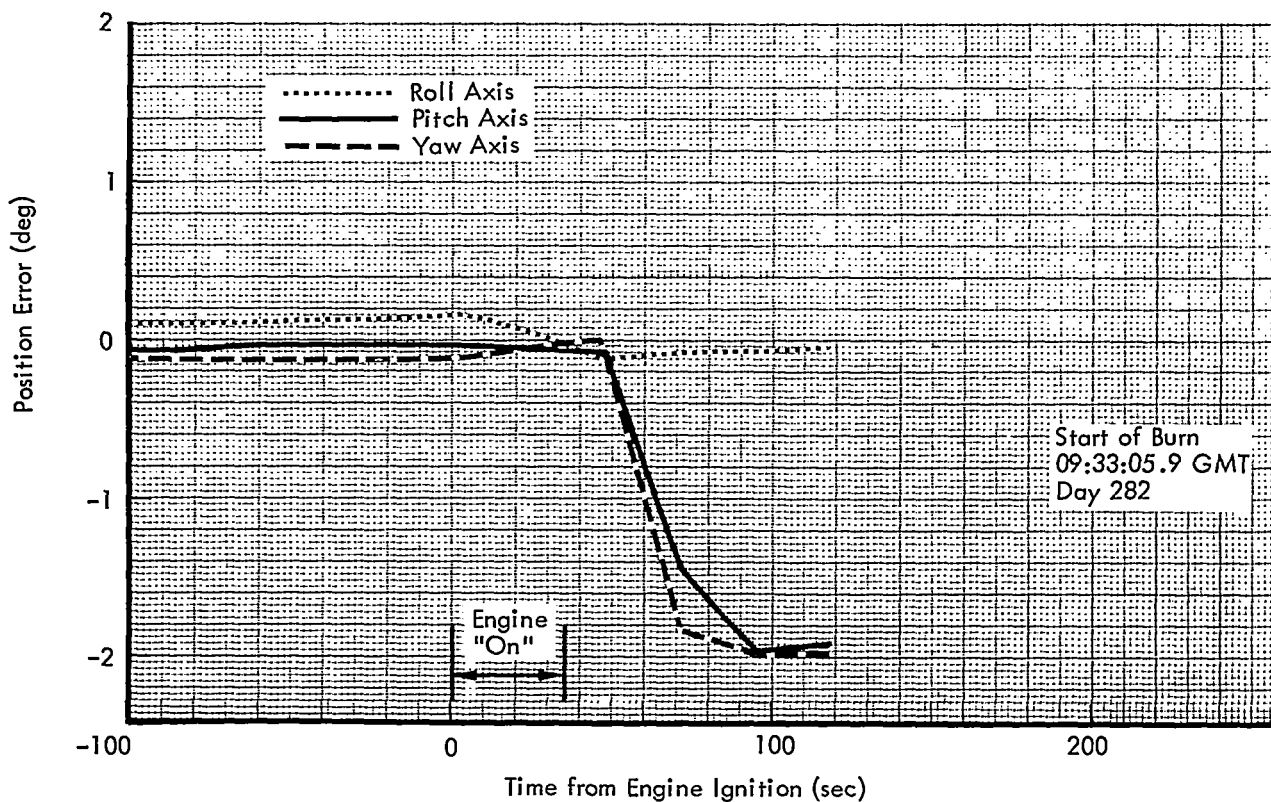


Figure 5-52: Spacecraft Position Error – Terminal Transfer Maneuver

Table 5-17: Mission III Velocity Maneuver Summary

Event	GMT Time Day of Year	ΔV m/sec	Burn Time (sec)	Average Thrust (lb)	Propellant Used (lb)*
Launch	0117 36 (1967)				**
Midcourse	1500 37	5.1	4.3	102.5	1.6
Injection	2154 39	704.3	542.5	100.0	195.9
Orbit Transfer	1814 43	50.7	33.7	100.2	12.2
Orbit Phasing for April 1967 eclipse	1640 102	5.5	3.5	102.8	1.3
Orbital lifetime adjust maneuver	0122 198	14.4	8.9	104.6	3.4
Maneuver into Apollo-type orbit	1939 242	198.3	127.1	97	44.6
Terminal transfer maneuver	0933 282	52.6	32.0	97.5	11.3
TOTAL		1,030.9	752.0		270.3

* Estimated assuming a specific impulse of 276 seconds

** 275.9 pounds propellant loaded at launch

Overall Subsystem Performance — During the photographic and extended mission, seven velocity maneuvers were performed. Significant information pertaining to each is summarized in Table 5-17. An analysis of system performance during each burn confirmed that the engine specific impulse averaged 276 seconds. The velocity control subsystem imparted a total velocity change to the spacecraft of 1,030.9 meters per second using 270.3 pounds of propellant, based on an engine specific impulse of 276. Experience from ground testing and Mission I has indicated the subsystem would impart a nominal velocity change of 1,026 meters per second to the spacecraft, based on actual propellants loaded and a 99% expulsion efficiency.

It was concluded, therefore, that the actual expulsion efficiency was slightly in excess of 99%.

5.3 SPECIAL FLIGHT TESTS

Special tests performed during the extended mission fall into two categories: (1) special experiments using the Lunar Orbiter spacecraft as a tool to obtain scientific data, and (2) special exercises that are tests of the spacecraft or equipment on board. Only the latter are reported herein; special experiments are to be reported by the particular agency requesting the experiment. However, subsystem performance during a special test designed to obtain scientific data, such as the orbit transfer maneuvers that were

designed to simulate the Apollo orbit, is reported in the general discussion on each subsystem.

5.3.1 Canopus Tracker Glint Mapping

The objective was to evaluate the effect of glint on Canopus tracker operation by simulating various Mission IV spacecraft conditions using the Sun, Moon, and Earth as the light source. Figure 5-53 depicts a typical proposed Mission IV photographic experiment showing the orbital position of the spacecraft at the time of roll update.

The test was performed at new Moon (Day 068) approximately 20 degrees before the p.m. terminator. Figure 5-54 describes the orbital

geometry existing at this time. Canopus is into the plane of the paper and the spacecraft was on-Sun and oriented toward Canopus. Table 5-18 is the sequence of events that was followed.

Data and Discussion — During Orbit 198, Day 068, with the spacecraft locked on the Sun and oriented toward Canopus, the star tracker was turned on approximately 20 degrees before the p.m. terminator (18:22:22 GMT) and immediately acquired Canopus with a star map between 3.28 and 3.38 volts. Since this was a higher-than-normal star map, it was concluded that a small amount of glint must have been adding to the star-map voltage. A roll-plus-360-degree maneuver was initiated 3 minutes prior to passing the

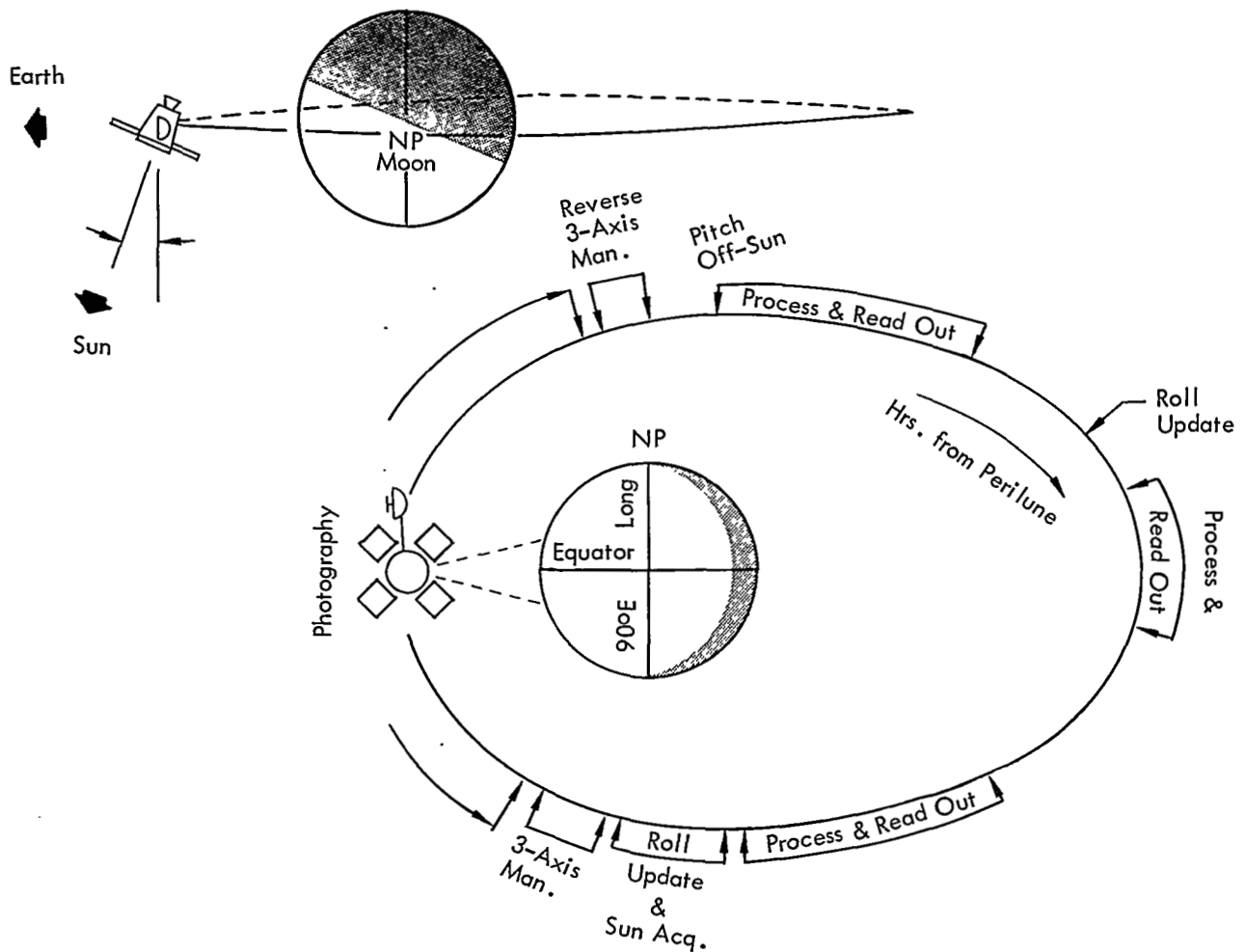


Figure 5-53: Typical Orbit Sequence — Star Tracker Test

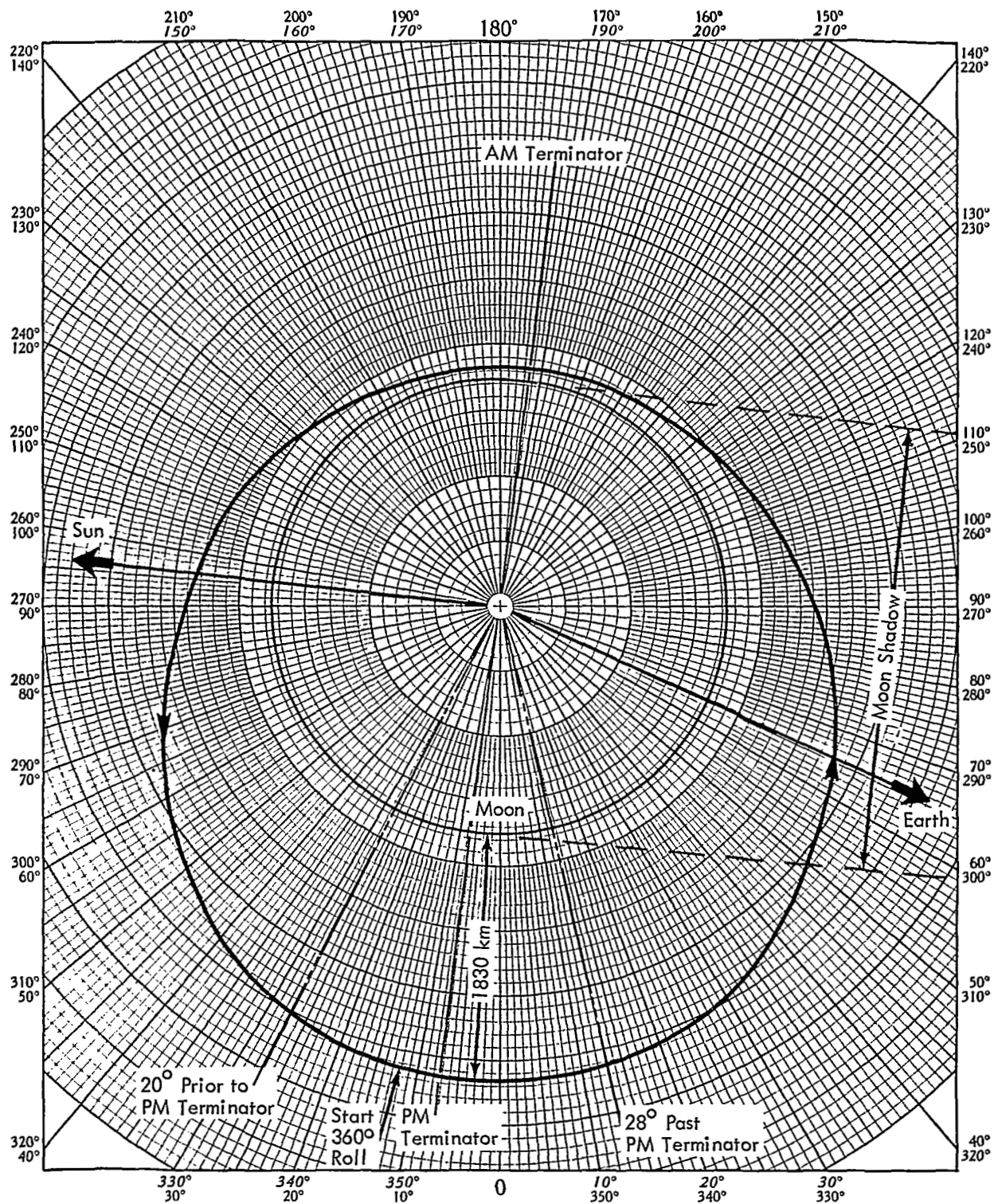


Figure 5-54: Orbital Geometry – Star Tracker Test

Table 5-18: Glint Mapping Sequence

Day: Hr: Min: Sec:	Event	Day: Hr: Min: Sec:	Event
068:15:25:45.8	Roll plus 0.11 deg	068: 21:25:00	Acquire Sun
15:35:00	Pitch and yaw fine sun sensors on	21:30:00	Pitch and yaw coarse sun sensors off
15:40:19	Acquire Sun	21:36:00	Canopus tracker on
16:00:40	Pitch and yaw coarse sun sensors off	21:39:24	Roll plus 80 deg
16:14:53	Sunset (Orbit 198)	21:50:52	20 deg before p.m. terminator
16:20:15	Canopus tracker on	22:12:53	Passed p.m. terminator
16:24:37	Roll minus 4.7 deg	22:38:33	Pitch minus 50 deg
16:31:00	Acquire Canopus	23:00:32	Pitch plus 50 deg
16:50:00	Canopus tracker off	23:11:54	Sunset (Orbit 200)
16:55:00	Roll plus 0.011 deg	23:45:18	Canopus tracker off
16:57:00	Pitch minus 50 deg	23:50:27	Pitch minus 50 deg
17:00:11	Sunrise	23:57:13	Sunrise
18:00:31	Pitch plus 50 deg	069:01:15:30	Pitch plus 50 deg
18:05:28	Acquire Sun	01:20:00	Acquire Sun
18:22:18	20 deg. before p.m. terminator	01:33:00	Canopus tracker on
18:22:22	Canopus tracker on	01:35:51	Pitch plus 360 deg
18:42:00	Roll plus 360 deg	01:41:26	Pass p.m. terminator
18:44:19	Pass p.m. terminator	01:55:29	Canopus tracker off
19:43:23	Sunset (Orbit 199)	02:00:00	Acquire Sun
20:10:00	Acquire Canopus	02:40:25	Sunset (Orbit 201)
20:20:15	Canopus tracker off	02:41:34	Canopus tracker on
20:22:36	Roll plus 0.011 deg	02:42:29	Roll plus 280.5 deg
20:24:00	Pitch and yaw coarse sun sensors on	02:58:00	Acquire Canopus
20:26:27	Pitch minus 50 deg	03:11:28	Pitch minus 50 deg
20:28:42	Sunrise	03:13:32	Canopus tracker off
21:20:35	Pitch plus 50 deg		

p.m. terminator. Figure 5-55 depicts the *a priori* star map, and Figure 5-56 shows the obtained star map. The stars observed between 0 and 232 degrees agree with the stars plotted on the

a priori star map. The star map shows relatively little glint until a roll angle of 313 degrees is reached. Glint was observed from this point through 355 degrees, with a peak voltage of 1.96

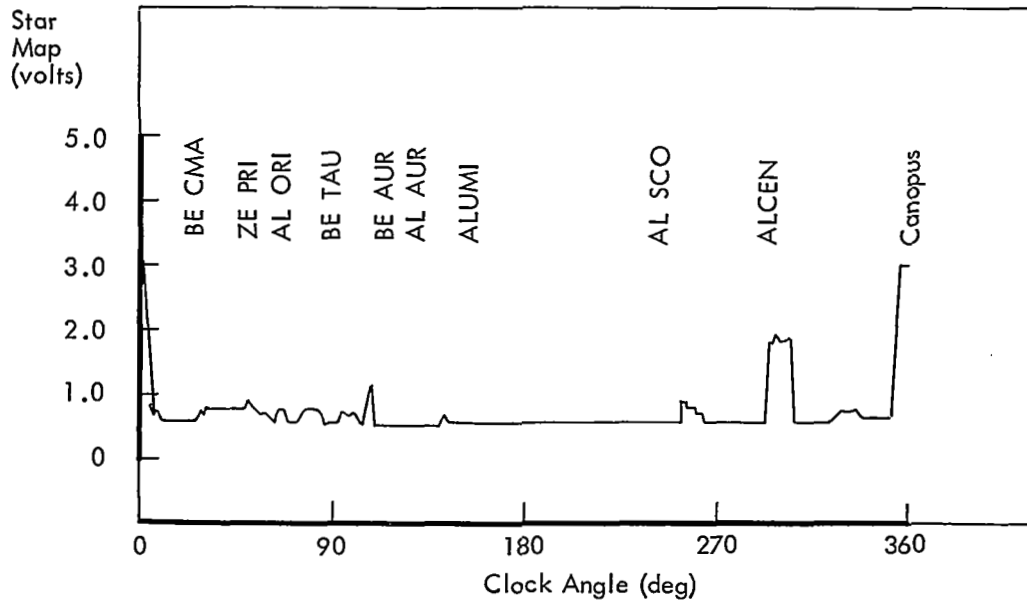
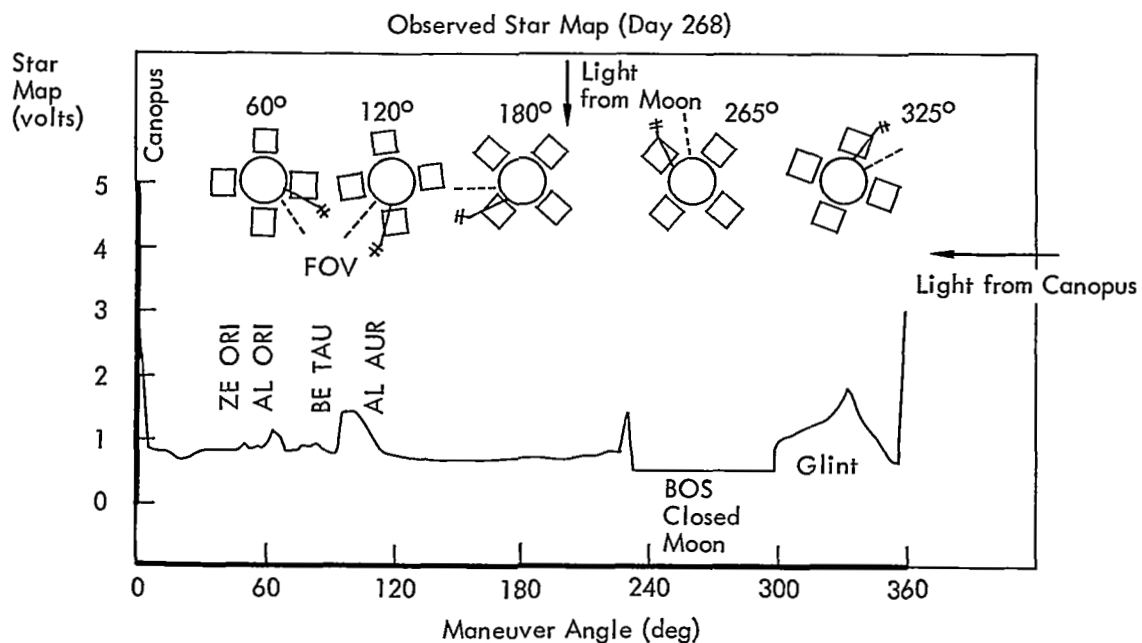


Figure 5-55: A Priori Star Map - Day 068, Orbit 198



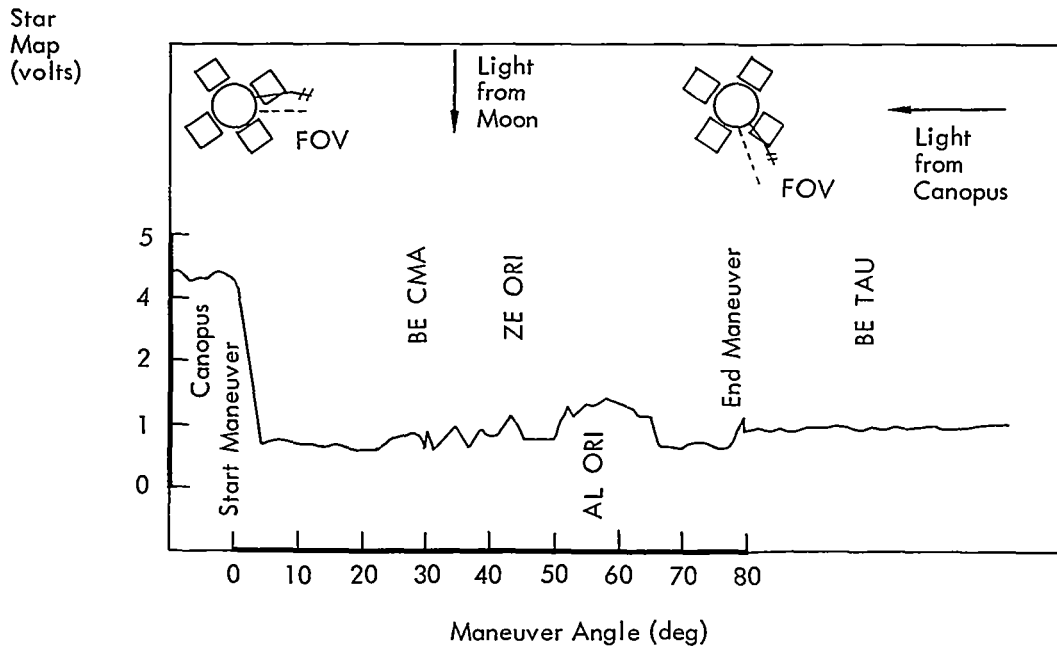
Notes FOV is centerline at tracker field of view.
S/C oriented with viewer looking at bottom of EMD.
Sunlight is from behind viewer.

Figure 5-56: Observed Star Map - Day 268

volts occurring at approximately 325 degrees. The bright-object sensor closed at 232 degrees and opened at 297 degrees as the spacecraft rolled past the Moon at an altitude of 1,830 kilometers, for a total angle of 65 degrees. There is a glint from the moon from 300 to 355 degrees. Comparing this with the light from the Moon that closed the BOS, we see about the same angular area of light, approximately 55 degrees, but the center is displaced 62 degrees later which indicates some object lit by the Moon and seen by the star tracker that is 60 polar degrees less than the star tracker centerline field of view. A polar map indicates that the power-resistor panel on the low-gain antenna is suspect. Therefore, it is concluded that light from the Moon is being reflected from the area of the low-gain antenna into the tracker baffle edges.

On Orbit 199, the spacecraft was rolled plus 80.32 degrees to point the +Y axis away from the Moon as the p.m. terminator was crossed.

Approximately 12 minutes prior to the orbital point defining 20 degrees before the p.m. terminator, a roll maneuver was executed. The star map for this maneuver was good and is a repeat of the first part of the 360-degree roll maneuver (see Figure 5-57). A small amount of background radiation was observed during the maneuver and the tracker ended the maneuver tracking the star Be Tau with a map voltage between 0.85 and 0.96 volt, which is larger than the predicted value of 0.11 times Canopus (predicted was approximately 0.7 volt). Evidently, a small amount of background is adding to the map voltage; however, no evidence of glint was observed. The spacecraft passed through the p.m. terminator tracking Be Tau. At 22:38:32 GMT, 26 minutes past the p.m. terminator, a 50-degree pitch-minus maneuver was initiated to obtain thermal relief. Some 22 minutes later, a pitch-plus maneuver of 50 degrees was executed. The tracker continued to track Be Tau throughout the two maneuvers.



Notes FOV is centerline of tracker field of view.
S/C oriented with viewer looking at bottom of EMD.
Sunlight is from behind viewer.

Figure 5-57: Star Map — Orbit 199

On Orbit 200, with the spacecraft rolled plus 80 degrees from Canopus, the star tracker was turned on 8 minutes prior to crossing the p.m. terminator. The tracker immediately acquired the star Be Tau and began tracking (Figure 5-58). No evidence of glint was seen. Six minutes prior to crossing the p.m. terminator, a pitch-plus 360-degree maneuver was initiated. At this time Be Tau was being tracked with a star map of 0.98 volt. When approximately 100 degrees of the maneuver were completed, Be Tau disappeared from the tracker field of view and the tracker apparently started into the search mode. At 270 degrees, the tracker viewed glint and the map voltage jumped to 1.3 volts. The tracker then locked on glint or background radiation at 0.7 volt and stayed through completion of the pitch maneuver. The 1.3 volts of glint and the 0.7 volt of noise are insufficient to degrade tracker operation. The tracker was then turned off and on and acquired Be Tau again. A roll of 280.5 degrees was initiated to place the spacecraft back in the orbital position. Figure 5-59 shows the star map from this maneuver. Since the maneuver was performed during sunset, the stars occulted by the Moon during the 360-degree roll maneuver were observed. Very little glint can be seen and the Canopus ratios of the

stars calculated from the star map data agree closely with the *a priori* calculated values, considering the overall degradation of 18% from *a priori* values.

Conclusions — The glint is low enough in the area of interest to allow tracking of stars much dimmer than Canopus. There is no problem anticipated in performing a mission similar to that simulated.

5.3.2 Tracker Degradation

The objective was to obtain data in support of Mission IV on Canopus star tracker degradation while in sunlight.

This experiment consisted of an on-off duty cycle of the tracker while the spacecraft was in sunlight (see Table 5-19). The tracker was turned on approximately 30 minutes prior to sunset on every third orbit and left on for approximately 40 minutes. Every 24 hours, a roll update was accomplished to keep Canopus within the tracker window and to prevent the tracker from looking at the Moon. The on-off duty cycles were started on Day 082, 02:50:00 and ceased on Day 085, 22:00:00. During this period, the tracker was turned on 13 times in the Sun.

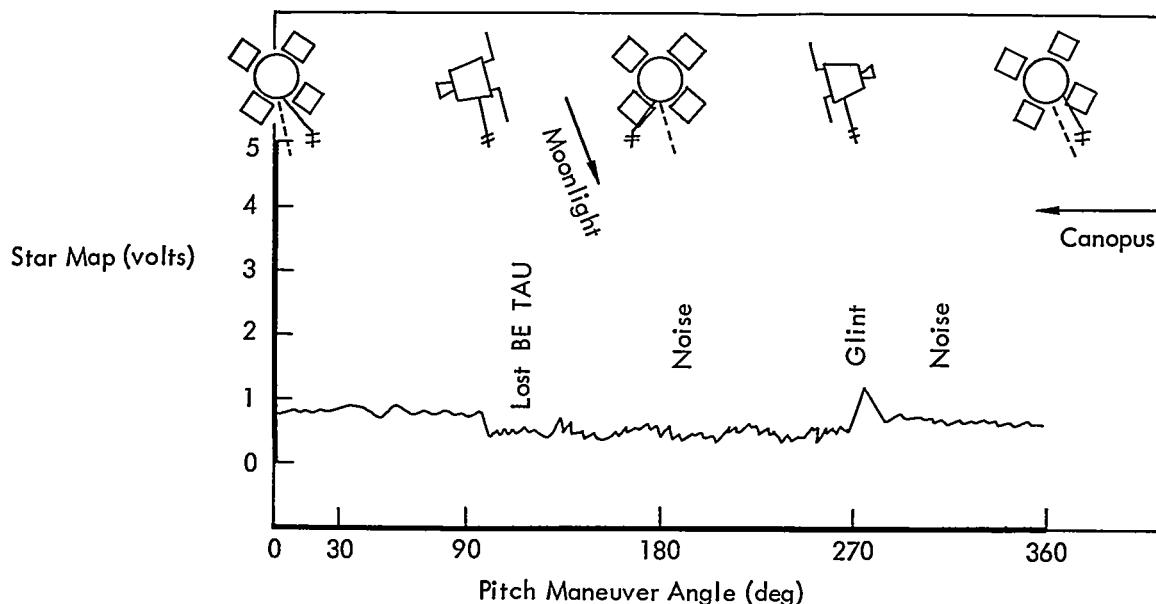


Figure 5-58: Star Map — Orbit 200

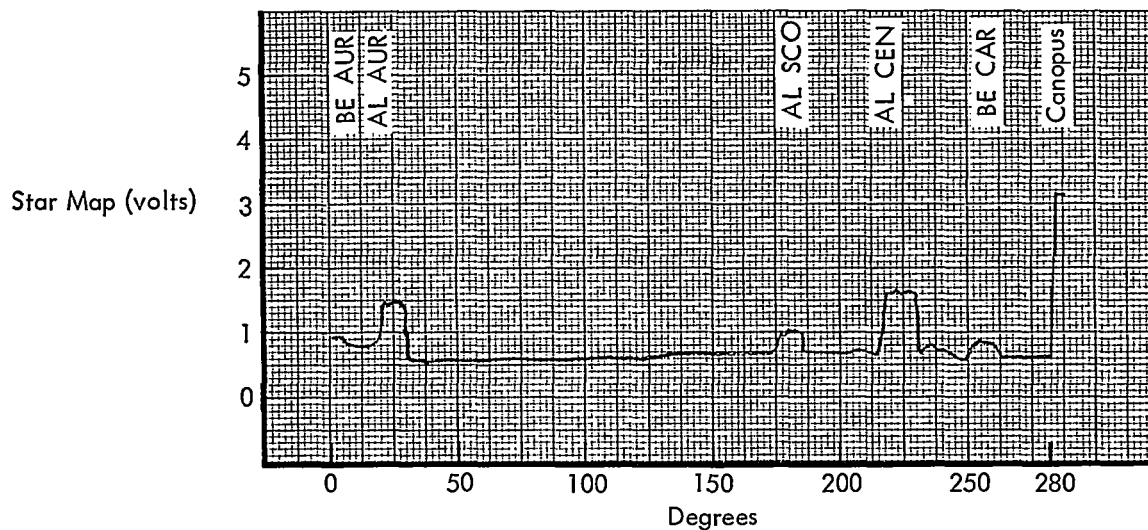


Figure 5-59: Star Map - Day 069, Orbit 200

Data and Discussion - The tracker accumulated a total of 13 on-off cycles and a total time of 3 hours, 29 minutes operational time in the Sun over a 4-day period. Figure 5-60 is a plot of star map voltage maxima and minima versus time. Readings were taken after sunset. The reference reading, 3.05 volts, was taken Day 078 during sunset. Readings of 2.65 volts on Day 083 and 2.87 volts on Day 086 were obtained, which

clearly are not on the same curve as the other readings. Possibly 0.3 volt of glint adds to the other readings, or that particular reading of 2.65 volts is dependent on a degraded portion of the photo multiplier tube. The average voltage when locked on Canopus in 0.2 deadband was 2.95 volts. The dotted lines in Figure 5-60 represent the weighted average of tracker degradation, which compares with that observed during the

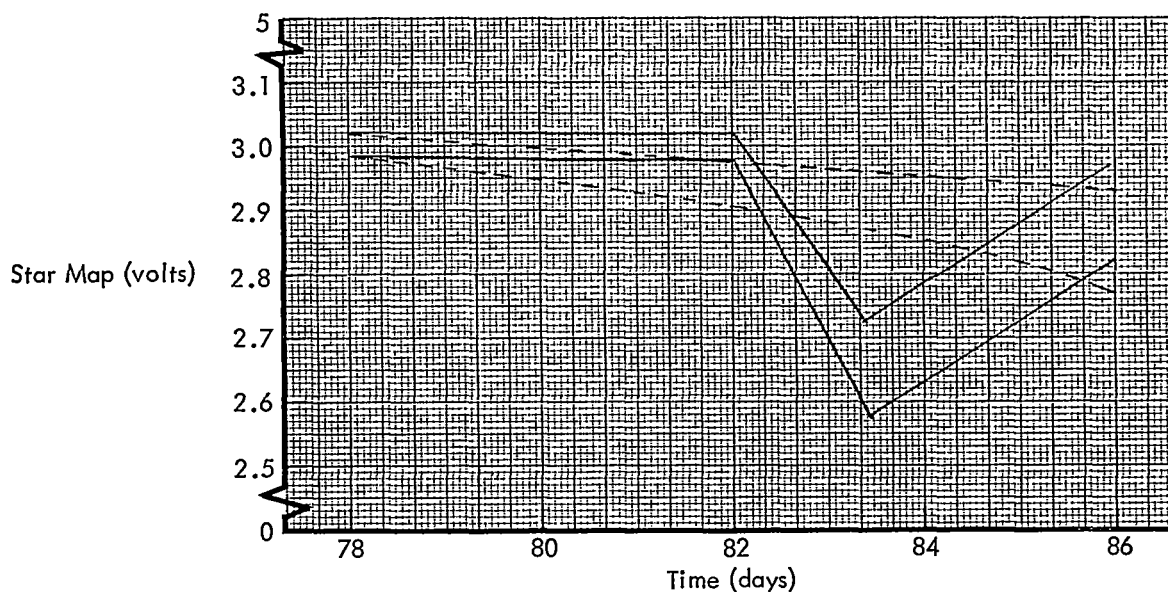


Figure 5-60: Star Map Degradation Test

Table 5-19: Star Tracker Degradation Exercise Sequence

GMT Day:Hr:Min:Sec	Event	Command		GMT Day:Hr:Min:Sec	Event	Command
081:16:00:40	Roll minus 26 deg	RTC		05:05:12	Acquire Sun	RTC
17:21:19	Tracker on	RTC		05:08:28	Tracker on	RTC
17:30:50	Roll minus 5 deg	RTC		05:15:12	Roll minus 5 deg	RTC
17:40:20	Tracker off	RTC		05:19:50	Tracker off	RTC
082:01:50:18	Acquire Sun	SPC		05:20:42	Tracker on	RTC
02:17:19	Pitch minus 50 deg	SPC		05:24:50	Roll plus 10 deg	RTC
02:50:00	Tracker on	SPC		05:34:30	Tracker off	RTC
03:27:29	Sunset			05:37:30	Tracker on	RTC
03:30:58	Tracker off	SPC		05:40:31	Tracker off	RTC
13:20:00	Tracker on	SPC		07:15:30	Sunset	
13:52:59	Sunset			07:42:00	Tracker on	SPC
14:00:58	Tracker off	SPC		07:52:00	Acquire Canopus	RTC
14:10:00	Roll plus 2.8 deg	SPC		07:56:00	Tracker off	SPC
23:50:58	Tracker on	SPC		10:42:00	Acquire Sun	SPC
083:00:18:29	Sunset			10:44:00	Sunset	
00:30:58	Tracker off	SPC		10:45:00	Tracker on	SPC
04:29:51	Sunrise			10:45:07	Acquire Canopus	SPC
05:04:27	0.2 deg dead zone	RTC		11:12:25	Tracker off	SPC

Table 5-19 (continued)

GMT Day:Hr:Min:Sec	Event	Command	GMT Day:Hr:Min:Sec	Event	Command
083:11:48:08	2 deg dead zone	SPC	14:51:38	Sunset	
11:49:00	Acquire Sun	SPC	15:10:58	Tracker off	RTC
20:53:00	Tracker on	SPC	18:14:41	Tracker on	RTC
21:09:31	Sunset		18:18:55	Sunset	
21:33:58	Tracker off	SPC	18:21:46	Tracker off	RTC
084:06:00:00	Acquire Sun	SPC	18:21:59	Earthset	
07:00:00	Tracker on	SPC	20:45:00	Acquire Sun	RTC
07:35:00	Sunset		20:49:49	Tracker on	RTC
07:40:58	Tracker off	SPC	21:20:00	Roll plus 10 deg	RTC
14:10:00	Roll minus 3.1 deg	SPC	21:47:48	Sunset	
17:30:00	Tracker on	SPC	21:48:58	Acquire Canopus	RTC
18:00:34	Sunset		22:00:00	Tracker off	RTC
18:10:58	Tracker off	RTC			
085:04:00:00	Tracker on	RTC			
04:26:06	Sunset				
04:40:58	Tracker off	RTC			
14:10:00	Roll plus 3.1 deg	SPC			
14:30:00	Tracker on	SPC			

prime mission. Although there is some indication of degradation, the time span of the experiment was not long enough to generate conclusive data on tracker degradation.

Conclusion — Although there was not enough time to attach an established rate to tracker degradation, there was definitely evidence of degradation under the influence of sunlight.

5.3.3 Squib Firing Interaction

The objective was to test the hypothesis that there is some interaction — either electrical or mechanical — between a squib being fired and the Canopus star tracker output and operation.

The Canopus star tracker was turned on. All axes were in the 2.0-degree deadband. An attitude change of plus 4.5 degrees roll was made to place the star Vega in the tracker field of view (Canopus was out of the tracker yaw field of view). The star Vega was acquired and the nitrogen shutoff squib valve was fired. See Table 5-20 for sequence of events.

Data and Discussion — The tracker was turned on in the Sun and went into the search mode. The tracker stayed in the search mode for approximately 13 minutes, with the star roll position error, cycling between minus 1.0 and minus 0.2 degree. Upon executing a roll of plus 3.0 degrees, the tracker locked up on glint, the roll error went to minus 4.1 degrees, and star map increased to 0.92 - 0.96 volts. At GMT 20:02 sunset occurred, and the glint disappeared. The tracker then acquired Vega with a star map of 1.50 volts. Dividing the obtained Vega star map

Table 5-20: Squib Firing Interaction Exercise Sequence		
GMT Day:Hr:Min:Sec	Event	Command
101:19:00:00	Acquire Sun	SPC
19:20:00	Pitch and yaw coarse sun sensors off	SPC
19:20:01	Pitch plus 0.011 deg.	SPC
19:30:00	Canopus tracker on	SPC
19:43:00	Roll plus 3.0 deg.	RTC
20:02:00	Sunset	
20:21:00	Roll plus 1.5 deg.	RTC
20:24:45	Fire nitrogen shutoff squib	RTC
20:25:10	Fire nitrogen shutoff squib backup	RTC

voltage by the Canopus value of 3.2 volts gives a ratio of 0.46 close to that calculated of 0.44. Vega was continuously tracked through the squib firing. Figure 5-61 indicates the roll, pitch, and yaw position outputs during the squib firing. Figure 5-62 indicates the star roll error. The spacecraft rates derived from the position change are shown in Table 5-21.

It is evident from Figure 5-61 that no significant rate changes occurred. Star map output and star roll error did not change during the squib firing.

Table 5-21: Position Error			
	<u>Before Squib Fire</u>	<u>After Squib Fire</u>	<u>Rate Change</u>
Roll	-0.0010 deg./sec.	-0.0018 deg./sec.	-0.0008
Pitch	+0.0040 deg./sec.	+0.0032 deg./sec.	-0.0008
Yaw	+0.0004 deg./sec.	+0.0004 deg./sec.	0

Conclusion — No attitude changes occurred as a result of squib firing. The tracker operation was unaffected, either electrically or mechanically, due to squib firing. This is, of course, not con-

clusive evidence that all squib firings will not mechanically affect tracker operation; however, it does prove that electrical noise generated by squib firing had no bearing on tracker operation.

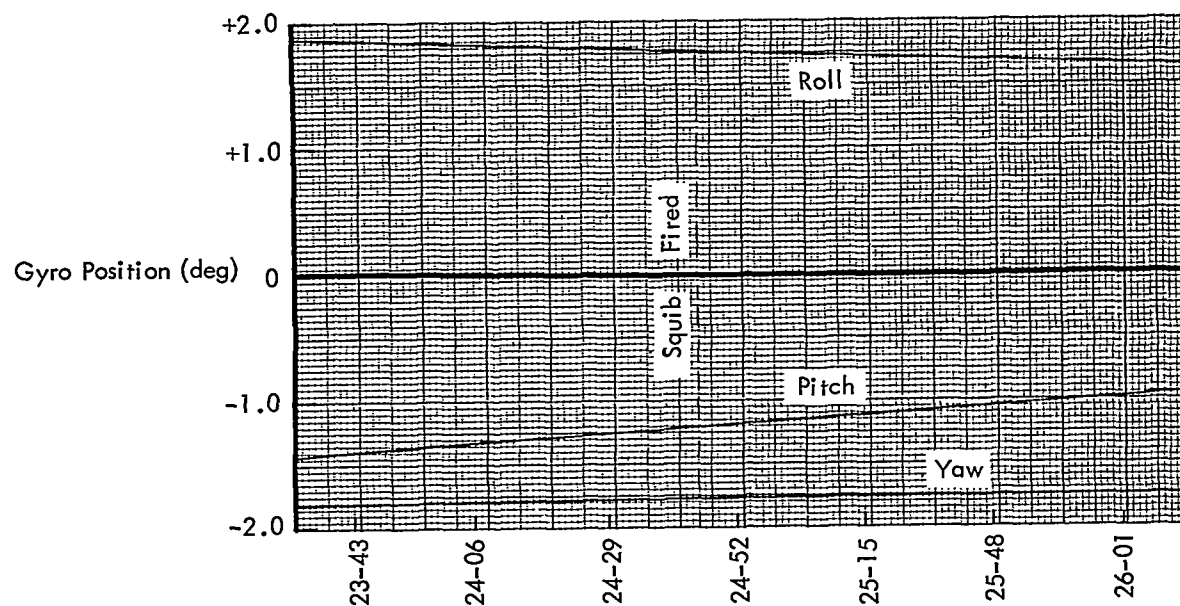


Figure 5-61: Gyro Position versus Time

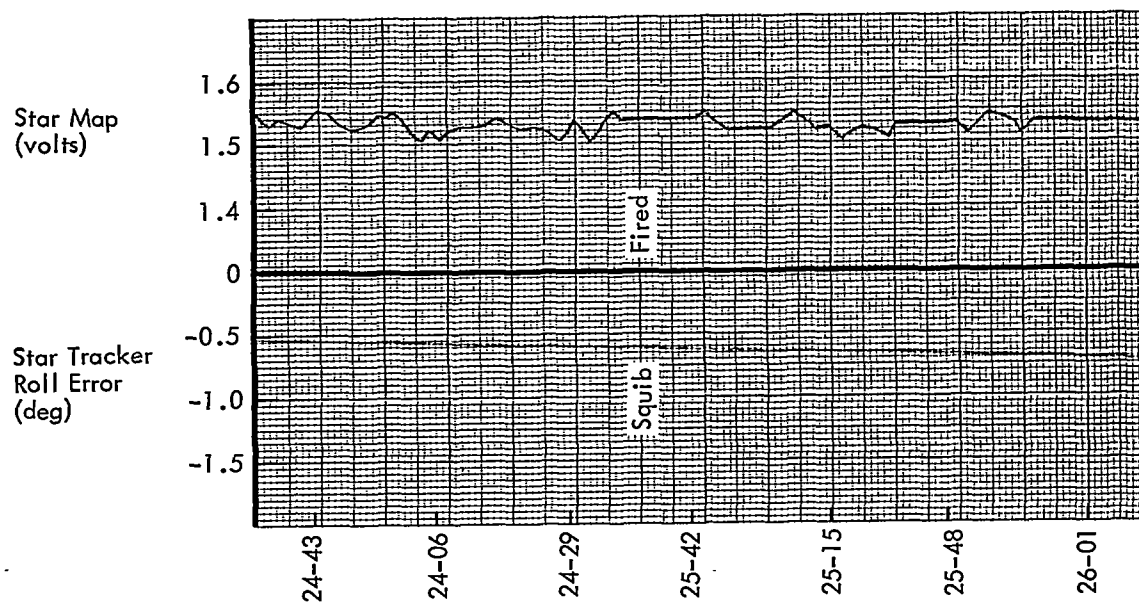


Figure 5-62: Star Map versus Time

5.3.4 Maneuver Accuracy

The objective was to determine the maneuver accuracy in roll, pitch, and yaw.

The test consisted of 360-degree maneuvers starting from and ending on a celestial reference. Pitch and yaw maneuvers were calculated from Sun position and the roll maneuver was calculated from the position of the star Canopus. The roll-plus maneuver was performed on Day 041; the other maneuvers were performed on Days 067 and 069. Gyro rate mode accuracy is not separable from the collective accuracy of the gyro and the voltage-to-frequency converter. The collective system accuracy for a particular axis is measured by commanding a 360-degree maneuver and noting the actual maneuver magnitude as indicated by the initial and final fine Sun sensor or star tracker position outputs.

The sequence of events is given in Table 5-22.

Table 5-22: Maneuver Accuracy Exercise Sequence	
GMT Day:Hr:Mn:Sec	Event
067:14:18:31	Acquire Sun
:14:21:36	Coarse Sun sensors off
:14:24:29	Yaw plus 360 deg
:14:44:29	Yaw minus 360 deg
:15:04:36	Acquire Sun
:19:40:19	Canopus tracker on
:19:43:30	Roll minus 360 deg
069:01:20:00	Acquire Sun
:01:35:51	Pitch plus 360 deg

Data and Discussion — The pitch-minus maneuver was not performed due to gas budget. Data on maneuver accuracies are given in Table 5-23.

The data indicate that the average error is on the order of $\pm 0.15\%$. This compares with Mission II spacecraft where the accuracy was within $\pm 0.10\%$.

Conclusion — It is evident from the above that the maneuver functions on the spacecraft are performing well within the design requirement of $\pm 0.3\%$.

5.3.5 Transponder Threshold

This test was designed to measure the transponder receiver threshold as a means of determining whether the transponder sensitivity and/or the telemetry AGC calibration had degraded.

The test was conducted using the acquisition aid antenna in place of the DSIF 85-foot antenna. Uplink power was gradually reduced until uplink lock was lost, as indicated by transponder AGC.

Data and Discussion — Each data point (Figure 5-63) is an average for the data obtained at one transmitter power setting and has been corrected to a temperature of 80°F. Transmitter power of 2 kilowatts through the acquisition aid antenna is equivalent to 1.26 watts through the 85-foot antenna.

Conclusions — The value for transponder threshold obtained during spacecraft testing was 143 dbm. Comparing this value with Figure 5-63, it was concluded that the spacecraft telemetry data are indicating the correct received signal strength at threshold. It is possible, however, that the data vary periodically as opposed to a constant degradation. Therefore, this test would have to be performed at various initial indicated signal strengths to make a more complete analysis. It is also possible that the AGC calibration is non-linear at the higher signal levels (-80 to -120 dbm), which were not measured during this exercise.

5.3.6 Focus Adjustment

The purpose of this exercise was to determine if a video signal variation (tiger striping) could be eliminated by making adjustments to the line scan tube focus.

Table 5-23: Maneuver Accuracy Data

Maneuver	Actual Magnitude (deg)	Maneuver Error (deg)	Percent Error
Roll plus 360.0 deg	360.19	+0.19	+0.05
Roll minus 360.0 deg	-359.74	-0.26	-0.07
Pitch plus 360.0 deg	360.45	+0.45	+0.13
Yaw plus 360.0 deg	360.56	+0.56	+0.16
Yaw minus 360.0 deg	-359.89	-0.11	-0.03

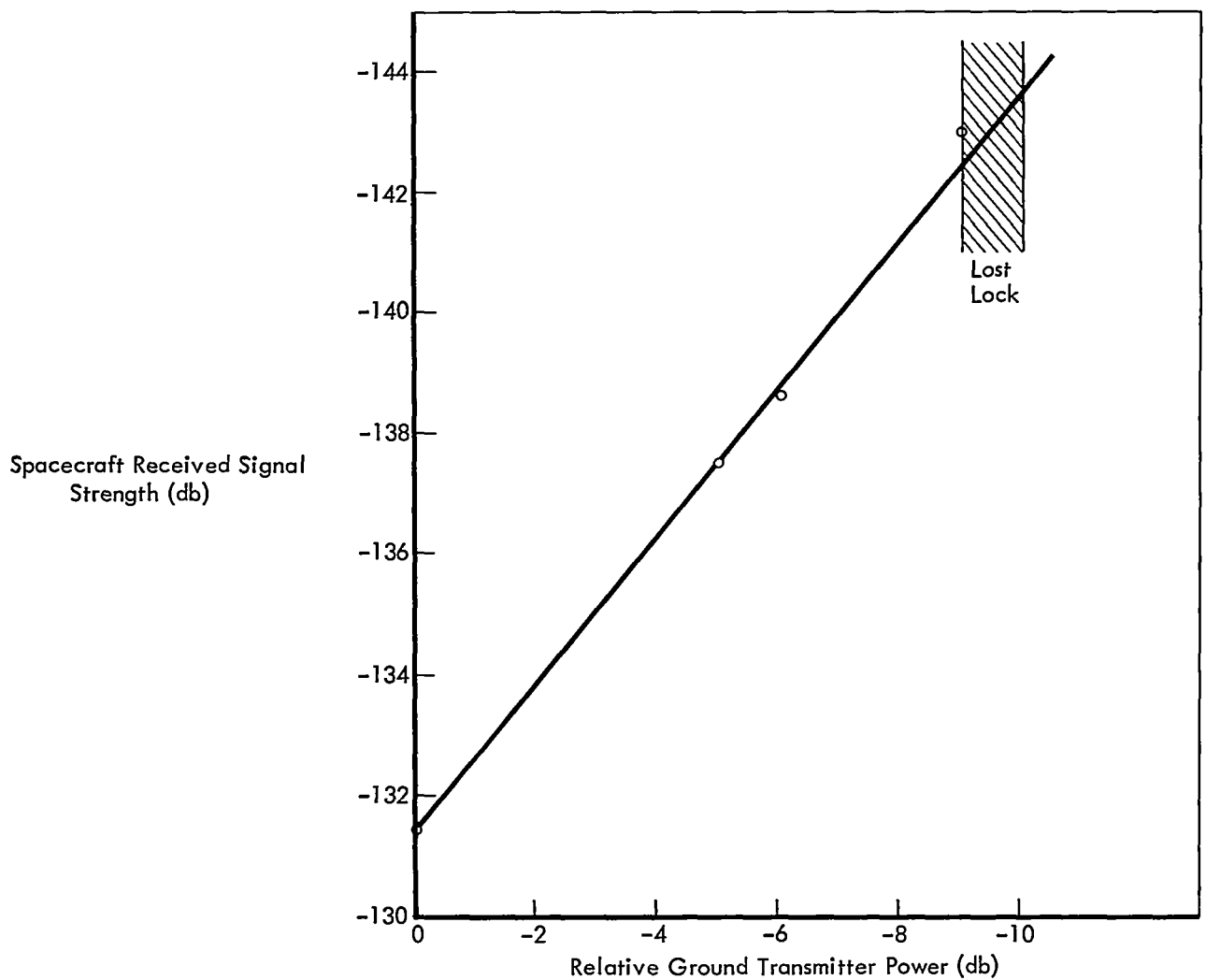


Figure 5-63: Transponder Threshold Test

Because of the failure of the high-voltage power supply, the photo subsystem could not be operated in the readout mode to support this exercise.

5.3.7 V/H Tracking Roll Limit

The objective of the exercise was to establish the spacecraft roll angle limit for V/H sensor tracking.

During the latter part of the photo mission, the V/H sensor was turned on with the camera thermal door closed. V/H sensor operation under this abnormal, zero-signal input condition resulted in the V/H sensor memory slewing (normally) to the high end of the scale (0.0508 rad/sec).

On Day 075, the V/H sensor was turned on for 6.6 minutes with the following orbital geometric parameters:

- Altitude — 62.9 to 65.8 km
- Sun angle — 98 to 77 deg
- Tilt angle — 73.4 to 67.7 deg
- Calculated V/H ratio — 0.0302 to 0.0288 rad/sec

The V/H ratio telemetry indicated off scale (0.0508 rad/sec) for the duration of the test, indicating failure of the sensor to lock on the Moon's surface under these conditions.

On Day 083, the exercise was again attempted with V/H sensor pointed toward the Moon near perilune in its normal operating mode. The sensor was turned on for 2 minutes with the following orbital parameters:

- Altitude — 65 to 70 km
- Sun angle — 92 to 85 deg
- Tilt angle — 6.47 to 0.98 deg (camera axis vertical)
- V/H ratio — 0.0291 to 0.0268 rad/sec

The V/H ratio telemetry locked in at 0.0273 rad/sec, indicating the V/H sensor was tracking properly. The spacecraft was then maneuvered to the following orbital parameters.

- Altitude — 97.34 to 337.64 km
- Sun angle — 72.76 to 48.05 deg
- Tilt angle — 67.79 to 66.14 deg
- V/H ratio — 0.0049 to 0.0022 rad/sec

The V/H ratio telemetry increased from its memory setting to "off scale" during the 8 minutes it was turned on, indicating failure of the sensor to lock on the Moon's surface.

Conclusions — The results of the exercise were inconclusive. On Day 075, the V/H sensor, operating in an abnormal mode (memory off scale), failed to track the lunar surface at a roll tilt angle of 67.7 degrees. On Day 083 the V/H sensor, operating in a normal mode but with the V/H ratio below the minimum specification value, failed to track the lunar surface at a roll tilt angle of 66.14 degrees. Orbital geometric parameters that would permit conduct of the test with all constraints satisfied were no longer available and further efforts were discontinued.

5.3.8 Canopus Tracker Glint Without Earthlight

The objective of the test was to determine glint conditions near the p.m. terminator with the Moon at or near full Moon (new earth).

The experiment was conducted during Orbits 316 and 317, with the spacecraft operating in the wide deadzone. The spacecraft was first oriented toward the Sun and Canopus. The Canopus tracker was turned on just prior to passing the p.m. terminator and turned off just after sunset (see table 5-24 for the test sequence).

Data and Discussion — During Orbit 316, the tracker was turned on approximately 5 minutes before the spacecraft passed the p.m. terminator. The tracker apparently locked up on a low-level star that does not appear on the *a priori* star map data shown in Figure 5-64. It does not appear to be tracking glint, as the roll error is not hard over (normal indication of glint). The star map reading was between 0.72 and 0.74 volt. The spacecraft passed the p.m. terminator on Day 085 at 20:55:00, with an altitude of approximately 1827 kilometers. The tracker continued to track this low-level star until Day 085 at 21:20:00, at which time a roll plus of 10 degrees was introduced into the spacecraft. Star map reading changed to between 2.78 and 2.96 volts and the tracker started to track Canopus. Figure 5-65 shows star-map and roll error for this period.

Table 5-24: Canopus Tracker Glint Without Earthlight Exercise Sequence

<u>GMT Day:Hr:Min:Sec</u>	<u>Event</u>	<u>Command</u>
085:20:45:00	Acquire Sun	RTC
:20:49:49	Canopus tracker on	RTC
:20:55:00	Pass p.m. terminator	
:21:20:00	Roll plus 10 deg	RTC
:21:47:48	Sunset	
:21:48:58	Acquire Canopus	RTC
:21:51:39	Earthset	
:22:00:00	Canopus tracker off	SPC
:22:39:39	Earthrise	
:22:40:02	Pitch minus 42 deg	RTC
:22:56:09	Roll plus 0.011 deg	RTC
:23:45:00	Acquire Sun	RTC
086:00:00:00	Canopus tracker on	RTC
:00:01:36	20 deg before p.m. terminator	
:00:06:26	Canopus tracker off	RTC
:00:06:50	Canopus tracker on	RTC
:00:14:53	Roll plus 5 deg	RTC
:00:19:06	Canopus tracker off	RTC
:00:19:52	Canopus tracker on	RTC
:00:24:06	Pass p.m. terminator	
:00:25:38	Pitch minus 50 deg	RTC
:00:45:20	Pitch plus 5 deg	RTC
:01:16:19	Sunset	
:01:20:10	Canopus tracker off	RTC

At sunset the roll error slope changed due to the sunset disturbance. During sunset an "Acquire Canopus" command was given. The star was acquired and the roll axis went to celestial hold. During Orbit 317, the tracker was turned on 22.5 minutes (approximately 20 degrees) before the spacecraft reached the p.m. terminator (see Figure 5-67). At this time, the tracker started into track with a roll error reading of about minus 1.0 degree and a star map reading of 0.72 to 0.78 volt. When the star map increased to 1.52 volts and roll error went hard over to a minus 4.0 degrees, it was obvious the tracker had locked up on glint. The glint level, as indicated by the star map output, continued to increase to a point 13 degrees before the p.m. terminator. At this time, since the star map read 1.84 volts, the tracker was cycled off-on. Figure 5-66 is a plot of roll, pitch, and yaw position and star map voltage during this period. The change in pitch position was more pronounced, pitch rate being approximately 0.003 degree per second, than that of the other axes. Apparently, the change in pitch is exposing the tracker to more glint. It would appear that the direction of change would expose more of the low-gain antenna resistor panel to the Sun, thus causing an increase in light on the tracker front baffle.

The tracker again locked up on glint after return on and the star map increased slowly to 2.36 volts at GMT 00:14:00 (10 degrees before the terminator). During this period, pitch position reached minus 2.0 degrees; yaw and roll remained steady. A 5-degree roll plus command was then executed. Star map dropped off rapidly to between .88 and 1.0 volt, although the tracker continued to lock up. At GMT 00:19:06 (approximately 5 degrees before the p.m. terminator), the tracker was cycled off-on, which resulted in the tracker acquiring Canopus, with a star map between 2.92 - 3.02 volts, star roll error being plus 0.144 degree. The problem of acquiring Canopus, discussed above, may well have occurred because of the nearness of Canopus to the edge of the tracker field of view, since after rolling plus 5 degrees the error was still plus 2.5 degrees. The tracker continued to track Canopus past the p.m. terminator (00:24:06) and through a pitch minus maneuver executed to obtain thermal relief. Upon completion of the PIM

50-degree maneuver, Canopus was just at the edge of the tracker field of view. Due to the maneuver, the star map decreased to 2.48 volts and remained at this level during and after sunset, indicating that degradation of star map was due to the photomultiplier tube and not to glint.

Conclusion — During the initial pass through the p.m. terminator, the tracker apparently locked up on a small celestial object unknown to the experimenter. Canopus was not in the roll field of view at this time. During the second

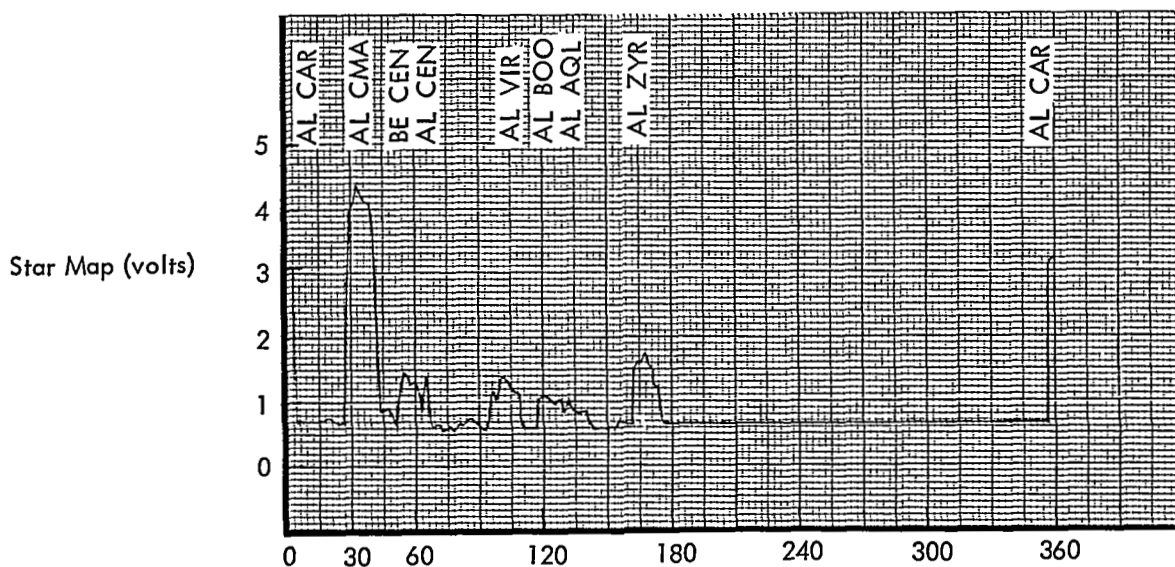


Figure 5-64: A Priori Star Map — Orbit 316

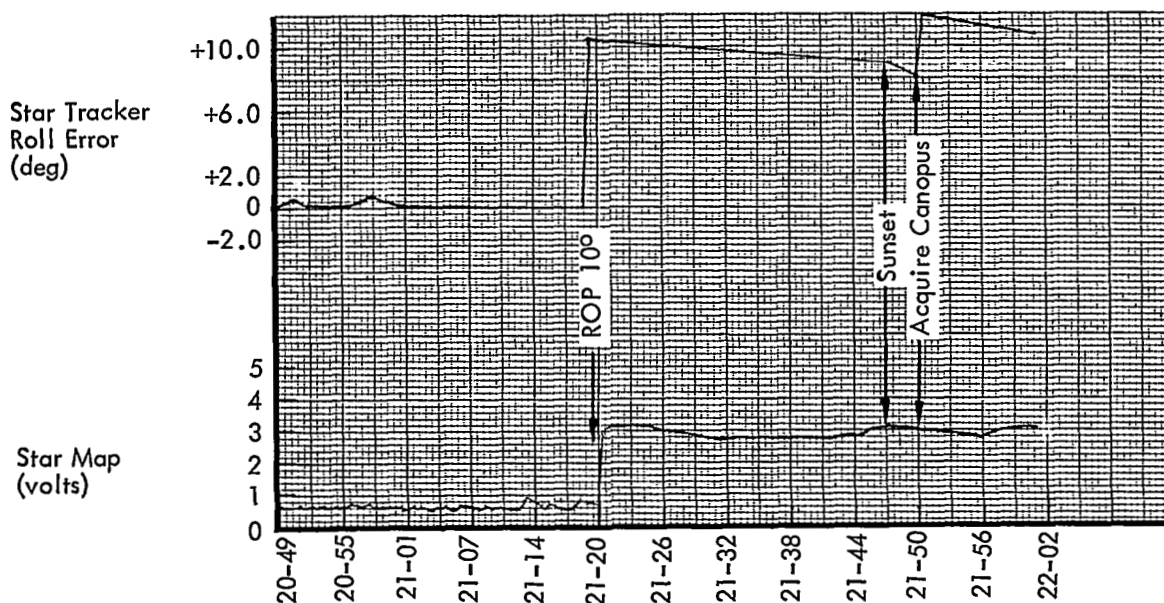


Figure 5-65: Star Map and Roll Error

pass through the p.m. terminator, the tracker locked on glint because the star was close to edge of the field of view. In this situation, unless the tracker electronically sweeps in the right direction the result is normally always baffle lockup.

Although the test results were not as good as expected, largely due to failure to center Canopus before turning on the tracker, it is probable that Canopus will be acquired within 20 degrees of the p.m. terminator, and highly probable that Canopus can be acquired at the p.m. terminator.

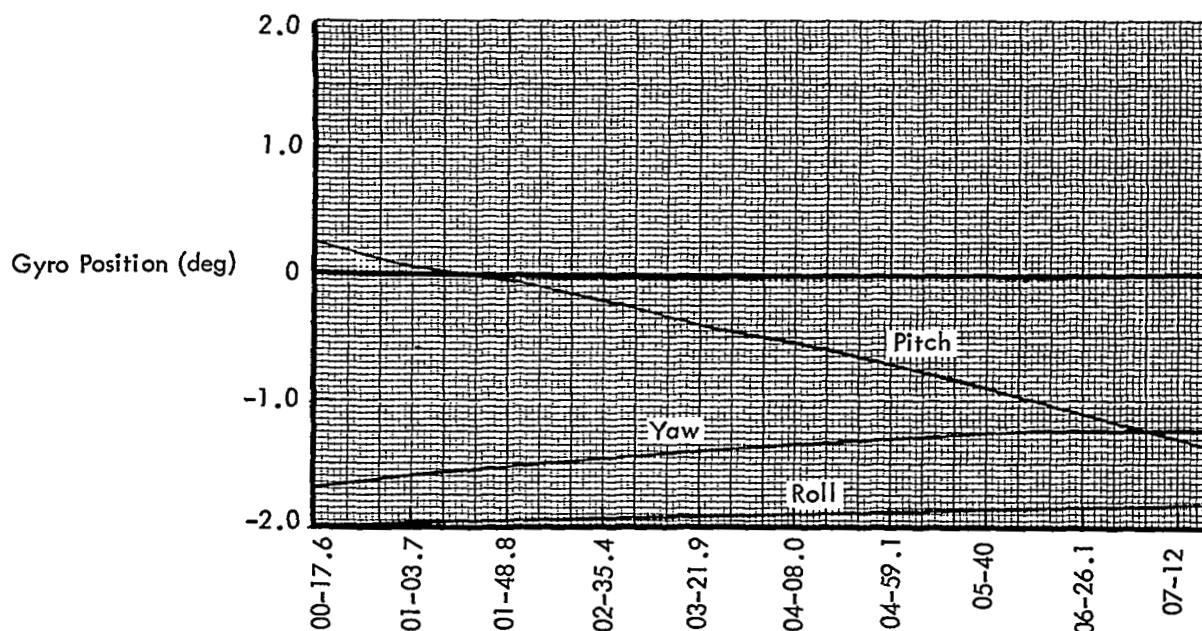


Figure 5-66: Gyro Position - Orbit 317

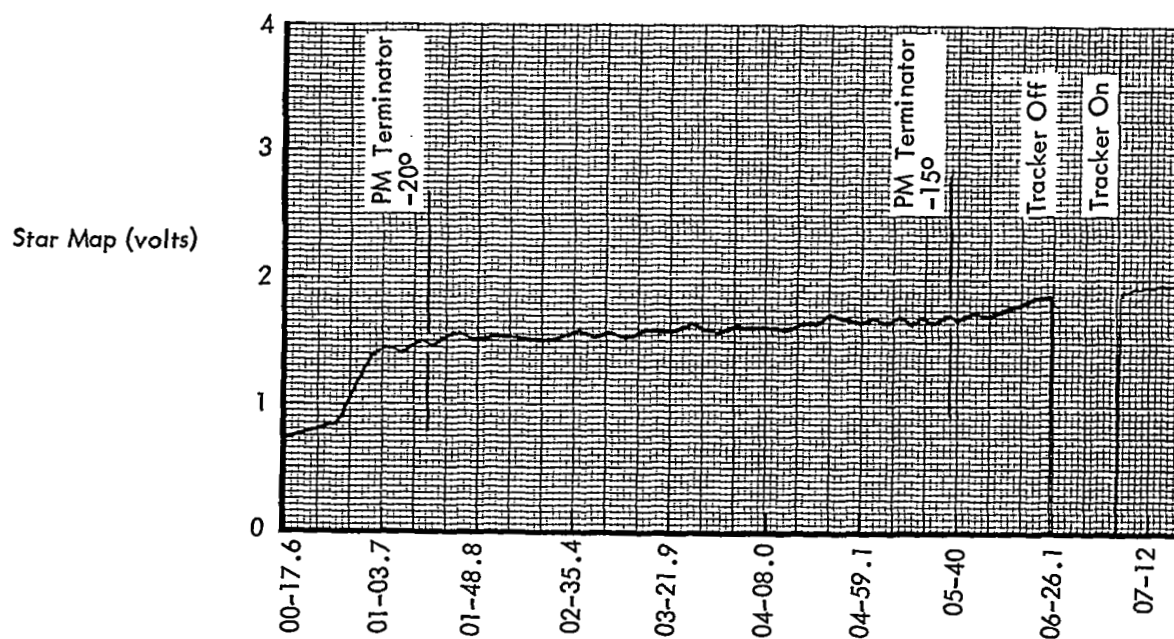


Figure 5-67: Star Map - Orbit 317